2015

Characterization of the SufC ATPase during Fe-S Cluster Assembly by the Suf Pathway in Escherichia coli

Khaleh Mykel Thomas
University of South Carolina

Characterization of the SufC ATPase during Fe-S Cluster Assembly by the Suf Pathway in *Escherichia coli*

by

Khaleh Mykel Thomas

Bachelor of Science
Valdosta State University, 2008

Submitted in Partial Fulfillment of the Requirements

For the Degree of Doctor of Philosophy in

Biochemistry

College of Arts and Sciences

University of South Carolina

2015

Accepted by:

F. Wayne Outten, Major Professor

James Sodetz, Committee Member

Qian Wang, Committee Member

Rekha Patel, Committee Member

Lacy Ford, Senior Vice Provost and Dean of Graduate Studies

DEDICATION

To my wife, godson, parents, and sisters

ABSTRACT

The gram-negative bacterium *E. coli* encodes the Suf pathway to assemble iron-sulfur (Fe-S) clusters under iron starvation and oxidative stress conditions. The ATPase activity of SufC is critical for *in vivo* Fe-S cluster assembly by the Suf pathway. SufC shares homology with the nucleotide binding domain (NBD) of ATP-binding cassette (ABC) transporters and belongs to the AAA+ (ATPases Associated with diverse cellular Activities) ATPase superfamily, a family of proteins that utilizes energy from ATP hydrolysis to perform a variety of cellular functions. SufC forms a stable $SufBC_2D$ complex with partner proteins SufB and SufD. The $SufBC_2D$ complex serves as a novel scaffold where iron and sulfide are assembled into an Fe-S cluster prior to transfer to the SufA carrier protein. The detailed mechanism of the $SufBC_2D$ complex is unknown; however, it is known that all three proteins are required for *in vivo* Fe-S cluster assembly. The present research focuses on understanding the role of the SufC ATPase as a part of the $SufBC_2D$ complex during the Suf Fe-S cluster assembly process. We establish that the ATPase activity of SufC is significantly enhanced in $SufBC_2D$ compared to SufC alone. Steady state and pre-steady state kinetic analysis of $SufBC_2D$ provides evidence of the existence of two conformations of $SufBC_2D$ with different ATPase activities. We explore the specific step in the ATP cycle that contributes to the observed differences in ATPase activity using fluorescent nucleotides mantATP and mantADP. We also observe that SufC has a weaker affinity for SufB in the absence of SufD. The

addition of ATP or ADP enhances the association of SufC with SufB to form a stable $SufB_2C_2$ complex. An affinity chromatography approach is used to investigate the *in vivo* protein-protein interactions between the Suf proteins. Chromosomally encoded polyhistidine-tagged SufC ($SufC_{His}$) interacts with partner proteins SufB and SufD and sulfur transferase proteins SufS and SufE *in vivo*. We discover that $SufC_{His}$ is also present as a monomer in normal and H_2O_2 stressed cells. The data from these *in vivo* studies suggest a role for SufC alone that is separate from its role when associated with SufB and SufD. Because Suf is a stress-responsive pathway, post-translational regulation could be used to maintain Suf in an inactive state during normal growth conditions when Suf is not the predominant Fe-S cluster assembly pathway. Mass spectrometry analysis of recombinant SufC and $SufC_{His}$ identifies phosphorylation sites at SufC residues Tyr241 and Ser10, respectively. Studies of the kinetics of the SufC ATPase in Fe-S scaffolds $SufBC_2D$ and $SufB_2C_2$, Suf protein-protein interactions *in vivo* and *in vitro*, and Suf post-translational modifications provide insight into the functional roles of the SufC ATPase and identify phosphorylation as a mode of SufC regulation during Fe-S cluster assembly by the Suf pathway.

TABLE OF CONTENTS

LIST OF TABLES

LIST OF FIGURES

LIST OF ABBREVIATIONS

AAA+……..ATPases Associated with diverse cellular Activities

ABC……...ATP-Binding Cassette

ADP…….Adenosine Diphosphate

ANS……...8-Anilinonaphthalene-1-sulfonic acid

Asp or D……..Aspartate

ATP…….Adenosine Triphosphate

βME…….2-Mercaptoethanol

DTT……..Dithiothreitol

FAS……...Ferrous Ammonium Sulfate

Fe-S……..Iron-Sulfur

FF……...Fast-Flow

Fur……...Ferric Uptake Regulator

H_2O_2……....Hydrogen peroxide

HIC…….Hydrophobic Interaction Chromatography

HscA……..Heat Shock Cognate A

HscB……..Heat Shock Cognate B

IHF……Integration Host Factor

IPTG……...Isopropyl-β-thiogalactopyranoside

IRP1……..Iron Regulatory Protein 1

Isc…….Iron Sulfur Cluster

kDa……kiloDalton

m/z……mass-to-charge ratio

Mant……2’-(or -3’)-*O*-(*N*-Methylanthraniloyl)

MWCO……Molecular Weight Cut-Off

NBD……..Nucleotide Binding Domain

Nif……...Nitrogen fixation

OD_{600}……....Optical Density at 600 nm

OxyR……Oxygen Regulator

PCR……Polymerase Chain Reaction

Phe or F……...Phenylalanine

PMS……Phenazine Methosulfate

SDS PAGE……...Sodium Dodecyl Sulfate Polyacrylamide Gel Electrophoresis

Ser or S……Serine

Suf……...Sulfur formation

Tyr or Y……...Tyrosine

Val……...Valine

WT……..Wildtype

CHAPTER 1

Introduction

1.1 Iron, Sulfur, and Iron-Sulfur clusters

Iron. Iron is the fourth most abundant element in the earth's crust and is essential for almost all organisms. Under physiological conditions, iron exists in primarily the +2 (ferrous) or +3 (ferric) oxidation states, but can also accommodate other oxidation states (+4 to +6). The redox properties of iron make it an efficient electron carrier, participating in important biological processes such as photosynthesis, nitrogen fixation, respiration, gene regulation, and DNA synthesis. The majority of intracellular iron is bound to iron-containing proteins or iron storage proteins due to the poor solubility of Fe^{3+} under aerobic conditions.[1] While iron is essential for many biological processes, excess iron is harmful to organisms because of the Fe^{2+}-triggered Fenton reaction (shown below) that produces harmful reactive oxygen species (ROS) such as hydroxyl radicals ($^{\bullet}OH$).[2, 3]

$$Fe^{2+} + H_2O_2 \rightarrow Fe^{3+} + {}^{-}OH + {}^{\bullet}OH$$

Its biological function is dependent upon its incorporation into proteins as mono- or bi-nuclear species, heme centers, or iron-sulfur (Fe-S) clusters.

Sulfur. Sulfur is a nonmetallic element required for the biosynthesis of many essential compounds in bacteria: amino acids (Cys and Met), vitamins (biotin, thiamine), and prosthetic groups (Fe-S clusters). In most organisms, the primary mechanism of sulfur incorporation is through cysteine biosynthesis.[4] Sulfur in cysteine can be mobilized

by a group of enzymes called desulfurases and combined with an iron (ferrous or ferric) source for Fe-S cluster cofactor synthesis.[5]

Iron-Sulfur (Fe-S) Clusters. Fe-S clusters are one of the most common prosthetic groups in biology. There are multiple types of Fe-S clusters but the most common are the rhombic [2Fe-2S] and the cubic [3Fe-4S] and [4Fe-4S] types (Figure 1.1).[6] Fe-S proteins typically coordinate the cluster by the thiol side chain of cysteine residues (Figure 1.2), but His and Asp residues can also function as Fe-S cluster ligands. Enzymes with Fe-S centers are widely distributed in modern biology and catalyze a diverse array of chemical reactions. The chemical reactivity of Fe-S clusters makes them a versatile cofactor, participating in reactions that involve electron transfer, substrate binding and activation, enzyme activity regulation, gene expression regulation, and redox sensing. Fe-S clusters are found in organisms from all domains of life (archaea, eubacteria, and eukaryotes) and participate in important biological processes like photosynthesis and respiration.[7, 8]

In the laboratory, Fe-S metalloproteins can be reconstituted chemically using iron and sulfide salts or enzymatically using purified physiological iron and sulfur donor proteins.[6, 9-11] *In vitro* reconstitution of Fe-S metalloproteins requires strict anoxic conditions because solvent exposed Fe-S clusters can readily react with oxygen. Fe-S clusters are generated *in vivo* via complex Fe-S cluster biogenesis pathways consisting of a system of proteins essential to maintain adequate levels of Fe-S clusters under normal and adverse cellular conditions. Decreased iron bioavailability, altered sulfur metabolism and trafficking, and damage to Fe-S proteins as a result of increased oxygen exposure can perturb Fe-S cluster metabolism.[12] Our lab studies the mechanism of an Fe-S cluster

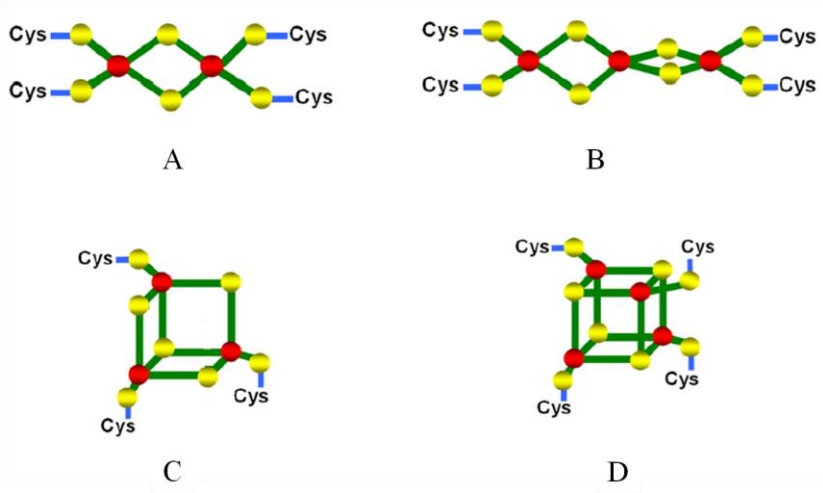

Figure 1.1 Types of Fe-S clusters: (A) rhombic [2Fe-2S], (B) linear [3Fe-4S], (C), cubic [3Fe-4S], and (D) cubic [4Fe-4S]. Red circles represent Fe atoms. Yellow circles represent S atoms. Fe-S clusters are typically ligated to the Cys residues of proteins (labeled).

biogenesis pathway that contributes to the survival of *E. coli* under conditions that normally disrupt Fe-S cluster metabolism: iron starvation and oxidative stress.

1.2 Iron-Sulfur (Fe-S) Cluster Biogenesis Pathways

Multiple Fe-S cluster biogenesis pathways in E. coli. To date, three Fe-S cluster biogenesis pathways have been identified in prokaryotes (Figure 1.2A).[13] Genetic studies in *Azotobacter vinelandii* led to the identification of the Nif (Nitrogen fixation) system, an Fe-S cluster biogenesis pathway required for the maturation of Fe-S containing nitrogenase enzyme.[14, 15] Isc (Iron-sulfur cluster) pathway was also discovered in *A. vinelandii.*[16] The Isc pathway has also been identified in eubacteria and most eukarya. The Suf (mobilization of Sulfur) pathway was initially identified in *E. coli* as a minor contributor to Fe-S cluster biogenesis.[17] Isc is the "housekeeping" Fe-S cluster biogenesis pathway in *E. coli*, assembling Fe-S clusters under normal cellular conditions (Figure 1.2B). Suf is an alternative Fe-S cluster biogenesis pathway to Isc, operating in response to oxidative stress and iron starvation cellular conditions.[18, 19] The Suf pathway is found in bacteria, archaea, the chloroplasts of plants, and parasites.[17] Many organisms encode for only one Fe-S cluster biogenesis system. In organisms that lack Isc and Nif homologues, Suf is the only Fe-S cluster biogenesis pathway and functions as the housekeeping Fe-S cluster assembly system.[12]

Specific proteins are required for Fe-S cluster assembly. Genetic and biochemical studies of each of the three Fe-S cluster biogenesis systems have shown that *in vivo* Fe-S cluster biogenesis often requires a cysteine desulfurase (NifS, IscS, SufS) that mobilizes sulfur from L-cysteine.[7, 8, 13, 20] Bacterial cysteine desulfurase enzymes are

A

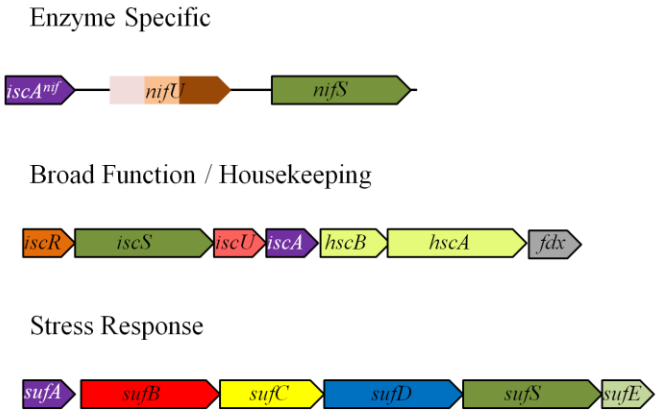

B

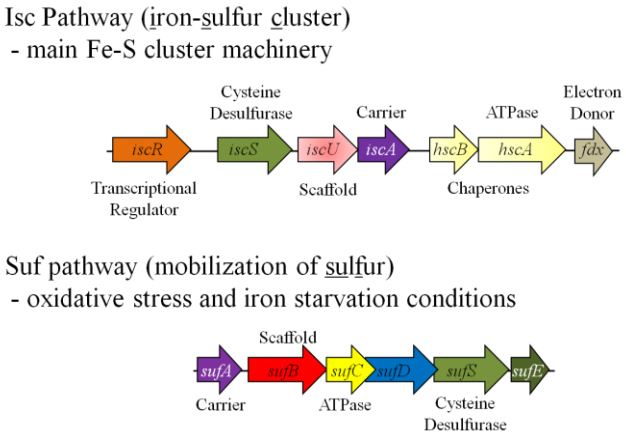

Figure 1.2 Fe-S cluster biogenesis operons. (A) Three Fe-S cluster biogenesis pathways have been identified. (B) *E. coli* encodes two Fe-S cluster biogenesis operons.

pyridoxal 5'-phosphate (PLP)-dependent homodimeric proteins that catalyze the decomposition of L-cysteine to L-alanine and sulfane sulfur.[21] *E. coli* contains three genes that encode cysteine desulfurase enzymes: *iscS*, *csdA*, and *sufS*. The proposed reaction mechanism involves an initial formation of a Schiff base between the substrate L-cysteine and the enzyme-bound PLP cofactor. This is followed by a nucleophilic attack of the cysteine sulhydryl group by a highly conserved cysteine residue, resulting in an enzyme-bound persulfide intermediate. This persulfide intermediate is then available for any downstream biosynthetic pathways generating sulfur-containing molecules (i.e. Fe-S clusters).[5, 22]

All pathways also contain a scaffold protein (IscU, NifU, SufB, and SufU). The scaffold functions as the intermediate assembly site for the Fe-S cluster.[13] The newly synthesized Fe-S cluster bound to the scaffold protein is often labile, facilitating the release of the Fe-S cluster after assembly. Though *in vitro* transfer studies show that the scaffold protein could theoretically directly transfer the assembled Fe-S cluster to Fe-S proteins, Fe-S cluster biogenesis pathways also encode for a carrier protein (IscA, SufA) to mediate downstream trafficking and targeting of the mature Fe-S cluster to the appropriate Fe-S metalloprotein.[23-27] *E. coli* contains three carrier proteins (IscA, ErpA, and SufA).[20]

The study of Fe-S cluster formation on ferredoxin (Fdx) in isolated hypotonically lysed spinach chloroplasts provided evidence that ATP hydrolysis and reduced nicotinamide adenine dinucleotide phosphate (NADPH) are required for Fe-S cluster formation. Takahashi et al. did not determine the specific ATP-dependent step in the Fe-S cluster formation pathway but did propose the idea of an ATP-dependent enzyme that

facilitates assembly and/or insertion of the Fe-S cluster into Fdx.[28] ATP hydrolyzing enzymes have been identified in both Fe-S cluster biogenesis pathways in *E. coli.* Heat shock cognate A (HscA) of the Isc pathway and SufC of the Suf pathway both display intrinsic ATPase activity.[29, 30] The role of HscA ATP hydrolysis in Isc cluster assembly has been well-characterized and will be discussed in detail in a later section. The contribution of SufC ATP hydrolysis to Suf cluster biogenesis is still unclear.

The physiological iron donor for Fe-S cluster assembly is undetermined. A critical gap in our knowledge of the *in vivo* Fe-S cluster biogenesis process is the iron donation step.[31, 32] Many potential iron donors have been proposed. The most accepted theory proposes the ferrous "labile" iron pool as the source of iron for *in vivo* Fe-S cluster assembly. The nature of the labile iron pool theory is not fully understood, however, because the majority of cellular iron is sequestered in iron metalloenzymes and iron storage proteins. Alternatively, a separate iron chaperone or iron storage protein could participate in the iron donation step. CyaY, the bacterial frataxin homolog, is the most extensively studied iron donor candidate.[33] CyaY binds ferrous iron with a binding affinity of K_d = 3.8 μM.[34] This binding affinity is weak compared to other metallochaperones that have metal-binding affinities of picomolar or tighter (i.e. cobalt metallochaperone AnhE K_d = 0.120 nM).[35] Other studies of CyaY's involvement in the Isc pathway also negate the possibility of CyaY as an iron chaperone.[36-38] *E. coli* contains four iron storage proteins that could potentially release iron for Fe-S cluster assembly: ferritin A (FtnA), ferritin B (FtnB), bacterioferritin (Bfr), and "DNA-binding protein from starved cells" (Dps). Previous genetic evidence indirectly links the Suf pathway to Bfr in the plant pathogen *Erwinia chrysanthemi* (recently renamed *Dickeya dadantii*, but

will be referred to as *E. chrysanthemi* throughout this text).[39] The mobilization of iron from iron storage proteins for Fe-S cluster assembly has not been studied extensively, though. Figure 1.3 summarizes the proteins involved in Fe-S cluster biogenesis.

1.3 Transcriptional regulation of Suf Fe-S cluster Assembly in *E. coli*

Fur represses suf expression in normal cellular conditions. The *suf* operon in *E. coli* consists of six genes *sufABCDSE* organized as a single polycistronic transcriptional unit. The *E. coli* Suf system is primarily used to augment the Isc "housekeeping" pathway under conditions of oxidative stress and iron starvation. Both the *isc* and *suf* operons are regulated in response to cellular iron status via the iron metalloregulatory protein ferric uptake regulator (Fur).[40] Fur senses cellular iron status by binding ferrous iron. In normal cells and iron-replete conditions, basal *suf* transcripts are maintained at low levels due to repression of transcription by Fe^{2+}-Fur bound at the *suf* promoter region (Figure 1.4A). Demetallation of Fur in response to iron limiting conditions leads to decreased binding of Fur at the promoter region, resulting in up-regulation of *suf* expression (Figure 1.4B).

IscR activates suf expression in response to oxidative stress. In *E. coli*, the *iscRSUA-hscBA-fdx* genes are transcriptionally regulated by IscR, which is encoded by the first gene of the *isc* operon. IscR accommodates a [2Fe-2S] cluster and functions as a repressor of *isc* operon transcription in its Fe-S-bound conformation.[41] Oxidative stress conditions are unfavorable for Fe-S maturation of IscR. Destabilization and ultimate removal of the Fe-S cluster in IscR or titration of Fe-S biogenesis machinery to replace damaged clusters in other proteins results in the accumulation of apo-IscR. Apo-IscR

causes derepression of the *isc* operon and activation of *suf* expression (Figure 1.4B).[42-44] Sensitivity of the Fe-S cluster in IscR to cellular conditions allows a mechanism of sensing Fe-S cluster homeostasis in the cell to regulate Fe-S cluster demand.

OxyR activates suf expression in response to oxidative stress. DNA microarray analysis of *E. coli* cells treated with hydrogen peroxide (H_2O_2) revealed *suf* expression was induced by H_2O_2 in an OxyR-dependent manner (Figure 1.4B).[45] OxyR is oxidized via disulfide bond formation in response to H_2O_2, stimulating the expression of *suf* genes and other antioxidant genes such as *katG* (hydrogen peroxidase I).[46]

1.4 The Isc Pathway

IscS, IscU, and IscA are critical components of the Isc system. IscS is the PLP-dependent cysteine desulfurase for the Isc Fe-S cluster biogenesis system. Sulfur is acquired from L-cysteine as a protein-bound persulfide at IscS catalytic residue Cys328 via the cysteine desulfurase mechanism then transferred to scaffold IscU. IscU is a U-type scaffold protein defined by its ability to assemble both [2Fe-2S] and [4Fe-4S] clusters and to transfer the assembled clusters to acceptor proteins. IscA binds a [2Fe-2S] or [4Fe-4S] cluster in *E. coli* but also has iron binding activity *in vivo* under aerobic conditions.[20] Initial studies proposed IscA as a bifunctional protein, serving as an alternative scaffold protein or iron chaperone depending on cellular conditions. However, current evidence assigns the role of IscA as an A-type carrier protein that shuttles Fe-S clusters from scaffold IscU to target proteins.[25-27] The specific contribution of IscA's iron binding capacity remains unanswered.

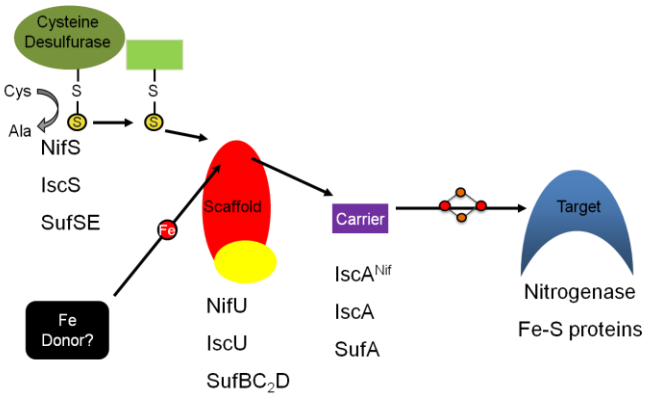

Figure 1.3 Proteins involved in Fe-S cluster biogenesis.

A

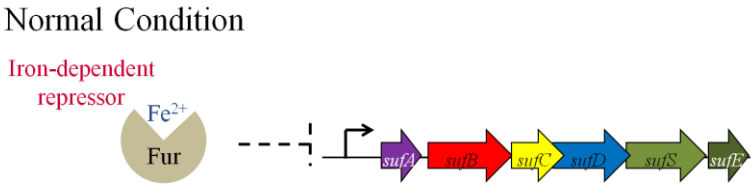

B

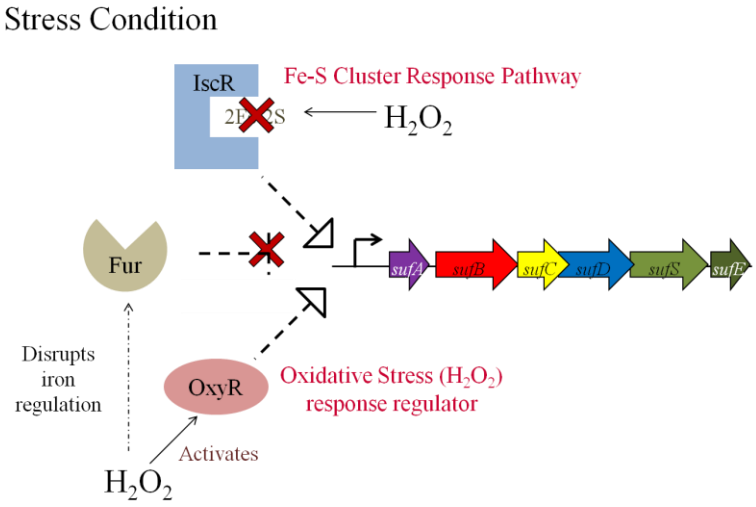

Figure 1.4 Transcriptional regulation of the *suf* operon in *E. coli* under (A) normal and (B) H_2O_2 stress conditions. (A) Fe^{2+}-bound Fur represses *suf* expression under normal growth conditions. (B) H_2O_2 stress depresses Fur regulation of *suf* and apo-IscR and OxyR activate *suf* expression.

HscA and HscB stimulate Fe-S cluster transfer from IscU. The Isc pathway also contains heat shock protein 70-kDa (Hsp70) -type chaperone HscA and Hsp40-type co-chaperone HscB. HscA displays intrinsic ATPase activity and interacts selectively with scaffold IscU and co-chaperone HscB to stimulate Fe-S cluster transfer from IscU to acceptor proteins.[47] ATP binding and hydrolysis allosterically regulate the affinity of HscA for IscU.[48] The interaction between HscA and IscU is facilitated by HscB, which serves as a bridge between ATP-bound HscA and the [2Fe-2S] cluster-bound state of IscU. Together, IscU and HscB stimulate the ATPase activity of HscA.[49] ATP hydrolysis results in a structural change in HscA that has a weaker affinity for HscB and a stronger affinity for the apo-state of IscU, leading to Fe-S cluster transfer from IscU.[48]

1.5 The Suf pathway

SufS and SufE are a sulfur-shuttle system. SufS is a PLP-dependent cysteine desulfurase enzyme that catalyzes the mobilization of sulfur from L-cysteine. SufE, a structural homolog of IscU, accepts the persulfide (R-S-SH) from SufS and traffics the persulfide to $SufBC_2D$ as a reduced sulfide (S^{2-}) for Fe-S cluster assembly.[50, 51] SufE enhances the cysteine desulfurase activity of SufS (Table 1.1).[52, 53] SufE-dependent SufS desulfurase activity enhancement is further increased by $SufBC_2D$.[54] Dai and Outten recently reported increased resistance to H_2O_2 during the cysteine desulfurase reaction by SufS-SufE compared to IscS-IscU. These results support a shielded persulfide transfer from SufS to SufE for protection against reactive oxygen species.[55] Selbach et al. also reported protected sulfur transfer from SufS to SufE in the presence of reducing agents DTT and TCEP.[56] The crystal structure of SufS[57] reveals the active site Cys (Cys364) is

hidden in a pocket at the dimer interface of the SufS subunits and appears to be solvent-limited. The structure of the SufSE complex has not been determined, but SufE-dependent cysteine desulfurase activity enhancement of SufS suggests a shielded persulfide transfer from SufS to SufE.

SufA is the Fe-S cluster carrier protein. Native SufA, isolated from cells co-expressing *sufABCDSE* genes, is a dimer and binds a [2Fe-2S] $^{2+}$ cluster. [2Fe-2S]-SufA from *E. coli* and *E. chrysanthemi* can efficiently transfer a [2Fe-2S] cluster to apo-Fdx and a [4Fe-4S] cluster to apo-AcnA to generate holo-forms of each protein *in vitro*.[58, 59] Initial studies proposed SufA as a Fe-S scaffold protein, but current data supports SufA involvement as an Fe-S cluster carrier protein for the Suf pathway (Table 1.1). Protein-protein interaction and *in vitro* Fe-S transfer studies indicate SufA preferentially binds Fe-S-bound $SufBC_2D$ and provide evidence of a unidirectional transfer of Fe-S clusters from $SufBC_2D$ to SufA.[23] SufA also binds Fe (1.0 Fe: SufA monomer), but Fe-bound SufA has not been shown to donate iron to $SufBC_2D$ for Fe-S cluster assembly.

SufB can assemble a [4Fe-4S] or [2Fe-2S] cluster. SufB has been most extensively studied in *E. coli* and *Erwinia chrysanthemi*. *E. coli* SufB has been established as an Fe-S scaffold protein for the Suf pathway. SufB assembles a stable $[4Fe\text{-}4S]^{2+}$ cluster when iron and sulfide salts are provided as starting materials under strictly anoxic conditions.[51, 60] Fe-S bound SufB is competent to transfer intact Fe-S clusters to native *E. coli* target proteins SufA, Fdx and aconitase A (AcnA).[24] $(His)_6$-SufB purifies with both $[4Fe\text{-}4S]^{2+}$ and linear [3Fe-4S] clusters after *in vivo* co-expression with the *sufCDSE* genes.[61] It was recently discovered that SufB can also assemble a oxygen-resistant [2Fe-2S] cluster.[62] SufB contains 13 total cysteine residues, 4 of which are

highly conserved. The N-terminus of SufB contains a putative Fe-S cluster binding motif (*CxxCxxxC*), but it has not been identified as the Fe-S cluster binding site.

SufD shares homology with SufB. SufD is a paralog of SufB. SufD and SufB share significant sequence similarity throughout their C-terminal helical domains. In *E. coli*, SufD interacts with SufC to form a $SufBC_2D$ complex[51] and also assembles a $SufC_2D_2$ complex in the absence of SufB. The C-terminal domain residues of SufD participate in the binding of SufD with SufC in the structure of the $SufC_2D_2$ complex.[63] The role of SufD in Fe-S cluster assembly has not been established, but our lab proposes a role in *in vivo* iron acquisition (Table 1.1). We previously discovered that in the absence of SufD, *in vivo* incorporation of iron on SufB during Fe-S cluster assembly is abolished while sulfide levels are only slightly diminished.[61] Saini proposed SufD works in concert with the ATPase enzyme SufC (explained in detailed in section 1.6) to facilitate active iron delivery into Suf against an unfavorable concentration gradient.

SufB, SufC, and SufD form stable SufBCD scaffold complexes. SufC is encoded along with the SufB scaffold protein in all identified *suf* operons. SufB and SufC interact along with partner protein SufD as a stable $SufBC_2D$ complex isolated from cells co-expressing the *sufABCDSE* genes. Similar to SufB alone, $SufBC_2D$ reconstitutes a [4Fe-4S] cluster *in vitro*. As mentioned previously, SufA and SufE have been shown to interact with SufB alone, but this interaction is enhanced in the $SufBC_2D$ complex.[23,51] Unidirectional cluster transfer from reconstituted Fe-S bound $SufBC_2D$ to apo-SufA further supports the role of $SufBC_2D$ as a novel Fe-S cluster scaffold complex.[23] A recent study demonstrated the [4Fe-4S] cluster on SufB is sensitive to oxidants and gets oxidized to a [2Fe-2S] cluster on SufB. The [2Fe-2S] cluster on SufB is five times more

stable to air than the [2Fe-2S] cluster on IscU. The observed resistance to air was greater in $SufBC_2D$. The [2Fe-2S] cluster on $SufBC_2D$ was completely stable at the experimental oxygen concentrations.[62] The protected Fe-S cluster environment is consistent with the SufSE desulfurase activity resistance to H_2O_2 stress, providing more evidence for a protected Fe-S cluster assembly process by the Suf pathway under oxidative stress conditions. $SufBC_2D$ has been established as the Fe-S cluster scaffold complex in *E. coli* and *T. thermophilus* HB8 (Table 1.1).[64]

His_6-SufB co-purifies with SufC and SufD as two distinct Suf complexes after *in vivo* co-expression with the *sufCDSE* genes. His_6-$SufBC_2D$ binds 1 equivalent of reduced flavin adenine dinucleotide ($FADH_2$) per $SufBC_2D$. The role of $FADH_2$ has not been established. Additionally, a His_6-$SufB_2C_2$ complex was isolated associated with minimal amounts of SufD. As purified His_6-$SufB_2C_2$ contained 3.2 Fe atoms and 4.2 S^{2-} per complex and displayed a UV-visible absorption spectrum similar to the spectra of an *in vitro* reconstituted [4Fe-4S] SufB or [4Fe-4S] $SufBC_2D$.[61] Reconstituted [4Fe-4S] His_6-$SufB_2C_2$ can transfer a [2Fe-2S] cluster to carrier protein SufA and Fe-S protein Fdx *in vitro*.[24] While the physiological relevance of $SufB_2C_2$ in *E. coli* is not well understood, this complex may reflect the active SufBC complex in organisms that lack SufD and have only the minimal *sufBC* operon.[12] A $SufC_2D_2$ complex can be isolated from cells expressing only *sufCD* genes[63], however, $SufC_2D_2$ is not an Fe-S scaffold complex. It is possible the $SufB_2C_2$ and $SufC_2D_2$ complexes carry out discrete steps in Fe-S cluster assembly, but their roles have not been conclusively shown.

Table 1.1 Proposed Functions of Suf Proteins during Fe-S Cluster Assembly

Suf protein	Proposed function	References
SufA	Fe-S carrier protein	23,24,58
SufB	Fe-S scaffold protein	23,24,60-62,64
SufC	ATPase	18,29,40,61,63,64,66,68,69,71
SufD	Iron trafficking	61
SufS	Cysteine desulfurase	50-57
SufE	Sulfur transfer shuttle	50-56

1.6 SufC is an ATPase.

SufC shares homology with the nucleotide-binding domain of ATP-binding cassette (ABC) transporters. The ATP binding cassette (ABC) transporters are the largest class of transporters in *E. coli*. Most ABC transporters are associated with the membrane and utilize energy from ATP hydrolysis to transport substrates across biological membranes. A full-length ABC transporter minimally consists of two hydrophobic transmembrane domains (TMDs) traversing the cytoplasmic (inner) membrane and two nucleotide-binding domains localized in the cytoplasm.[65] Primary sequence analysis of SufC reveals the presence of signature motifs commonly found in the nucleotide-binding domains (NBD) of ABC transporters. SufC shows the highest degree of sequence similarity with HisP, the NBD of the histidine permease from *Salmonella typhimurium* (Figures 1.5 and 1.6). Similarly to the NBDs of ABC transporters, SufC has an overall L-shaped structure divided into two domains.[66] The RecA-like catalytic domain contains the Walker A (GxxxxGKT/S) (Figure 1.6, red) and Walker B (hhhhD, where h is a hydrophobic residue) (Figure 1.6, blue) motifs. In ABC NBDs, the Walker A and B motifs directly participate in ATP binding and hydrolysis.[65] The helical domain of SufC contains the strictly conserved ABC signature motif (L/FSGGQ/E) (Figure 1.6, magenta). Upon nucleotide-induced dimer formation, the Walker A and B motifs of one SufC subunit should orient with the ABC signature motif of the opposing SufC subunit to create two head-to-tail ATP-binding sites, both buried at the dimer interface.[66]

The D-loop is a flexible structure that coordinates and activates the catalytic water for ATP hydrolysis in ABC NBDs.[67] A dimer model of SufC, generated by

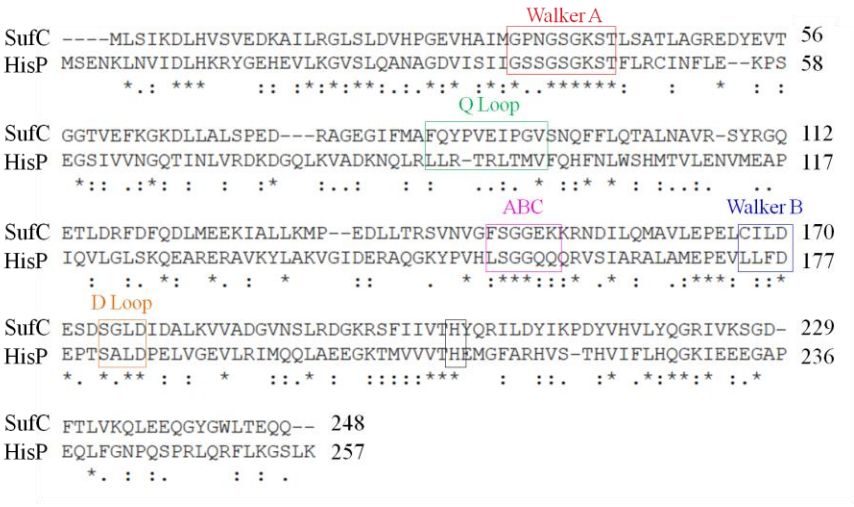

Figure 1.5 Sequence alignment of *E. coli* SufC and ABC NBD HisP from *S. typhimurium*. Residues of conserved motifs are indicated with color-coded boxes: Walker A (red), Q-loop (green), ABC signature (magenta), Walker B (blue), and D-loop (orange). A conserved His residue is indicated in a black box. Identical residues are starred. Alignment was generated using the ClustalW2 multiple sequence alignment tool.

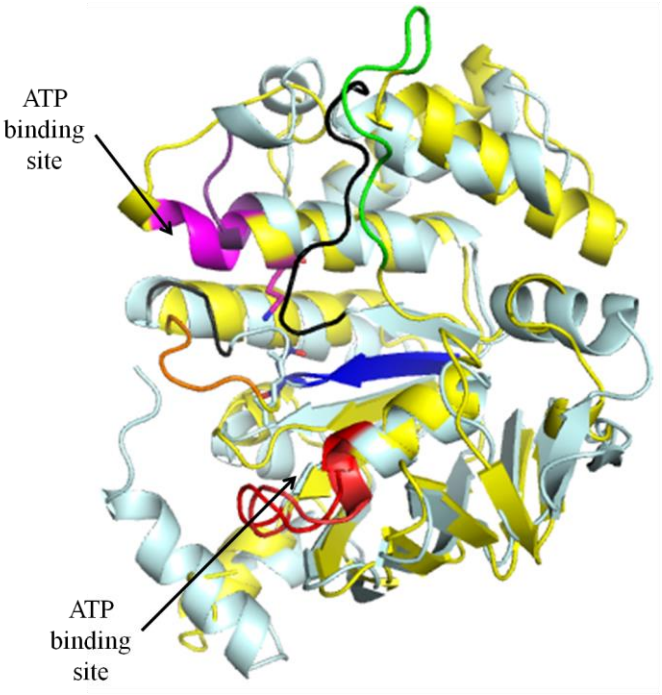

Figure 1.6 Structural alignment of *E. coli* SufC monomer (yellow) and *S. typhimurium* HisP (light grey). Walker A (red), Walker B (blue), ABC signature (magenta-SufC; purple-HisP), D-loop (orange-SufC; grey-HisP) and Q-loop (green-SufC; black-HisP) conserved motifs are shown in color. ATP binding sites are labeled. Alignment was generated using the FATCAT Pairwise Alignment tool.

superimposing the structure of SufC monomer onto the structure of ATP-bound ABC NBD HlyB (H662A) dimer from *E. coli*, reveals possible steric hindrance of SufC dimer formation due to protrusion of the D-loops into the putative dimer interface.[66] This feature distinguishes SufC from the ABC transporter NBDs. Another structural difference between SufC and ABC NBDs is at the Q-loop structure. In ABC transporters, the TMDs are structurally heterogeneous yet share the common feature of interacting at the Q-loops of the NBDs. The conserved Gln of the Q-loop participates in ATP binding and is proposed to participate in the coupling of ATP hydrolysis to structural dynamics in the TMDs.[65] In the SufC monomer structure, the Q-loop is positioned away from the ATP binding site and the conserved Gln (Gln85) is not available for participation in ATP hydrolysis. The Q-loop in SufC putatively participates in the interaction of SufC with partner proteins SufB and SufD.

Many of the residues involved in ATP binding and hydrolysis in NBDs are conserved in SufC. Residues of the Walker A motif stabilize the nucleotide in the binding pocket via hydrogen bonding with the phosphate groups of the bound ATP molecule. A Val residue in SufC (aromatic residue in ABC proteins) interacts with the adenine base of the ATP molecule via a hydrophobic interaction. Walker B motif residues coordinate an essential catalytic Mg^{2+} ion to the ATP molecule. The proposed kinetic mechanism of ATP hydrolysis requires properly positioned motifs for binding the phosphates of ATP and catalyzing the attack of water on the γ-phosphate of ATP for hydrolysis.[65] The primary catalytic base residue for SufC has not been determined and is ambiguous for NBDs of ABC transporters. A highly conserved Glu residue immediately following the Walker B motif is the proposed catalytic residue for ATP hydrolysis in

ABC NBDs (although this has not been conclusively shown for all ABC NBDs or SufC). In structures of ABC NBDs, this Glu residue interacts with ATP via a catalytic water molecule.[65] In SufC, this Glu residue (Glu171) is rotated away from the ATP binding site and forms a salt bridge with Lys152, a residue positioned adjacent to the ABC signature motif in the helical domain (Figure 1.7B).[66] Residues Lys152 and Glu171 are conserved in all SufC proteins, and the Lys152 – Glu171 salt-bridge is also observed in nucleotide-free and ADP-bound SufC structures from *T. thermophilus*.[68]

The structure of a $SufC_2D_2$ complex isolated from *E. coli* revealed that the SufC catalytic site is remodeled as a result of its interaction with SufD (Figure 1.7A). The Glu171 – Lys152 salt bridge is cleaved and Glu171 is repositioned toward the ATP binding pocket (Figure 1.7B). The D-loop is also rotated away from the dimer interface, making the ATP-binding site of SufC more accessible, ultimately facilitating the dimerization of SufC for ATP hydrolysis.[63] These structural changes appear to be controlled by SufC interaction with its partner protein(s) indicating an appreciable degree of coordinated regulation of SufC ATPase activity. Kinetic studies report the intrinsic ATPase activity of SufC alone is quite low but is significantly enhanced when SufC forms a complex with either SufB or SufD.[29, 69] It is proposed that the salt-bridge in the SufC monomer structure is used to down-regulate ATP hydrolysis when SufC is not bound to partner proteins SufB or SufD. At present the exact function of SufC in the Fe-S cluster biogenesis process is unknown.

A

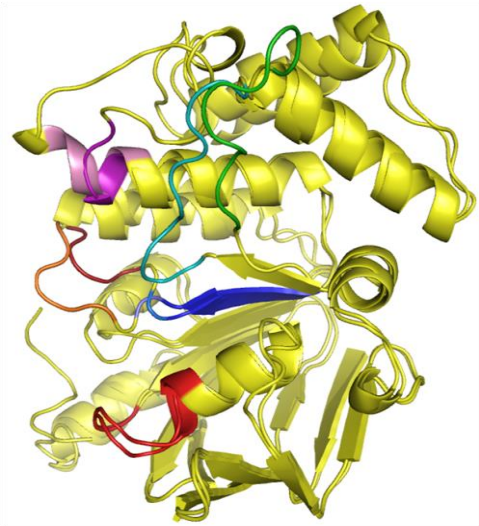

B

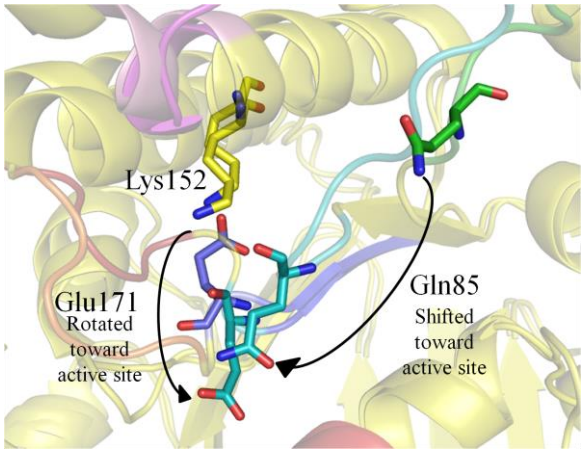

Figure 1.7 (A) Structural alignment of SufC monomer and one SufC subunit from the $SufC_2D_2$ complex (both yellow). Walker A (red) and Walker B (blue) motifs are colored the same as in Figure 1.6. The Q-loop is colored green (SufC monomer) or cyan ($SufC_2D_2$). The D-loop is colored orange (SufC monomer) or brick red ($SufC_2D_2$). The ABC signature motif is colored purple (SufC monomer) or lavender ($SufC_2D_2$). (B) Close-up view of panel A. Black arrows indicate positional changes of residues going from SufC monomer to SufC from $SufC_2D_2$. Gln85 (green to cyan), Lys152 (yellow), and Glu171 (blue to cyan) are shown as sticks. Alignment was generated using the FATCAT Pairwise Alignment tool.

1.7 Research Aims

A critical gap in the knowledge of Suf function is the role of ATP binding and hydrolysis by SufC. As mentioned previously, SufC shares homology with the nucleotide binding domain of ABC transporters. Figure 1.8 shows a major difference between the full-length ABC transporter $BtuC_2D_2$ and the $SufBC_2D$ complex (both isolated from *E. coli*). The nucleotide binding domains BtuD are cytoplasmic and the partner proteins BtuC are associated with the membrane for ATP-dependent import of vitamin B12.[70] In contrast, $SufBC_2D$ is completely cytoplasmic and participates in Fe-S cluster assembly. It was previously established that ATP hydrolysis is required for Fe-S cluster formation.[28] $SufBC_2D$ and $SufB_2C_2$ complexes reconstitute an Fe-S cluster when supplemented with iron and sulfide *in vitro*.[51] Our lab previously determined that SufC ATPase activity is not required for Fe-S cluster transfer to [2Fe-2S] target proteins.[24] SufC ATPase activity is also not required for SufSE cysteine desulfurase activity enhancement by $SufBC_2D$.We initially proposed a role of ATP in the conversion of the multiple Suf complexes containing SufC: $SufBC_2D$, $SufB_2C_2$, and $SufC_2D_2$. We tested nucleotide induced formation of the more stable $SufBC_2D$ from a mixture of $SufB_2C_2$ and $SufC_2D_2$. We also tested nucleotide induced decomposition of $SufBC_2D$ into its individual components SufB, SufC, and SufD. We tested if ADP altered the rate of cluster assembly on $SufBC_2D$ during *in vitro* enzymatic reconstitution.

SufC alone has intrinsic ATPase activity that is enhanced by SufB or SufD. This implies that SufC monomer plays a role in *in vivo* Fe-S cluster assembly that is separate from its role in the $SufBC_2D$ or $SufB_2C_2$ scaffold complexes. We investigated Suf *in vivo* protein-protein interactions to determine if SufC is present as a monomer or

A

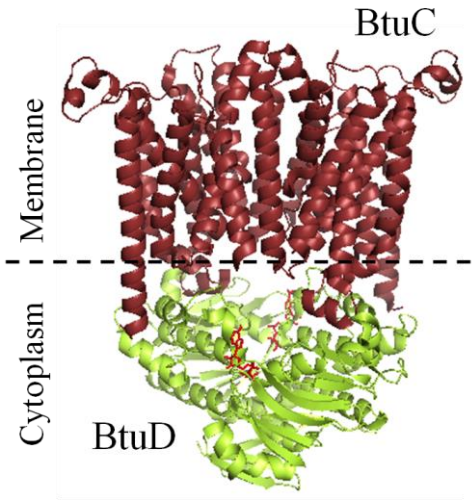

B

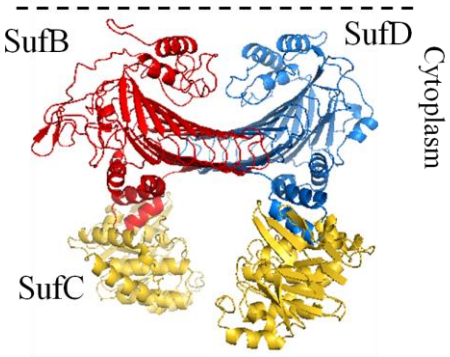

Figure 1.8 (A) Crystal structure of AMP-PNP bound ABC transporter $BtuC_2D_2$ from *E. coli* (PDB entry 4FI3). BtuC is brick red; BtuD is green-yellow. AMP-PNP molecules are shown as red sticks. (B) Model structure of $SufBC_2D$ from *E. coli* generated by modeling SufB on one chain of the $SufC_2D_2$ structure. SufB is red, SufC is yellow, and SufD is blue.

solely associated with a SufBCD complex. *In vivo* protein-protein interaction studies were repeated with added exogenous Mg-ATP to determine if nucleotide shifts any available SufC monomer into complex with SufB and SufD. Suf is a stress-responsive Fe-S cluster assembly system in *E. coli.* Suf interactions were observed from normal cells and cells treated with H_2O_2 to understand the critical interactions that occur between the Suf proteins under different cellular conditions.

The kinetics of ATP binding and hydrolysis of $SufB_2C_2$ and $SufC_2D_2$ complexes from *T. maritima* have been reported.[71] The ATPase activity of $SufBC_2D$ has not been extensively studied in *E. coli* or other species. We provide steady state and transient kinetic analysis of the ATP hydrolysis cycle of $SufBC_2D$ compared to SufC alone and the proposed alternative scaffold $SufB_2C_2$.

1.8 Biomedical Relevance

Mycobacterium tuberculosis is the causative agent of tuberculosis. The worldwide emergence of antibiotic resistant strains of *M. tuberculosis* has led to the need for development of novel antibiotics that inhibit its essential functions. The Suf machinery, which functions under oxidative stress and iron limiting conditions in *E. coli*, is the only Fe-S cluster assembly system in *M. tuberculosis*.[72] Fe-S clusters are incorporated into metalloproteins essential to survival of the bacterial cells in the host during infection. Lack of a direct Suf homologue in humans makes the Suf pathway an attractive drug target. The aim of our research is to provide a biochemical foundation of Suf function in *E. coli* to lead to the development of novel antibiotics against pathogens such as *M. tuberculosis* that encode only the Suf pathway.

1.9 References

1. Andrews, S. C., Robinson, A. K., and Rodriguez-Quinones, F. (2003) Bacterial iron homeostasis. *FEMS Microbiol Rev* 27, 215-237.

2. Touati, D. (2000) Iron and oxidative stress in bacteria. *Arch Biochem Biophys* 373, 1-6.

3. Winterbourn, C. C. (1995) Toxicity of iron and hydrogen peroxide: the Fenton reaction. *Toxicol Lett* 82-83, 969-974.

4. Wirtz, M., and Droux, M. (2005) Synthesis of the sulfur amino acids: cysteine and methionine. *Photosynth Res* 86, 345-362.

5. Mihara, H., and Esaki, N. (2002) Bacterial cysteine desulfurases: their function and mechanisms. *Appl Microbiol Biotechnol* 60, 12-23.

6. Beinert, H., Holm, R. H., and Munck, E. (1997) Iron-sulfur clusters: nature's modular, multipurpose structures. *Science* 277, 653-659.

7. Fontecave, M., and Ollagnier-de-Choudens, S. (2008) Iron-sulfur cluster biosynthesis in bacteria: Mechanisms of cluster assembly and transfer. *Arch Biochem Biophys* 474, 226-237.

8. Johnson, D. C., Dean, D. R., Smith, A. D., and Johnson, M. K. (2005) Structure, function, and formation of biological iron-sulfur clusters. *Annu Rev Biochem* 74, 247-281.

9. Kennedy, M. C., and Beinert, H.(1988) The state of cluster SH and S^{2-} of aconitase during cluster interconversions and removal. A convenient preparation of apoenzyme. *J Biol Chem* 263, 8194-8198.

10. Kennedy, M. C., Emptage, M. H., Dreyer, J. L., and Beinert, H. (1983) The role of iron in the activation-inactivation of aconitase. *J Biol Chem* 258, 11098-11105.

11. Malkin, R., and Rabinowitz, J. C. (1966) The reconstitution of clostridial ferredoxin. *Biochem Biophys Res Commun* 23, 822-827.

12. Boyd, E. S., Thomas, K. M., Dai, Y., Boyd, J. M., and Outten, F. W. (2014) Interplay between oxygen and Fe-S cluster biogenesis: insights from the Suf pathway. *Biochemistry* 53, 5834-5847.

13. Ayala-Castro, C., Saini, A., and Outten, F. W. (2008) Fe-S cluster assembly pathways in bacteria. *Microbiol Mol Biol Rev* 72, 110-125.

14. Jacobson, M. R., Brigle, K. E., Bennett, L. T., Setterquist, R. A., Wilson, M. S., Cash, V. L., Beynon, J., Newton, W. E., and Dean, D. R. (1989) Physical and genetic map of the major *nif* gene cluster from *Azotobacter vinelandii*. *J Bacteriol* 171, 1017-1027.

15. Jacobson, M. R., Cash, V. L., Weiss, M. C., Laird, N. F., Newton, W. E., and Dean, D. R. (1989) Biochemical and genetic analysis of the *nifUSVWZM* cluster from *Azotobacter vinelandii*. *Mol Gen Genet* 219, 49-57.

16. Zheng, L., Cash, V. L., Flint, D. H., and Dean, D. R. (1998) Assembly of iron-sulfur clusters. Identification of an *iscSUA-hscBA-fdx* gene cluster from *Azotobacter vinelandii*. *J Biol Chem* 273, 13264-13272.

17. Takahashi, Y., and Tokumoto, U. (2002) A third bacterial system for the assembly of iron-sulfur clusters with homologs in archaea and plastids. *J Biol Chem* 277, 28380-28383.

18. Nachin, L., Loiseau, L., Expert, D., and Barras, F. (2003) SufC: an unorthodox cytoplasmic ABC/ATPase required for [Fe-S] biogenesis under oxidative stress. *Embo J* 22, 427-437.

19. Outten, F. W., Djaman, O., and Storz, G. (2004) A *suf* operon requirement for Fe-S cluster assembly during iron starvation in *Escherichia coli*. *Mol Microbiol* 52, 861-872.

20. Roche, B., Aussel, L., Ezraty, B., Mandin, P., Py, B., and Barras, F. (2013) Iron/sulfur proteins biogenesis in prokaryotes: formation, regulation and diversity. *Biochim Biophys Acta* 1827, 455-469.

21. Mihara, H., Kurihara, T., Yoshimura, T., and Esaki, N. (2000) Kinetic and mutational studies of three NifS homologs from *Escherichia coli*: mechanistic difference between L-cysteine desulfurase and L-selenocysteine lyase reactions. *J Biochem* 127, 559-567.

22. Zheng, L., and Dean, D. R. (1994) Catalytic formation of a nitrogenase iron-sulfur cluster. *J Biol Chem* 269, 18723-18726.

23. Chahal, H. K., Dai, Y., Saini, A., Ayala-Castro, C., and Outten, F. W. (2009) The SufBCD Fe-S scaffold complex interacts with SufA for Fe-S cluster transfer. *Biochemistry* 48, 10644-10653.

24. Chahal, H. K., and Outten, F. W. (2012) Separate Fe-S scaffold and carrier functions for $SufB_2C_2$ and SufA during *in vitro* maturation of [2Fe-2S] Fdx. *J Inorg Biochem* 116, 126-134.

25. Ollagnier-de-Choudens, S., Sanakis, Y., and Fontecave, M. (2004) SufA/IscA: reactivity studies of a class of scaffold proteins involved in [Fe-S] cluster assembly. *J Biol Inorg Chem* 9, 828-838.

26. Vinella, D., Brochier-Armanet, C., Loiseau, L., Talla, E., and Barras, F. (2009) Iron-sulfur (Fe/S) protein biogenesis: phylogenomic and genetic studies of A-type carriers. *PLoS Genet* 5, e1000497.

27. Vinella, D., Loiseau, L., Ollagnier de Choudens, S., Fontecave, M., and Barras, F. (2013) *In vivo* [Fe-S] cluster acquisition by IscR and NsrR, two stress regulators in *Escherichia coli*. *Mol Microbiol* 87, (3), 493-508.

28. Takahashi, Y., Mitsui, A., Fujita, Y., and Matsubara, H. (1991) Roles of ATP and NADPH in formation of the Fe-S cluster of spinach ferredoxin. *Plant Physiol* 95, 104-110.

29. Rangachari, K., Davis, C. T., Eccleston, J. F., Hirst, E. M., Saldanha, J. W., Strath, M., and Wilson, R. J. (2002) SufC hydrolyzes ATP and interacts with SufB from *Thermotoga maritima*. *FEBS Lett* 514, 225-228.

30. Silberg, J. J., and Vickery, L. E. (2000) Kinetic characterization of the ATPase cycle of the molecular chaperone Hsc66 from *Escherichia coli*. *J Biol Chem* 275, 7779-7786.

31. Outten, F. W. (2014) Recent advances in the Suf Fe-S cluster biogenesis pathway: Beyond the Proteobacteria. *Biochim Biophys Acta* 1853, 1464-1469.

32. Outten, F. W. (2014) A stress-responsive Fe-S cluster biogenesis system in bacteria-the *suf* operon of Gammaproteobacteria. In *Iron-Sulfur Clusters in Chemistry and Biology*, Rouault, T. A., Ed. de Gruyter:; 297-323.

33. Ding, H., Yang, J., Coleman, L. C., and Yeung, S. (2007) Distinct iron binding property of two putative iron donors for the iron-sulfur cluster assembly: IscA and the bacterial frataxin ortholog CyaY under physiological and oxidative stress conditions. *J Biol Chem* 282, 7997-8004.

34. Bou-Abdallah, F., Adinolfi, S., Pastore, A., Laue, T. M., and Dennis Chasteen, N. (2004) Iron binding and oxidation kinetics in frataxin CyaY of *Escherichia coli*. *J Mol Biol* 341, 605-615.

35. Okamoto, S., Van Petegem, F., Patrauchan, M. A., and Eltis, L. D. (2010) AnhE, a metallochaperone involved in the maturation of a cobalt-dependent nitrile hydratase. *J Biol Chem* 285, 25126-25133.

36. Adinolfi, S., Iannuzzi, C., Prischi, F., Pastore, C., Iametti, S., Martin, S. R., Bonomi, F., and Pastore, A. (2009) Bacterial frataxin CyaY is the gatekeeper of iron-sulfur cluster formation catalyzed by IscS. *Nat Struct Mol Biol* 16, 390-396.

37. Iannuzzi, C., Adinolfi, S., Howes, B. D., Garcia-Serres, R., Clemancey, M., Latour, J. M., Smulevich, G., and Pastore, A. (2011) The role of CyaY in iron sulfur cluster assembly on the *E. coli* IscU scaffold protein. *PLoS One* 6, e21992.

38. Prischi, F., Konarev, P. V., Iannuzzi, C., Pastore, C., Adinolfi, S., Martin, S. R., Svergun, D. I., and Pastore, A. (2010) Structural bases for the interaction of frataxin with the central components of iron-sulphur cluster assembly. *Nat Commun* 1, 95.

39. Expert, D., Boughammoura, A., and Franza, T. (2008) Siderophore-controlled iron assimilation in the enterobacterium *Erwinia chrysanthemi*: evidence for the involvement of bacterioferritin and the Suf iron-sulfur cluster assembly machinery. *J Biol Chem* 283, 36564-36572.

40. Nachin, L., El Hassouni, M., Loiseau, L., Expert, D., and Barras, F. (2001) SoxR-dependent response to oxidative stress and virulence of *Erwinia chrysanthemi*: the key role of SufC, an orphan ABC ATPase. *Mol Microbiol* 39, 960-972.

41. Schwartz, C. J., Giel, J. L., Patschkowski, T., Luther, C., Ruzicka, F. J., Beinert, H., and Kiley, P. J. (2001) IscR, an Fe-S cluster-containing transcription factor, represses expression of *Escherichia coli* genes encoding Fe-S cluster assembly proteins. *Proc Natl Acad Sci U S A* 98, 14895-14900.

42. Giel, J. L., Rodionov, D., Liu, M., Blattner, F. R., and Kiley, P. J. (2006) IscR-dependent gene expression links iron-sulphur cluster assembly to the control of O_2-regulated genes in *Escherichia coli*. *Mol Microbiol* 60, 1058-1075.

43. Lee, K. C., Yeo, W. S., and Roe, J. H. (2008) Oxidant-responsive induction of the *suf* operon, encoding a Fe-S assembly system, through Fur and IscR in *Escherichia coli*. *J Bacteriol* 190, 8244-8247.

44. Yeo, W. S., Lee, J. H., Lee, K. C., and Roe, J. H. (2006) IscR acts as an activator in response to oxidative stress for the *suf* operon encoding Fe-S assembly proteins. *Mol Microbiol* 61, 206-218.

45. Zheng, M., Wang, X., Templeton, L. J., Smulski, D. R., LaRossa, R. A., and Storz, G. (2001) DNA microarray-mediated transcriptional profiling of the *Escherichia coli* response to hydrogen peroxide. *J Bacteriol* 183, 4562-4570.

46. Zheng, M., Aslund, F., and Storz, G. (1998) Activation of the OxyR transcription factor by reversible disulfide bond formation. *Science* 279, 1718-1721.

47. Chandramouli, K., and Johnson, M. K. (2006) HscA and HscB stimulate [2Fe-2S] cluster transfer from IscU to apoferredoxin in an ATP-dependent reaction. *Biochemistry* 45, 11087-11095.

48. Kim, J. H., Tonelli, M., Frederick, R. O., Chow, D. C., and Markley, J. L. (2012) Specialized Hsp70 chaperone (HscA) binds preferentially to the disordered form, whereas J-protein (HscB) binds preferentially to the structured form of the iron-sulfur cluster scaffold protein (IscU). *J Biol Chem* 287, 31406-31413.

49. Silberg, J. J., Tapley, T. L., Hoff, K. G., and Vickery, L. E. (2004) Regulation of the HscA ATPase reaction cycle by the co-chaperone HscB and the iron-sulfur cluster assembly protein IscU. *J Biol Chem* 279, 53924-53931.

50. Sendra, M., Ollagnier de Choudens, S., Lascoux, D., Sanakis, Y., and Fontecave, M. (2007) The SUF iron-sulfur cluster biosynthetic machinery: sulfur transfer from the SUFS-SUFE complex to SUFA. *FEBS Lett* 581, 1362-1368.

51. Layer, G., Gaddam, S. A., Ayala-Castro, C. N., Ollagnier-de Choudens, S., Lascoux, D., Fontecave, M., and Outten, F. W. (2007) SufE transfers sulfur from SufS to SufB for iron-sulfur cluster assembly. *J Biol Chem* 282, 13342-13350.

52. Loiseau, L., Ollagnier-de-Choudens, S., Nachin, L., Fontecave, M., and Barras, F. (2003) Biogenesis of Fe-S cluster by the bacterial Suf system: SufS and SufE form a new type of cysteine desulfurase. *J Biol Chem* 278, 38352-38359.

53. Ollagnier-de-Choudens, S., Lascoux, D., Loiseau, L., Barras, F., Forest, E., and Fontecave, M. (2003) Mechanistic studies of the SufS-SufE cysteine desulfurase: evidence for sulfur transfer from SufS to SufE. *FEBS Lett* 555, 263-267.

54. Outten, F. W., Wood, M. J., Munoz, F. M., and Storz, G. (2003) The SufE protein and the SufBCD complex enhance SufS cysteine desulfurase activity as part of a sulfur transfer pathway for Fe-S cluster assembly in *Escherichia coli*. *J Biol Chem* 278, 45713-45719.

55. Dai, Y., and Outten, F. W. (2012) The *E. coli* SufS-SufE sulfur transfer system is more resistant to oxidative stress than IscS-IscU. *FEBS Lett* 586, 4016-4022.

56. Selbach, B. P., Pradhan, P. K., and Dos Santos, P. C. (2013) Protected sulfur transfer reactions by the *Escherichia coli* Suf system. *Biochemistry* 52, 4089-4096.

57. Lima, C. D. (2002) Analysis of the *E. coli* NifS CsdB protein at 2.0 A reveals the structural basis for perselenide and persulfide intermediate formation. *J Mol Biol* 315, 1199-1208.

58. Gupta, V., Sendra, M., Naik, S. G., Chahal, H. K., Huynh, B. H., Outten, F. W., Fontecave, M., and Ollagnier de Choudens, S. (2009) Native *Escherichia coli* SufA,

coexpressed with SufBCDSE, purifies as a [2Fe-2S] protein and acts as an Fe-S transporter to Fe-S target enzymes. *J Am Chem Soc* 131, 6149-6153.

59. Ollagnier-de Choudens, S., Nachin, L., Sanakis, Y., Loiseau, L., Barras, F., and Fontecave, M. (2003) SufA from *Erwinia chrysanthemi*. Characterization of a scaffold protein required for iron-sulfur cluster assembly. *J Biol Chem* 278, 17993-18001.

60. Wollers, S., Layer, G., Garcia-Serres, R., Signor, L., Clemancey, M., Latour, J. M., Fontecave, M., and Ollagnier de Choudens, S. (2010) Iron-sulfur (Fe-S) cluster assembly: the SufBCD complex is a new type of Fe-S scaffold with a flavin redox cofactor. *J Biol Chem* 285, 23331-23341.

61. Saini, A., Mapolelo, D. T., Chahal, H. K., Johnson, M. K., and Outten, F. W. (2010) SufD and SufC ATPase activity are required for iron acquisition during *in vivo* Fe-S cluster formation on SufB. *Biochemistry* 49, 9402-9412.

62. Blanc, B., Clemancey, M., Latour, J. M., Fontecave, M., and Ollagnier de Choudens, S. (2014) Molecular investigation of iron-sulfur cluster assembly scaffolds under stress. *Biochemistry* 53, 7867-7869.

63. Wada, K., Sumi, N., Nagai, R., Iwasaki, K., Sato, T., Suzuki, K., Hasegawa, Y., Kitaoka, S., Minami, Y., Outten, F. W., Takahashi, Y., and Fukuyama, K. (2009) Molecular dynamism of Fe-S cluster biosynthesis implicated by the structure of the $SufC_2$-$SufD_2$ complex. *J Mol Biol* 387, 245-258.

64. Tian, T., He, H., and Liu, X. Q. (2013) The SufBCD protein complex is the scaffold for iron-sulfur cluster assembly in *Thermus thermophilus* HB8. *Biochem Biophys Res Commun* 443, 376-381.

65. Rees, D. C., Johnson, E., and Lewinson, O. (2009) ABC transporters: the power to change. *Nat Rev Mol Cell Biol* 10, 218-227.

66. Kitaoka, S., Wada, K., Hasegawa, Y., Minami, Y., Fukuyama, K., and Takahashi, Y. (2006) Crystal structure of *Escherichia coli* SufC, an ABC-type ATPase component of the SUF iron-sulfur cluster assembly machinery. *FEBS Lett* 580, 137-143.

67. Jones, P. M., and George, A. M. (2012) Role of the D-loops in allosteric control of ATP hydrolysis in an ABC transporter. *J Phys Chem A* 116, 3004-3013.

68. Watanabe, S., Kita, A., and Miki, K. (2005) Crystal structure of atypical cytoplasmic ABC-ATPase SufC from *Thermus thermophilus* HB8. *J Mol Biol* 353, 1043-1054.

69. Eccleston, J. F., Petrovic, A., Davis, C. T., Rangachari, K., and Wilson, R. J. (2006) The kinetic mechanism of the SufC ATPase: the cleavage step is accelerated by SufB. *J Biol Chem* 281, 8371-8378.

70. Korkhov, V. M., Mireku, S. A., and Locher, K. P. (2012) Structure of AMP-PNP-bound vitamin B12 transporter BtuCD-F. *Nature* 490, 367-372.

71. Petrovic, A., Davis, C. T., Rangachari, K., Clough, B., Wilson, R. J., and Eccleston, J. F. (2008) Hydrodynamic characterization of the SufBC and SufCD complexes and their interaction with fluorescent adenosine nucleotides. *Protein Sci* 17, 1264-1274.

72. Huet, G., Castaing, J. P., Fournier, D., Daffe, M., and Saves, I. (2006) Protein splicing of SufB is crucial for the functionality of the *Mycobacterium tuberculosis* SUF machinery. *J Bacteriol* 188, 3412-3414.

CHAPTER 2

Suf protein-protein interactions *in vitro* and *in vivo*

Abstract

Multiple recombinant SufBCD complexes have been isolated from *E. coli*. $SufBC_2D$, $SufB_2C_2$, and $SufC_2D_2$ have in common the presence of two SufC subunits that participate in ATP binding and hydrolysis. There has been considerable characterization of the Fe-S cluster on $SufBC_2D$ and $SufB_2C_2$ scaffold proteins; however, little is known about *in vivo* Suf protein complex assembly. We investigate the effect of nucleotide on SufC complex formation *in vitro* but also study the *in vivo* interactions of the Suf proteins at native levels under normal and H_2O_2 stress conditions. We establish that the addition of nucleotide enhances the interaction between SufC and SufB proteins in the absence of SufD. We confirm the existence of a complex consisting of SufB, SufC, and SufD proteins and also discover SufS and SufE association with SufC *in vivo*.

2.1 Introduction

The Suf pathway consists of six proteins that work together to mobilize iron and sulfide for Fe-S cluster biogenesis. SufS and SufE mobilize sulfide via a cysteine desulfurase mechanism. SufB, SufC, and SufD interact to form a stable $SufBC_2D$ complex. SufA is a carrier protein that transfers intact Fe-S clusters from the $SufBC_2D$ scaffold to target apo-proteins.[1] SufC shares strong sequence and structural homology with the nucleotide binding domain (NBD) of ABC transporters and has been reported to have intrinsic ATPase activity.[2-8] Highly conserved Walker A, Walker B, and ABC signature motifs in SufC contribute to ATP binding and hydrolysis. The Q- and D-loops participate in interactions with partner proteins SufB and SufD and SufC dimer formation, respectively. In many ABC NBDs, a highly conserved Glu residue immediately following the Walker B motif interacts with ATP in the active site and acts as a catalytic base for ATP hydrolysis.[9-11] Nucleotide-free and ADP-bound SufC monomer structures from *E. coli* and *T. thermophilus* HB8 have been resolved.[3, 8] In these structures, the conserved glutamate residue (Glu171 in *E. coli*) is rotated away from the ATP binding site and forms a salt-bridge with Lys152. The crystal structure of *E. coli* $SufC_2D_2$ (Figure 2.1) reveals cleavage of the Glu171-Lys152 salt bridge and rotation of Glu171 towards the ATP-binding pocket.[7] The Q-loop is the putative site of interaction between SufC and partner protein SufD. A dramatic shift of Q-loop residue Gln85 towards the ATP binding site in the $SufC_2D_2$ structure accompanies the Glu171 rotation (Figure 2.2). These changes appear to be controlled by the binding of SufD to SufC. SufB and SufD share sequence homology in the C-terminus α-helical region shown to interact with SufC. SufB is presumed to interact similarly with SufC

A

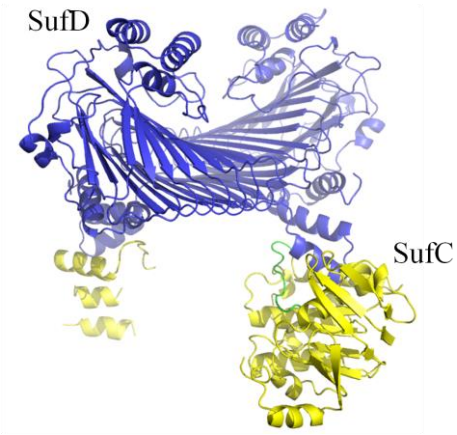

B

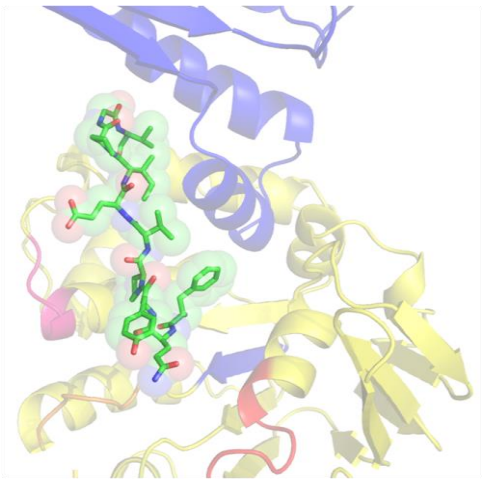

Figure 2.1 (A) *E. coli* $SufC_2D_2$ structure.[7] SufC Q-loop (green) is the proposed binding site for SufD (and SufB). (B) Close-up view of panel A. SufC Q-loop residues (green) interact with C-terminal α-helical region of SufD (blue).

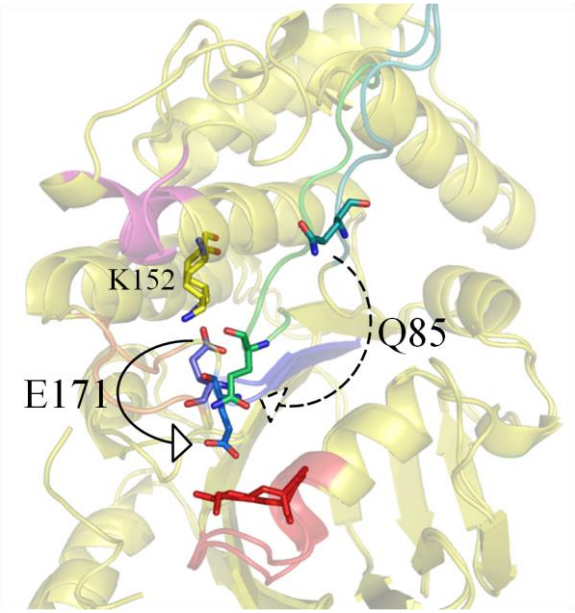

Figure 2.2 Structural alignment of *E. coli* SufC monomer[3] and SufC subunit from $SufC_2D_2$.[7] Walker A (red), Walker B (blue), ABC signature (magenta), D-loop (orange), and Q-loop (green) motifs are colored. Solid arrow indicates Lys152-Glu171 salt bridge cleavage and positional change of Glu171 residue from SufC alone to SufC from $SufC_2D_2$. Dashed arrow indicates positional change of Q-loop Gln85 residue from SufC alone to SufC from $SufC_2D_2$.

The Isc pathway is the main Fe-S cluster assembly system in *E. coli.* Along with the Isc proteins, the *isc* operon encodes molecular chaperones HscA (Heat Shock Cognate A) and HscB (Heat Shock Cognate B).[12] HscA is a Hsp70-type chaperone and characteristically has intrinsic ATPase activity. HscB is an Hsp40-type co-chaperone.[13-16] Molecular chaperones are characterized by their ability to prevent protein aggregation and to facilitate proper folding of denatured proteins into their native conformations.[17] We previously investigated the chaperone-like activity of $SufBC_2D$. We observed that $SufBC_2D$ suppressed the aggregation of rhodanese and the aggregation was further suppressed when ATP was added. However, $SufBC_2D$ could not facilitate the refolding of denatured luciferase (H.K. Chahal and F.W. Outten, unpublished data). At present it is not clear if $SufBC_2D$ plays a role as a molecular chaperone.

In recent studies, Kim et al. reported nucleotide binding allosterically regulates the affinity of the substrate binding domain on HscA for scaffold IscU.[13, 14] Nucleotide binding to HscA modulates its interaction with IscU. This transient interaction is stabilized only when formation of the HscA-IscU complex is necessary for enhanced Fe-S cluster transfer from IscU to target acceptor proteins.[15, 16, 18] SufC is not a direct homologue of HscA, but we propose a similar role of SufC ATP binding in the coordination of Suf protein-protein interactions. Such a role of the SufC ATPase cycle could be associated with the stabilization or dissociation of a Suf multi-protein complex. In this study, we find that an unstable interaction between SufC and His_6-SufB is stabilized in the presence of ATP or ADP. This suggests nucleotide binding causes structural rearrangements in SufC and/or SufB to enhance the interaction. The structural shifts observed in the crystal structure of $SufC_2D_2$ indicate the changes in SufC caused by

the binding of its partner protein SufD (Figure 2.2). A dramatic shift in Q-loop residue Gln85 towards the nucleotide binding site suggests nucleotide binding to SufC could communicate with SufD (SufB) via the Q-loop, thus also generating structural changes in SufD. In this study, we explore the effect of nucleotide on Suf interactions *in vitro*. We also construct an *E. coli* strain with a polyhistidine tag sequence encoded at the C-terminus of *sufC* in the *suf* operon on the chromosome. Chromosomally encoded $SufC_{His}$ is isolated from normal and H_2O_2 stressed cells to investigate *in vivo* Suf interactions at native Suf levels and endogenous ATP and ADP concentrations. Results support previously reported *in vivo* interactions of SufC with SufB and SufD.[4, 5, 19]

2.2 Materials and Methods

Strains, growth conditions, and protein purification of recombinant Suf proteins. The pETDuet-1 (Novagen) vector containing only *sufBC* genes was used to over-express His_6-SufBC in *E. coli* BL21 (DE3) strain. 2 L cultures were grown in LB at 37°C to an OD_{600} of 0.7 and induced with 200 µM IPTG. After 18 hour induction at 18°C, cells were harvested and cell pellets frozen at -80°C. His_6-SufBC was purified anaerobically. Cells were resuspended in anaerobic Hisprep buffer A (25 mM Tris, pH 8.0, 300 mM NaCl, 10 mM Imidazole, 10 mM βME) containing 1 mM phenylmethanesulfonyl fluoride (PMSF), followed by anaerobic sonication on ice (power = 50%, pulse on = 5 seconds, pulse off = 20 seconds, total time = 1.5 minutes per 1 L culture) and centrifugation (16,000 x g, 40 minutes, 4°C) to remove cellular debris. Cleared lysate was loaded onto a Hisprep FF (20 mL) (GE Healthcare) column equilibrated with Hisprep buffer A. After 4 column volume washes with 10% Hisprep buffer B (25 mM Tris, pH 8.0, 300 mM

NaCl, 500 mM imidazole, 10 mM βME), bound proteins were eluted stepwise with 25%, 50%, and 100% Hisprep buffer B. His_6-SufBC eluted as a single peak at 25% Hisprep buffer B. Fractions were pooled and concentrated. Note: Keep protein in anaerobic chamber @ 4 ºC until ready to proceed to the 2nd column. SufB will aggregate if left aerobic for too long. Concentrated His_6-SufBC was then loaded onto a HiLoad 16/60 Superdex-200 column equilibrated in aerobic buffer C (25 mM Tris, pH 8.0, 150 mM NaCl, 2 mM DTT). Fractions containing pure His_6-$SufB_2C_2$ were concentrated and stored at -80°C immediately following concentration.

The pBAD/*Myc*-His C vector (Invitrogen) containing the entire *suf* operon under control of an arabinose-inducible promoter was used to over-express *sufABCDSE* in *E. coli* TOP10 strain.[19] 4 L cultures were grown in LB at 37°C to an OD_{600} of 0.5 and induced with 0.2% (w/v) L-arabinose. After 3 hour induction at 37°C, cells were harvested by centrifugation and cell pellets frozen at -80°C. $SufBC_2D$ was purified as described previously.[20]

The over-expression plasmid pET3a (Novagen) expressing *sufC* was transformed into *E. coli* strain BL21(DE3).[20] 2 L cultures were grown in LB at 37°C to an OD_{600} of 0.7 then induced with 1 mM IPTG for 3 hours at 37°C. Cells were harvested and cell pellets frozen at -80°C. For purification, cells were resuspended in cold extract buffer (25 mM Tris-HCl, pH 8.0, 50 mM NaCl, 10 mM βME) containing 1 mM PMSF, lysed via sonication on ice (power = 50%, pulse on = 2 seconds, pulse off = 18 seconds, total time = 1 minutes per 1 L culture), and centrifuged for lysate collection after treatment with 2% streptomycin sulfate. Cleared lysate was loaded onto a HiLoad 16/10 Q Sepharose High Performance column (20 mL) (GE Healthcare) equilibrated with Q

buffer A (25 mM Tris-HCl, pH 8.0, 50 mM NaCl, 4 mM DTT). Fractions containing SufC eluted at 30-45% Q buffer B (25 mM Tris-HCl pH 8.0, 1 M NaCl, 4 mM DTT). SufC fractions were diluted 1:1 with Phenyl buffer A (25 mM Tris-HCl pH 7.5, 100 mM NaCl, 1 M $(NH_4)_2SO_4$, 10 mM βME) and loaded onto a Phenyl FF column (20 mL) (GE Healthcare). Fractions containing SufC eluted at 100% Phenyl buffer B (25 mM Tris-HCl, pH 7.5, 10 mM βME). Fractions were pooled and concentrated then loaded onto a HiLoad 16/60 Superdex-75 column in buffer containing 50 mM Tris-HCl, pH 7.5, 200 mM NaCl, and 4 mM DTT. Fractions with pure SufC were concentrated and stored at -80°C.

SufD was expressed in the pET3a plasmid (Novagen) in BL21(DE3) pLysS strain.[20] 2 L cultures were grown in LB at 37°C to late exponential phase (OD_{600} = 0.7) then induced with 50 μM IPTG at 18°C for 18 hours. Cells were harvested and resuspended in anaerobic extract buffer for anaerobic sonication on ice (sonication conditions same as for His-SufB_2C_2). Cleared lysate was diluted with 3 M ammonium sulfate (2:1) and loaded onto a Phenyl FF column. SufD eluted at 100% Phenyl buffer B. Pooled fractions were diluted with Q buffer A (1:3) and loaded onto a Q Sepharose column. Fractions containing SufD were concentrated and loaded onto an equilibrated HiLoad 16/60 Superdex 200 column. SufD fractions were collected from the center of the peak, concentrated, and stored at -80°C. For all preps, purity was determined by SDS PAGE and protein concentrations were measured by Bradford assay.

Preparation of 100 mM Mg^{2+}-ATP and 100 mM ADP stocks. Dissolve 1.10 g Adenosine 5'-Triphosphate (ATP) disodium salt hydrate (Sigma-Aldrich A7699) in 15 mL MilliQ water. Add 0.41 g $MgCl_2$ and dissolve. Adjust to pH ~7.0 with 3 M NaOH

added dropwise with stirring. Add water to a final volume of 20 mL. Filter the Mg-ATP solution and store in aliquots at -20°C. Mg-ATP stocks are stable at -20°C for six months. Dissolve 42.7 mg Adenosine 5'-Diphosphoate (ADP) sodium salt (Sigma-Aldrich A2754) in 1 mL desired buffer. The pH of the ADP stock solution does not need to be adjusted. ATP and ADP concentrations were determined by absorbance at 259 nm using ε_{259} =15,400 M^{-1} cm^{-1}.

Suf interactions mediated by ATP or ADP monitored by affinity chromatography. 1 mL Histrap column (GE Healthcare) was equilibrated with binding buffer (25 mM Tris-HCl pH 7.5, 300 mM NaCl, 10 mM $MgCl_2$, 10 mM imidazole) containing 0.5 mM ATP or ADP. 300 µg (6 µM) His_6-$SufB_2C_2$ pre-incubated with 1 mM ATP or 1 mM ADP was loaded on the column. The column was then washed with 10 column volumes of binding buffer. His_6-SufB was eluted with buffer containing 300 mM imidazole. To investigate the interaction of $SufC_2D_2$ with His_6-$SufB_2C_2$, 150 µg (3 µM) His_6-$SufB_2C_2$ was incubated with 200 µg pre-mixed SufC (30 µM) and SufD (15 µM) and 1 mM ATP for 5 min at room temperature. The proteins were loaded onto an equilibrated 1 mL Histrap column. The column was washed with 10 mL binding buffer, then His_6-SufB and any interacting proteins were eluted with buffer containing 300 mM imidazole. All wash and elution fractions were collected separately and analyzed by SDS PAGE. For comparison, His_6-$SufB_2C_2$ and His_6-$SufBC_2D$ without nucleotide were loaded, washed, and eluted on a 1 mL Histrap column equilibrated with buffer containing no nucleotide.

Suf interactions with ATP or ADP monitored by size exclusion. Analytical Superdex 200 10/300 column was equilibrated with buffer containing 50 mM Tris-HCl pH 7.5, 100 mM KCl, 5 mM $MgCl_2$, and 1 mM DTT. 1 mM Mg-ATP was added to 50

μM $SufBC_2D$, 30 μM SufC, or 30 μM SufC mixed with 30 μM SufD and incubated at room temperature for 5 minutes prior to loading (in 250 μL). Controls with only $SufBC_2D$ or SufC without nucleotide were also performed for comparison. The apparent molecular weight ($MW_{apparent}$) was calculated from gel filtration standards. All fractions were collected and analyzed by SDS PAGE.

In vitro Fe-S reconstitution. 50 μM $SufBC_2D$ was incubated in an anaerobic glove box (Coy) in 250 μL reconstitution buffer (25 mM Tris, pH 8.0, 100 mM NaCl, 50 mM KCl, 5 mM $MgCl_2$) with 4 mM DTT for 1 hr. 0.2 μM SufS and 0.2 μM SufE were added first and allowed to incubate for 5 minutes prior to addition of 6-fold excess ferrous ammonium sulfate (FAS) and 8-fold excess L-cysteine to initiate the reaction. 1 mM ADP was added immediately after the L-cysteine. $SufBC_2D$ without nucleotide was also reconstituted for comparison. Cluster formation was monitored by UV-Vis during the reconstitution. Reconstituted proteins were purified using a 5 mL HiTrap desalting column (GE Healthcare) in line with an Akta FPLC system. Fractions containing $SufBC_2D$ were collected and concentrated. Iron content and acid-labile sulfide content were determined by a previously reported method.[21, 22]

Enrichment of $SufC_{His}$ and in vivo Suf protein-protein interactions. MG1655*$sufC_{His}sufD$* strain was constructed as described in Appendix A (this study). MG1655*$sufC_{His}sufD$* was grown in 8 L LB at 37°C to an OD_{600} of 0.5 and treated with 300 μM H_2O_2 for 10 minutes prior to harvesting. For normal growth conditions, *$sufC_{His}sufD$* was grown to an OD_{600} of 0.5 and harvested. Cells were washed twice with 1 X TBS (50 mM Tris-HCl, pH 8.0, 150 mM NaCl), resuspended in 20 mL cold extract buffer (50 mM Tris-HCl, pH 8.0, 50 mM NaCl, 2 mM DTT) with 1 mM PMSF, and

lysed via sonication on ice (power = 50%, pulse on = 2 seconds, pulse off = 18 seconds, total time = 1 minutes per 1 L culture). The lysate was collected by spinning at 16,000 x g for 25 min at 4°C. Cleared lysate was loaded onto a HiPrep Q XL 16/10 column (20 mL) (GE Healthcare) in line with a Biologic DuoFlow FPLC system. After a two column volume wash with binding buffer (25 mM Tris-HCl, pH 8.0, 2 mM DTT), $SufC_{His}$ was eluted with an increasing gradient of 0-1 M NaCl. $SufC_{His}$ eluted at 30-70% 1 M NaCl. Pooled fractions were diluted with Hisprep buffer A (25 mM Tris-HCl, pH 8.0, 300 mM NaCl, 2 mM imidazole) and loaded onto a Hisprep FF column (20 mL) (GE Healthcare). After 4 column volume washes with 10% Hisprep buffer B (buffer A + 500 mM imidazole), bound proteins were eluted stepwise with 25%, 50%, and 100% buffer B. $SufC_{His}$ eluted at 25% buffer B. Immunoblots were used to monitor $SufC_{His}$ protein levels in fractions from each column. Fractions containing $SufC_{His}$ were pooled and concentrated in a 50-kDa MWCO filter (Millipore). Proteins not retained in the 50-kDa MWCO filter were further concentrated in a 10-kDa MWCO filter. Concentrated $SufC_{His}$ retained in the 50- or 10-kDa MWCO filter was loaded onto a Superdex-200 or Superdex-75 10/300 column, respectively. Fractions containing $SufC_{His}$ were concentrated and stored at -80°C. Sample purity was determined by SDS PAGE.

To monitor *in vivo* $SufC_{His}$ interactions with added Mg^{2+}-ATP, *sufC*$_{His}$*sufD* cells were prepared and purified as previously described with minor modifications. Briefly, cells were grown in 6 L LB and induced with 300 µM H_2O_2 for 10 minutes. Washed cells were lysed via sonication and loaded onto a Q XL column. Fractions containing $SufC_{His}$ were pooled and split into two equal volumes. The first sample was further purified with no modifications to the procedure. The second sample was treated with 1

mM Mg^{2+}-ATP for 1 hr at 4°C then purified on a Hisprep FF column with 0.200 mM ATP added to all buffers. $SufC_{His}$ fractions were pooled and concentrated in a 50-kDa MWCO filter. Proteins not retained in the 50-kDa MWCO filter were further concentrated in a 10-kDa MWCO filter. Presence of Suf proteins was detected by immunoblot.

Immunoblots. Equal total protein amounts were loaded and separated on a 12% SDS PAGE gel. Proteins were then transferred to a nitrocellulose membrane and blocked overnight with 80% Odyssey blocking buffer (Li-Cor) in 1 X TBS (50 mM Tris-HCl pH 8.0, 150 mM NaCl) at 4°C (α-SufB, α-SufC, α-SufD) or 10% BlkHenII buffer (Avēs) in MilliQ H_2O at room temperature with shaking (α-SufS, α-SufE). Primary antibody incubations with α-SufB (1:3000), α-SufC (1:3000), or α-SufD (1:5000) (rabbit, polyclonal) were performed in 40% blocking buffer in 1 X TBST (TBS + 0.001% Tween-20). α-SufS (1:5000) or α-SufE (1:3000) (chicken, polyclonal) incubations were performed in 1 X TBST only. After 2 hours incubation at room temperature with shaking, membranes were washed 5 times (10 min each) with copious amounts of 1 X TBST. Then, α-SufB, α-SufC, and α-SufD probed membranes were incubated with goat α-rabbit secondary antibody (1:20,000) at room temperature with shaking for 45 min. The α-SufS and α-SufE probed membranes were incubated with donkey α-chicken secondary antibody (1:20,000). Membranes were washed with 1 X TBS and scanned using an Odyssey Infrared Imager (Li-Cor).

2.3 Results

SufC does not undergo nucleotide-induced dimerization in the absence of partner proteins SufB and/ or SufD. SufC shares homology with the ATPase component of ABC transporters. SufC has the intrinsic ability to hydrolyze ATP and its ATPase activity has been well characterized in *Thermotoga maritima*, *Plasmodium falciparum*, and *Erwinia chrysanthemi*.[2, 4-6, 23] ABC-ATPases form a dimer as a catalytic step for ATP hydrolysis. This nucleotide-induced dimerization is transient and difficult to capture under most *in vitro* experimental conditions. Over-expressed recombinant SufC from *E. coli* exists as a monomer in solution. We investigated the possible nucleotide-induced dimerization of SufC using size exclusion chromatography (Figure 2.3). SufC was incubated with 2 mM Mg-ATP for 5 min prior to separation on a size exclusion column. Elution of SufC was monitored by absorbance at 280 nm. SufC alone had an apparent molecular weight of 31.2 ± 2.4 kDa. SufC with Mg-ATP had a similar apparent molecular weight, 31.7 kDa. Our data is consistent with the presence of a monomeric species in solution even in the presence of nucleotide. This result, similar to the observed behavior of SufC from *T. maritima*[2], suggests either SufC does not form a dimer in the presence of nucleotide or SufC forms a transient dimer that could not be isolated under our experimental conditions. Disulfide cross-linking and native PAGE analysis data showed that SufC does form a dimer in the presence of Mg-ATP when it is in a complex with SufD.[7] Nucleotide-induced dimerization of SufC may be specific to SufC bound in a complex with partner protein. In this study, we investigated nucleotide-induced structural changes of SufC as a part of His_6-$SufB_2C_2$, $SufC_2D_2$, and $SufBC_2D$ complexes.

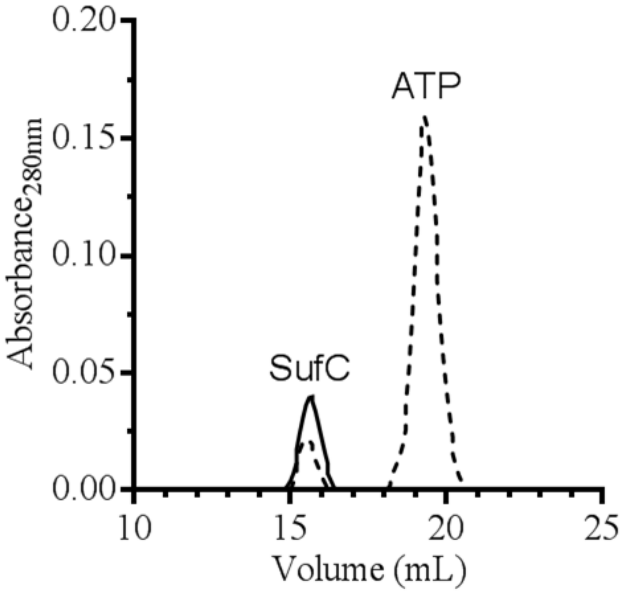

Figure 2.3 Size exclusion analysis of as-purified SufC in the presence of 2 mM Mg-ATP (dashed). SufC without Mg-ATP was run for comparison (solid).

SufC association with His_6-SufB and SufD is enhanced by ATP or ADP in the His_6-$SufB_2C_2$ and $SufC_2D_2$ complexes. A His_6-$SufB_2C_2$ complex can be isolated if *sufB* and *sufC* are co-expressed in-trans.[24] His-tagged SufB was used because native SufB aggregates and is difficult to purify in a soluble form.[2] His_6-$SufB_2C_2$ is somewhat unstable, as determined by the observed dissociation of SufC during size exclusion chromatography (Figure 2.4A). Study of the kinetic mechanism for *T. maritima* SufC ATPase reports the presence of SufB enhances the interaction of SufC with fluorescently tagged analogues mantATP and mantADP.[2, 6, 23] The enhanced binding event provides evidence that a structural change must occur in SufC to better accommodate the nucleotide. We used affinity chromatography to test if changes in SufC mediated by the presence of nucleotide could stabilize the interaction between SufC and His_6-SufB. We observed that when as-isolated His_6-$SufB_2C_2$ was loaded onto a Histrap column without nucleotide, untagged SufC almost completely dissociated from His_6-SufB. When repeated with 1mM ATP or 1mM ADP added to His_6-$SufB_2C_2$ (with 0.5 mM ATP or ADP in the column buffers), SufC was retained on the column and co-eluted with His_6-SufB (Figure 2.4B). His_6-$SufBC_2D$ was also tested. We observed that both SufC and SufD remained tightly associated with His_6-SufB even without nucleotide (data not shown). His_6-$SufB_2C_2$ seems to be a transient complex that is relevant for Suf function but is only maintained if SufC can access nucleotide.

SufC and SufD also interact to form a $SufC_2D_2$ complex.[7, 23, 25] We investigated the potential nucleotide-enhanced interaction of SufC and SufD (both untagged) using size exclusion chromatography. The theoretical molecular weight for the $SufC_2D_2$ complex is 142 kDa. When SufC and SufD are mixed without nucleotide, the elution

A

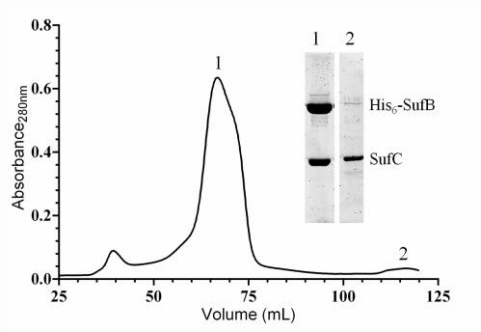

B

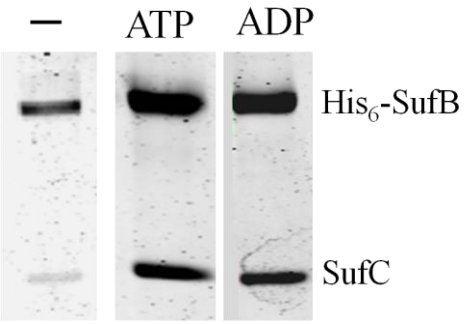

Figure 2.4 (A) Superdex 200 size exclusion elution profile of as-purified His_6-$SufB_2C_2$. *Inset*, SDS PAGE of fractions collected from peak 1 (His_6-$SufB_2C_2$) and peak 2 (SufC). (B) SDS PAGE of elution fractions from His_6-$SufB_2C_2$ interaction studies. Purified His_6-$SufB_2C_2$ (-) or His_6-$SufB_2C_2$ pre-incubated with 1mM ATP or ADP was loaded onto a 1 mL Histrap column equilibrated with buffer only or buffer containing 0.5 mM ATP or ADP, respectively. Proteins interacting with His_6-SufB co-elute with buffer containing 300 mM imidazole.

profile shows a broad peak at a volume consistent with the molecular weight of a newly formed $SufC_2D_2$ complex ($MW_{apparent}$ = 130.8 kDa). When 1 mM Mg-ATP is added to pre-mixed SufC and SufD, we observed sharpening of the $SufC_2D_2$ peak (144.7 kDa) and the presence of a shoulder off of the main peak at a $MW_{apparent}$ consistent with a SufD dimer (82.9 kDa) (Figure 2.5). The altered elution profile suggests the formation of a complex that migrates more tightly as a single species in the presence of nucleotide; however, a more sensitive technique should be used for confirmation.

Protein interactions in $SufBC_2D$ are not altered by Mg-ATP. $SufBC_2D$ is the most stable complex isolated from cells over-expressing the entire *suf* operon.[20] $SufB_2C_2$ and $SufC_2D_2$ complexes can also be isolated from cells over-expressing *sufBC* and *sufCD* genes, respectively. We tested if the addition of Mg-ATP to $SufBC_2D$ would disrupt protein-protein interactions within the $SufBC_2D$ complex and convert into complexes containing only SufBC or SufCD proteins. Size exclusion analysis indicated $SufBC_2D$ (165.6 kDa) and $SufBC_2D$-Mg-ATP (177.5 kDa) eluted as a single symmetrical peak and have similar apparent molecular weights (Figure 2.6). The results confirm $SufBC_2D$ is a stable complex that does not undergo nucleotide-induced dissociation into SufBC and/or SufCD complexes.

We also wanted to investigate if the $SufB_2C_2$ and $SufC_2D_2$ complexes were formed as a precursor to the ultimate $SufBC_2D$ complex. We tested the possibility of ATP mediating these shifts in protein complex conformations by repeating the 1 mL Histrap ATP interaction studies with His_6-$SufB_2C_2$ and adding untagged SufC and SufD pre-mixed to form a $SufC_2D_2$ complex (confirmed by size exclusion chromatography). As-purified His_6-$SufB_2C_2$ was added to pre-assembled $SufC_2D_2$ then incubated with 1

mM Mg-ATP prior to loading on the Histrap column. His_6-SufB still only eluted with SufC bound. The pre-assembled $SufC_2D_2$ was not retained on the column (Figure 2.7). The results confirmed ATP stabilizes the His_6-$SufB_2C_2$ and $SufC_2D_2$ complexes, but the lack of SufD association with His_6-SufB revealed ATP does not cause conversion of the His_6-$SufB_2C_2$ and $SufC_2D_2$ complexes to $SufBC_2D$.

ADP decreases rate of Fe-S cluster reconstitution on $SufBC_2D$. Conformational changes in HscA caused by ATP binding and hydrolysis contributes to HscA's transient interaction with co-chaperone HscB and Fe-S scaffold protein IscU.[15, 16] HscA and HscB are required for enhanced Fe-S cluster transfer from IscU to target proteins *in vivo*. The rate of cluster transfer is significantly stimulated in the presence of Mg-ATP.[18] The $SufBC_2D$ protein complex has been identified as the scaffold for cluster assembly in *E. coli* and *T. thermophilus* HB8.[26-28] Both $SufBC_2D$ and $SufB_2C_2$ can assemble a [4Fe-4S] cluster *in vitro* and donate the intact cluster to SufA. We previously tested the effect of Mg-ATP on Fe-S cluster transfer from $SufBC_2D$ and His_6-$SufB_2C_2$ complexes to carrier protein SufA. The addition of Mg-ATP did not enhance cluster transfer but rather slightly inhibited the rate of cluster transfer from both complexes.[27] These results revealed the ATPase cycle of SufC contributes to a different role than Fe-S cluster transfer enhancement in the Suf pathway.

In this study, we tested the effect of nucleotide on $SufBC_2D$ Fe-S cluster reconstitution *in vitro*. It was previously reported that the presence of ATP during reconstitution does not alter the type or amount of cluster reconstituted on $SufBC_2D$.[25] We monitored the rate of Fe-S cluster reconstitution of $SufBC_2D$ in the presence of ADP. We observed a 37.9 ± 4.1% decrease in rate of cluster formation in the presence of ADP

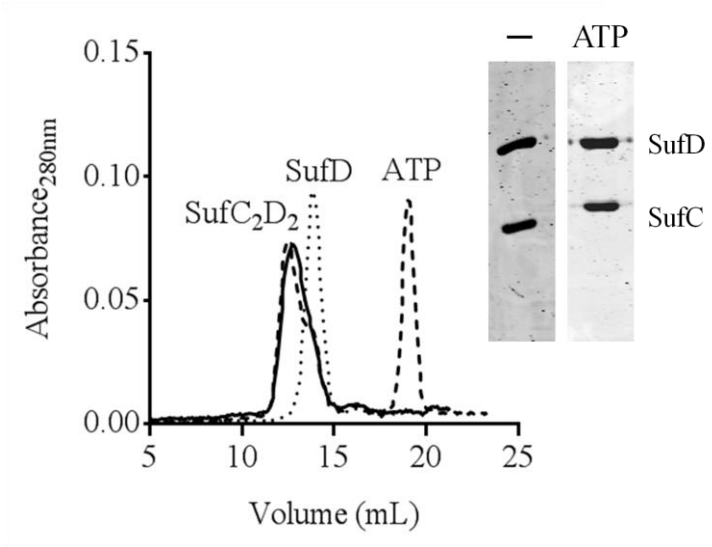

Figure 2.5 Formation of $SufC_2D_2$ complex by mixing equimolar amounts of SufC and SufD without (solid) or with (dashed) 1 mM ATP. SufD with 1 mM ATP was run for comparison (dotted). *Inset*, SDS PAGE of fractions collected from the $SufC_2D_2$ peak.

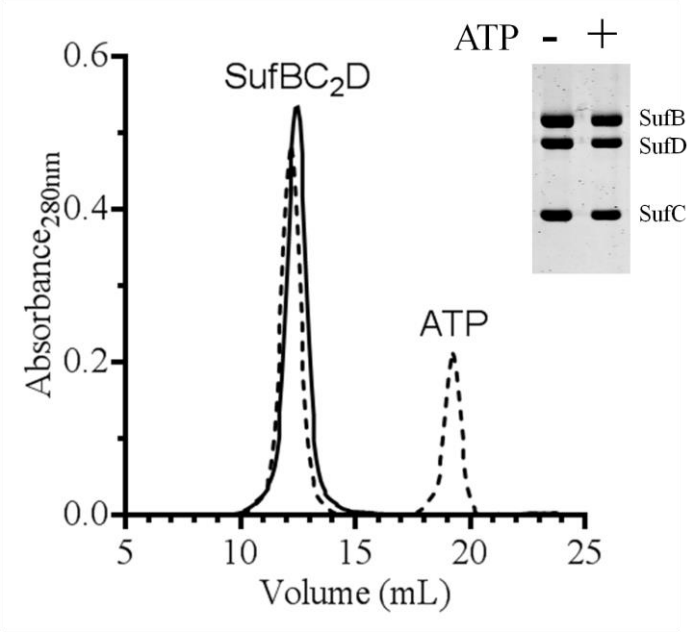

Figure 2.6 Size exclusion analysis of as-purified $SufBC_2D$ pre-incubated with 2 mM Mg-ATP (dashed). $SufBC_2D$ without Mg-ATP was run for comparison (solid). *Inset*, SDS PAGE of fractions collected from the $SufBC_2D$ peak.

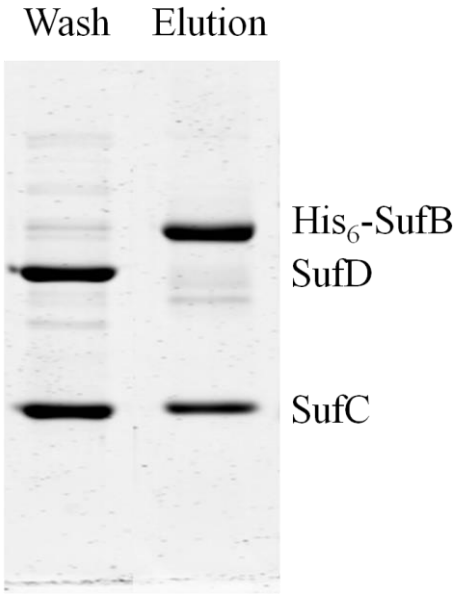

Figure 2.7 His_6-$SufB_2C_2$ interaction with $SufC_2D_2$ in the presence of 1 mM ATP. His_6-$SufB_2C_2$ with 1 mM ATP was bound to a 1 mL Histrap column. Equimolar pre-formed $SufC_2D_2$ with 1 mM ATP was passed over the column. Equal volumes of wash (lane 1) and elution (lane 2) fractions were analyzed for protein content by SDS PAGE.

compared to without nucleotide (Figure 2.8). The observed decrease in rate could be the result of structural changes in $SufBC_2D$ that make SufB less available for Fe-S cluster assembly. The most common cluster binding sites in proteins are cysteine residues. SufB has 13 cysteine residues. The residues involved in cluster binding on SufB have not been identified. The observed decrease in Fe-S cluster reconstitution as a result of ADP binding suggests a structural difference in the $SufBC_2D$-ADP complex that may be significant in elucidating the $SufBC_2D$ mechanism of Fe-S cluster assembly.

$SufC_{His}$ forms a stable complex with partner proteins SufB and SufD in vivo. A stable $SufBC_2D$ complex can be isolated from cells over-expressing the entire *suf* operon.[19, 20] His_6-SufB isolated from cells co-expressing *sufBCDSE* interacts with SufC and SufD as two distinct complexes: His_6-$SufBC_2D$ and His_6-$SufB_2C_2$.[24] A $SufC_2D_2$ complex can be isolated from cells co-expressing *sufCD*.[7, 23] We used the newly constructed *$sufC_{His}$sufD* strain (this study) to isolate chromosomally expressed SufC bound to SufB and SufD *in vivo* at native Suf protein levels from normal and H_2O_2 treated cells.

Intracellular levels of Suf proteins are low. Isolating enough of the Suf proteins to detect *in vivo* protein-protein interactions required an enrichment technique. We engineered a polyhistidine tag at the C-terminus of *sufC* on the *E. coli* chromosome (MG1655*$sufC_{His}$sufD* strain). Because SufC contained a polyhistidine tag, we initially attempted a one-step purification on the Hisprep FF column. $SufC_{His}$ purity was poor due to low intracellular levels of Suf and a number of contaminating *E. coli* proteins with affinity for the nickel resin (data not shown).[29] Recombinant SufC is initially isolated from cellular lysate on a strong anion exchange column.[20] SufC binds tightly to the Q

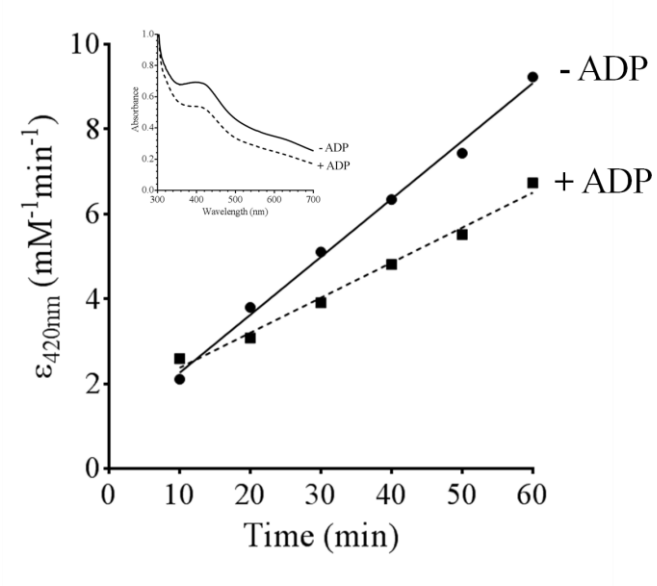

Figure 2.8 Representative data of Fe-S cluster reconstitution on $SufBC_2D$ with and without ADP. The rate of reconstitution was measured by monitoring absorbance at 420 nm over time. *Inset*, UV-Vis spectra of Fe-S cluster reconstituted on $SufBC_2D$ after 1 hour. The feature at 420 nm is indicative of a [4Fe-4S] cluster.

Sepharose column at pH 8.0. Taking this into account, we used a HiPrep Q XL 16/10 column as the initial enrichment step for $SufC_{His}$ prior to affinity chromatography on the Hisprep column (Figure 2.9). Addition of the anion exchange step helped reduce the amount of proteins nonspecifically binding the nickel resin (determined by SDS PAGE).

The theoretical molecular weight of monomeric $SufC_{His}$ is ~32 kDa. Upon binding SufB and/or SufD, the complex is larger than 50 kDa. To determine if $SufC_{His}$ always interacts with partner proteins SufB and SufD *in vivo*, we used a 50-kDa MWCO filter to separate the complexes from $SufC_{His}$ monomer. Suf levels were enriched enough in the H_2O_2 stressed sample to visualize $SufC_{His}$ and interacting partner proteins by SDS PAGE after the affinity column step (Figure 2.10A). Using this approach, we observed that SufB and SufD co-purify with $SufC_{His}$ isolated from normal cells as well as from cells treated with 300 μM H_2O_2. Immunoblots confirmed the interaction of $SufC_{His}$ with SufB and SufD (Figure 2.10B) Results were consistent with previous yeast-two hybrid, β-galactosidase activity, and pull-down studies reporting *in vivo* interactions between SufC and SufB and SufD.[4, 5] Further analysis of the sample by size exclusion chromatography revealed $SufC_{His}$ migrates as a single peak with SufB and SufD. The experimental molecular weight ($MW_{apparent}$) was 177.2 kDa, comparable to recombinant $SufBC_2D$ ($MW_{apparent}$ = 172 kDa).[19] $SufC_{His}$ interacts tightly with predominantly SufB and SufD *in vivo* during H_2O_2 stress (Figure 2.11).

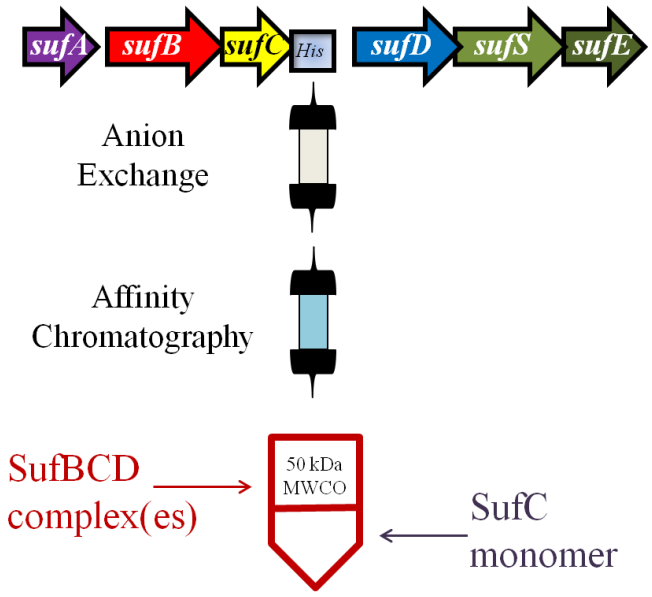

Figure 2.9 Scheme for enrichment of chromosomally encoded $SufC_{His}$.

$SufC_{His}$ interacts with SufS and SufE in vivo in normal cells. Suf levels were not as enriched in the sample from normal cells, making elution of Suf complexes by size exclusion chromatography difficult to monitor by simple absorbance at 280 nm. Instead, fractions containing $SufC_{His}$ were determined by immunoblot. Concentrated fractions containing $SufC_{His}$ analyzed by SDS PAGE revealed $SufC_{His}$ was not in a pure complex with only SufB and SufD (Figure 2.12A). The additional bands could be proteins that specifically bind $SufC_{His}$ or they could be the product of low Suf protein levels. Some of the SDS PAGE bands migrated at molecular weights similar to other Suf proteins. The presence of co-eluting Suf proteins was investigated by immunoblot detection (Figure 2.12B). As observed in the H_2O_2 treated cells, partner proteins SufB and SufD interact with $SufC_{His}$ in normal growth conditions. Interestingly, sulfur mobilization proteins SufS and SufE were also detectable. It was previously reported that SufE preferentially binds SufB when it is in complex with SufC *in vitro*.[20] We report a possible *in vivo* Suf multi-protein complex containing SufB, SufC, SufD, SufS, and SufE proteins. Chahal et al. reported SufA preferentially binds Fe-S cluster bound $SufBC_2D$ *in vitro*.[26] The presence of SufA was not determined because α-SufA antibodies were not available. Additional bands were not further identified by mass spectrometry.

$SufC_{His}$ and SufD are not solely in complex with SufB. Any isolated $SufC_{His}$ not retained in the 50-kDa MWCO filter was collected and concentrated in a 10-kDa MWCO filter. A new finding as a result of this approach was that $SufC_{His}$ monomer is also present in normal and H_2O_2 stressed cells (Figure 2.13). The data suggests SufC may have a function in the Suf pathway separate from its function when it interacts with SufB and SufD. Another interesting finding was the presence of SufD retrieved in the 10-kDa

MWCO filter. Previous reports reveal SufD is a homo-dimer in solution.[30] If SufD were interacting with SufC as a $SufC_{His}D$ heterodimer, the theoretical molecular weight of this complex is ~79 kDa and would be retained in the 50-kDa MWCO filter. It seems SufD once interacted with $SufC_{His}$ (allowing it to be retained on the Hisprep column) but subsequently dissociated from $SufC_{His}$ during subsequent purification and concentration. Native SufD does not nonspecifically bind the nickel resin based on the fact that recombinant SufD did not bind the Histrap column in the previously described His_6-$SufB_2C_2$ interaction studies. It is also possible that $SufC_{His}$ and SufD dissociated from SufB as an artifact of the purification process, although this seems unlikely because recombinant $SufBC_2D$ is a stable complex (this study). The presence of SufB unassociated with $SufC_{His}$ could not be determined because the molecular weight of SufB is larger than 50 kDa and thus SufB was retained in the 50-kDa filter with the $SufBC_{His}D$ complexes.

Previous *in vitro* ATP interaction studies with the SufBCD proteins revealed nucleotide-induced stabilization of His_6-$SufB_2C_2$ and $SufC_2D_2$ complexes (Figures 2.4B and 2.5). We added Mg^{2+}-ATP to an enriched sample of Suf proteins from H_2O_2 stressed cells to test if the observed $SufC_{His}$ monomer was an artifact of the dilution of any endogenous nucleotide during the purification process. Based on our *in vitro* studies, ATP addition should enhance the interaction of $SufC_{His}$ with partner proteins SufB and SufD. ATP was added after the anion exchange step to minimize the number of other proteins that may utilize ATP. After 1 hour incubation at 4°C, $SufC_{His}$ was further purified by affinity chromatography and separated into $SufBC_{His}D$ complexes (50-kDa MWCO filter) and $SufC_{His}$ monomer (10-kDa MWCO filter). Antibodies against SufC

and SufD were used to detect $SufC_{His}$ and SufD protein levels, and the integrated intensity of each band was determined (Table 2.1). Immunoblots of $SufC_{His}$ and SufD protein levels revealed slightly diminished SufD protein levels retained in the 10-kDa filter from the fractions incubated with ATP compared to without ATP (Figure 2.14). The ratio of SufD retained in the 50 kDa filter to the 10 kDa filter (50/10) was 6.07 in the sample incubated with Mg-ATP compared to 3.75 in the sample not treated with Mg-ATP. The results revealed more SufD was retained in the 50-kDa filter in the presence of nucleotide. The 50/10 ratios for $SufC_{His}$ with or without added Mg-ATP were similar (3.42 and 2.72, respectively). The $SufC_{His}$ retained in the 10-kDa MWCO filter does not appear to be an artifact of the purification process. $SufC_{His}$ could be a monomer that has a separate function from $SufC_{His}$ associated with the $SufBC_{His}D$ complexes or $SufC_{His}$ could interact with an unknown protein as a stable complex smaller than 50 kDa. Previous cross-linking and label transfer studies revealed strong interactions between SufA and SufC *in vitro*. The extent of label transfer from SufA to SufC was weakened when SufC was a part of the very stable $SufBC_2D$ complex, suggesting a disrupted interaction between SufA and SufC.[26] The purpose of this SufA-SufC interaction was not explored. Presence of SufA interaction with $SufC_{His}$ could not be observed because α-SufA antibodies were not available.

2.4 Discussion

Previous structural and kinetics studies emphasize the role of partner proteins SufB and SufD on SufC ATPase activity.[2, 6, 7, 23] Structural rearrangements of conserved motifs in SufC occur upon partner protein binding that enhance ATP binding and

A

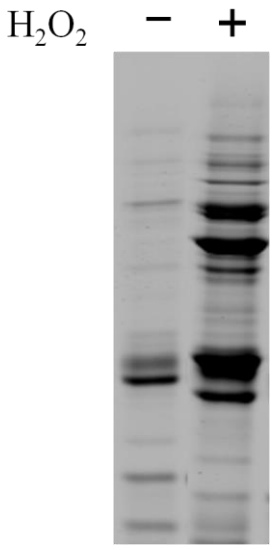

B

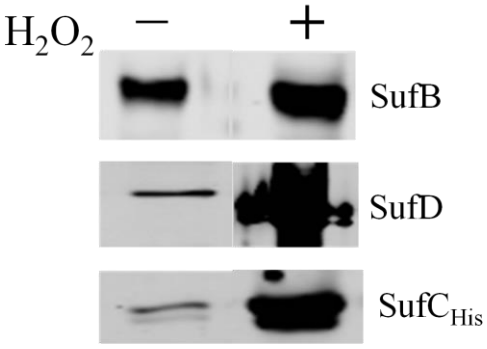

Figure 2.10 (A) SDS PAGE of $SufC_{His}$ and co-eluting proteins after two-column enrichment. (B) Immunoblots of SufB (top), SufD (middle), and SufC (bottom) protein levels in samples isolated from normal (lane 1) or H_2O_2 stressed (lane 2) cells. $SufC_{His}$ containing protein complexes were retained in a 50-kDa MWCO filter during concentration.

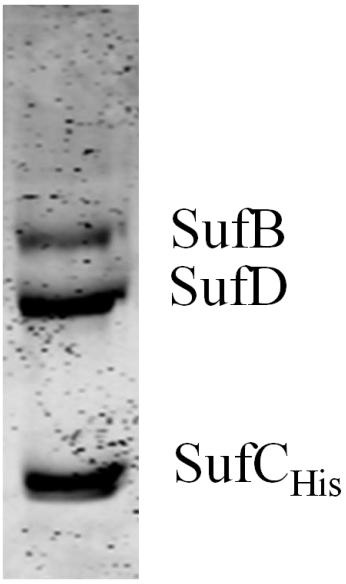

Figure 2.11 SufC$_{His}$ interacts with SufB and SufD to form a stable SufBCD complex *in vivo*. SufC$_{His}$ fractions from the size exclusion column were visualized by SDS PAGE. SufC$_{His}$ was isolated from H_2O_2 stressed cells.

A

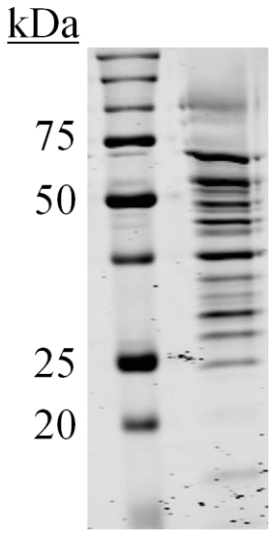

B

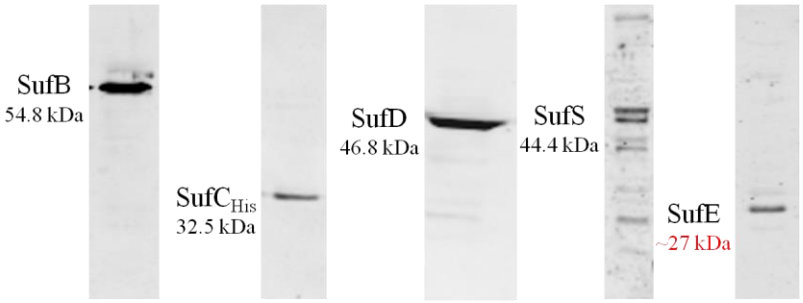

Figure 2.12 (A) SDS PAGE of fractions containing $SufC_{His}$ collected from size exclusion column. (B) Immunoblots of SufB, SufC, SufD, SufS, and SufE proteins using respective α-Suf antibodies. Proteins isolated from cells grown under normal conditions.

A

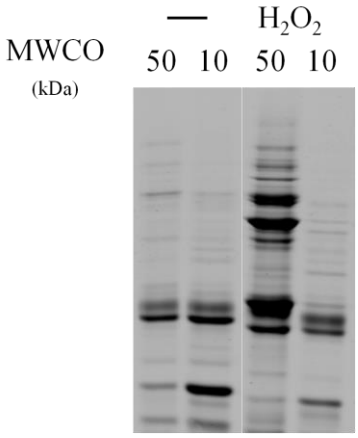

B

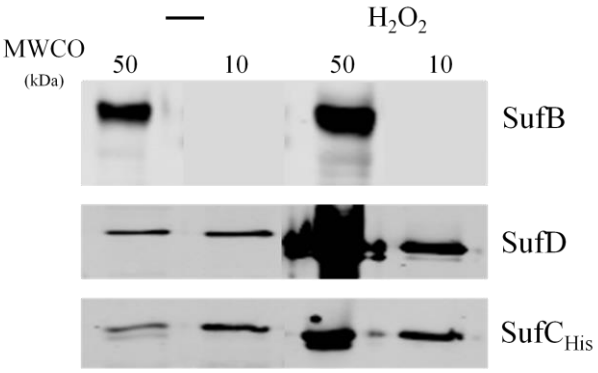

Figure 2.13 (A) SDS PAGE of $SufC_{His}$ and co-eluting proteins after two-column enrichment. (B) Immunoblots of SufB (top), SufD (middle), and SufC (bottom) protein levels in $SufC_{His}$ samples isolated from normal (lanes 1-2) or H_2O_2 stressed (lanes 3-4) cells. $SufC_{His}$ protein complexes were retained in a 50-kDa MWCO filter during concentration (lanes 1 and 3). $SufC_{His}$ monomer was collected and concentrated in a 10-kDa MWCO filter (lanes 2 and 4).

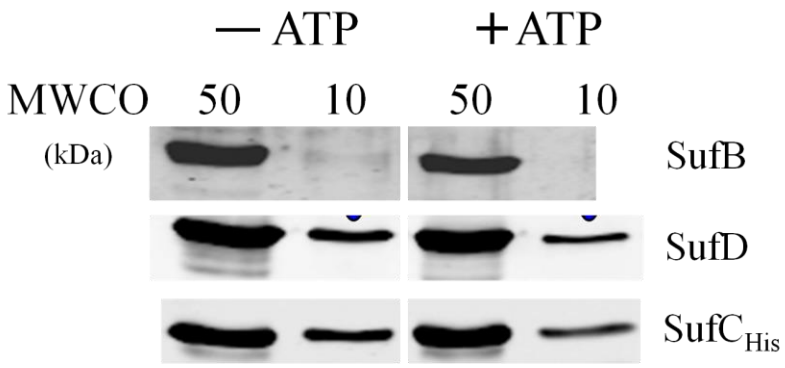

Figure 2.14 Effect of ATP on $SufC_{His}$ complex formation. $SufC_{His}$ isolated from cells stressed with 300 µM H_2O_2. Fractions from anion exchange column were split and purified (left) or treated with exogenous ATP prior to subsequent purification (right). $SufC_{His}$ protein complexes were retained in a 50-kDa MWCO filter (lanes 1 and 3). $SufC_{His}$ monomer was collected in a 10-kDa MWCO filter (lanes 2 and 4). Immunoblots of $SufC_{His}$ and co-eluting SufB and SufD after two-column enrichment.

Table 2.1 $SufC_{His}$ and SufD protein levels in presence of Mg-ATP

Protein[a]	ATP[b]	MWCO 50 kDa[c]	MWCO 10 kDa[c]	50:10 Ratio[d]
SufC	-	56.71	20.84	2.72
	+	49.60	14.51	3.42
SufD	-	200.69	53.53	3.75
	+	160.48	26.41	6.07

[a]Proteins eluted from Hisprep column and retained in 50-kDa or 10-kDa MWCO filter. Suf proteins detected by immunoblots. 0.53 mg/ml of total protein loaded in 20 µL. [b]1 mM Mg-ATP added to fractions containing $SufC_{His}$ from anion exchange. [c]Fractions containing $SufC_{His}$ concentrated in 50-kDa- or 10-kDa MWCO filters. [d]Ratio of intensities measured in 50-kDa MWCO to 10-kDa MWCO. Intensities of bands shown in arbitrary units.

hydrolysis in the active site of SufC.[7] In this study, we investigated if nucleotide-induced structural changes in the SufC ATP-binding site are communicated to SufB and SufD in the $SufB_2C_2$, $SufC_2D_2$, and $SufBC_2D$ complexes.

We establish that *E. coli* SufC does not undergo nucleotide-induced dimerization in the absence of SufB and SufD. SufC has been shown to form a dimer in the presence of Mg-ATP in the $SufC_2D_2$ complex.[7] If the mechanism of ATP hydrolysis is similar to the NBDs of ABC transporters, SufC must form a dimer prior to ATP hydrolysis. This dimerization was not observed under our experimental conditions, meaning SufC dimer formation is transient or specific to SufC in complex with SufB or SufD.

We noticed decreased solubility of SufBC proteins when purified aerobically. We established an alternative protocol to isolate His_6-$SufB_2C_2$ under anaerobic conditions. This approach increased solubility and decreased the aggregation of SufB. The binding affinity of SufB for SufC has not been measured, but dissociation of SufC from His_6-SufB during size exclusion chromatography leads us to assume the affinity of SufB for SufC is weaker in His_6-$SufB_2C_2$ compared to $SufBC_2D$. We observed that more SufC dissociated from His_6-SufB as we continued to dilute the proteins during purification. Further dissociation of SufC suggests a weak interaction between SufC and His_6-SufB observed at lower protein concentrations. Both Mg-ATP and ADP resulted in increased interaction between SufC and His_6-SufB even at lower protein concentrations. We did not directly observe Mg-ATP enhancement of the binding of SufC and SufD in the $SufC_2D_2$ complex, but sharpening of the $SufC_2D_2$ peak suggests the formation of a complex that migrates more tightly as a single species in the presence of nucleotide.

We observed that $SufBC_2D$ is a stable complex and does not undergo nucleotide-induced dissociation. Also, mixing His_6-$SufB_2C_2$ and $SufC_2D_2$ in the presence of Mg-ATP did not result in conversion to a $SufBC_2D$ complex. This study along with the hydrodynamic characterization of SufBC and SufCD complexes in *T. thermotoga*[23] provide evidence that the $SufB_2C_2$ and $SufC_2D_2$ complexes are probably only maintained if SufC can access ATP. From our results, we can conclude that multiple Suf complexes can exist with independent functions. Though it cannot be concluded if ATP binding or hydrolysis is the greatest contributing factor, the presence of ATP is essential for Suf pathway function in conjunction with SufC interacting with its partner proteins (SufB and SufD). Additional studies are needed to provide more insight into how each separate complex is initially assembled and to determine if the complexes interchange.

The $SufC_2D_2$ structure reveals a significant rearrangement of a conserved Gln (Gln85) residue toward the nucleotide binding site compared to SufC monomer structure.[7] In ABC transporters, this conserved Q-loop Gln residue has been shown to interact with the Mg^{2+} cofactor bound to ATP in the active site, interact with the putative catalytic H_2O for ATP hydrolysis, or interact with other residues within the ATP binding site to transmit changes to the bound transmembrane proteins.[31] With SufB or SufD bound at the Q-loop of SufC, Gln85 may be used to sense nucleotide binding and transmit changes to SufB or SufD to activate or deactivate $SufBC_2D$ Fe-S scaffold function in the Suf pathway.

$SufBC_2D$ is a novel Fe-S cluster scaffold protein that assembles a [4Fe-4S] cluster *in vitro* and transfers the cluster to [2Fe-2S] proteins SufA and ferredoxin and [4Fe-4S] protein aconitase. IscU is the scaffold protein for the Isc pathway. HscA has ATPase

activity and its ATP hydrolysis is used to drive Fe-S cluster transfer from scaffold protein IscU to target proteins.[13-15, 18] It was previously determined that Mg-ATP does not enhance Fe-S cluster transfer from $SufBC_2D$ to Fe-S proteins SufA, Fdx, or AcnB.[27] We recently determined that $SufBC_2D$ hydrolyzes Mg-ATP rapidly. (K.M. Thomas and F.W. Outten, unpublished) Under the reported Fe-S cluster transfer conditions, $SufBC_2D$ would have hydrolyzed Mg-ATP multiple times before the first measurement at 10 minutes. At the reported ATP and $SufBC_2D$ concentrations, ADP accumulation could also be the cause of the diminished rate of Fe-S transfer. We tested the effect of ADP on the rate of Fe-S cluster reconstitution on $SufBC_2D$. We found that ADP-bound $SufBC_2D$ assembled an Fe-S cluster at approximately 40% the rate of $SufBC_2D$ with no nucleotide bound. The results suggest a structural change in ADP-bound $SufBC_2D$ that does not accept cluster as readily. In future studies, we plan to map the solvent accessible regions of $SufBC_2D$ using hydrogen-deuterium exchange mass spectrometry (HDX-MS). The protection of amides in $SufBC_2D$ induced by ADP binding could lead to a decrease in deuterium incorporation in the backbone and may assist in the identification of the nucleotide-induced structural changes that occur in $SufBC_2D$. Based on the Fe-S reconstitution results, the regions on $SufBC_2D$ that show decreased deuterium exchange would provide information about the residues essential for Fe-S cluster assembly.

Yeast two-hybrid and pull-down assays using recombinant MBP- and His-tagged Suf proteins revealed SufB, SufC, and SufD proteins interact in *E. chrysanthemi*.[5] In this study, we investigated Suf protein interactions at native Suf protein levels in *E. coli*. Though the native Suf protein levels have not been quantified, incorporation of a polyhistidine tag fused at the C-terminus of SufC allowed us to isolate endogenously

expressed SufC along with any *in vivo* physiological binding partners. We confirmed the existence of an *in vivo* Suf complex with SufB, SufC, and SufD proteins. Previous studies reporting $SufBC_2D$ isolation used recombinant protein from cells over-expressing the *suf* operon.[19, 20, 25] We isolated an assembled $SufBC_2D$ complex from normal and H_2O_2 stressed cells. Our results reveal SufB, SufC, and SufD proteins assemble into a $SufBC_2D$ complex even when the Suf pathway is not the predominant Fe-S cluster assembly pathway (normal growth conditions).

SufS and SufE also co-eluted with $SufC_{His}$ from normal cells. SufS and SufE form a sulfur relay system onto SufB for Fe-S cluster assembly *in vitro*.[19, 20] Previous cross-linking and Surface Plasmon Resonance (SPR) data reported SufE interacts with $SufBC_2D$ at SufB[19, 20]; therefore, we cannot conclude if SufS and SufE directly bind $SufC_{His}$ or indirectly co-elute via interaction with SufB or SufD. Purified recombinant SufE migrates at a molecular weight consistent with a SufE monomer (~16 kDa) as determined by SDS PAGE and immunoblot detection with antibodies against SufE (data not shown). Chromosomally expressed SufE, purified using the His-tagged SufC construct, migrated at a molecular weight consistent with a SufE dimer (~30 kDa) (Figure 2.12). The observed variation in migration suggests SufE forms a stable dimer that cannot be reduced by DTT or SufE is tightly bound to an unidentified partner protein. SufS and SufE did not interact with $SufBC_2D$ isolated from H_2O_2 stressed cells. It seems that H_2O_2 stress caused disruption of the protein-protein interactions. This disruption may be necessary for $SufBC_2D$ to transfer assembled Fe-S clusters to proteins needed to restore homeostasis after oxidative stress exposure.

An interesting observation was the isolation of SufC monomer from normal cells and cells stressed with H_2O_2. We also observed SufD monomer. Purified recombinant SufD is a homo-dimer in solution.[7, 30] The presence of SufD monomer instead of SufD dimer could be explained by results from the hydrodynamic characterization of SufCD from *T. maritima*. The increasing retention times of serial dilutions during analytical size exclusion suggested a tetramer-dimer model for the SufC-SufD interaction. Petrovic et al. observed a mixture in equilibrium between a SufCD hetero-dimer and $SufC_2D_2$ tetramer in solution.[23] As mentioned previously, intracellular Suf protein levels are relatively low. The observed SufD monomer could be derived from dissociation of a residual SufCD complex. The fact that both SufC and SufD monomers could still be isolated even after the addition of exogenous Mg-ATP suggests the two species exist *in vivo*. We previously reported an interaction between SufA and SufC monomer *in vitro*.[26] Chahal proposed a role of SufC in SufA recruitment to $SufBC_2D$ for Fe-S cluster transfer. Determination of SufA interaction with SufC monomer or $SufBC_2D$ *in vivo* will help us better understand the physiological role of the interaction between SufA and SufC observed *in vitro*.

Construction of a polyhistidine tag on *sufC* in the *E. coli* chromosome allowed us to isolate native levels of the Suf proteins to study *in vivo* protein-protein interactions. In the future, we will use this approach to study Suf protein interactions during iron starvation conditions for comparison to interactions observed in response to oxidative stress. All purifications for this study were performed aerobically, but the purification protocol can be performed anaerobically and optimized to isolate enough $SufBC_2D$ for Fe-S cluster characterization. We also hope to use this technique to isolate an *in vivo* iron donor or other accessory proteins required for Suf function.

2.5 References

1. Ayala-Castro, C., Saini, A., and Outten, F. W. (2008) Fe-S cluster assembly pathways in bacteria. *Microbiol Mol Biol Rev* 72, 110-125.

2. Eccleston, J. F., Petrovic, A., Davis, C. T., Rangachari, K., and Wilson, R. J. (2006) The kinetic mechanism of the SufC ATPase: the cleavage step is accelerated by SufB. *J Biol Chem* 281, 8371-8378.

3. Kitaoka, S., Wada, K., Hasegawa, Y., Minami, Y., Fukuyama, K., and Takahashi, Y. (2006) Crystal structure of *Escherichia coli* SufC, an ABC-type ATPase component of the SUF iron-sulfur cluster assembly machinery. *FEBS Lett* 580, 137-143.

4. Kumar, B., Chaubey, S., Shah, P., Tanveer, A., Charan, M., Siddiqi, M. I., and Habib, S. (2012) Interaction between sulphur mobilisation proteins SufB and SufC: evidence for an iron-sulphur cluster biogenesis pathway in the apicoplast of *Plasmodium falciparum*. *Int J Parasitol* 41, 991-999.

5. Nachin, L., Loiseau, L., Expert, D., and Barras, F. (2003) SufC: an unorthodox cytoplasmic ABC/ATPase required for [Fe-S] biogenesis under oxidative stress. *Embo J* 22, 427-437.

6. Rangachari, K., Davis, C. T., Eccleston, J. F., Hirst, E. M., Saldanha, J. W., Strath, M., and Wilson, R. J. (2002) SufC hydrolyzes ATP and interacts with SufB from *Thermotoga maritima*. *FEBS Lett* 514, 225-228.

7. Wada, K., Sumi, N., Nagai, R., Iwasaki, K., Sato, T., Suzuki, K., Hasegawa, Y., Kitaoka, S., Minami, Y., Outten, F. W., Takahashi, Y., and Fukuyama, K. (2009) Molecular dynamism of Fe-S cluster biosynthesis implicated by the structure of the $SufC_2$-$SufD_2$ complex. *J Mol Biol* 387, 245-258.

8. Watanabe, S., Kita, A., and Miki, K. (2005) Crystal structure of atypical cytoplasmic ABC-ATPase SufC from *Thermus thermophilus* HB8. *J Mol Biol* 353, 1043-1054.

9. Moody, J. E., Millen, L., Binns, D., Hunt, J. F., and Thomas, P. J. (2002) Cooperative, ATP-dependent association of the nucleotide binding cassettes during the catalytic cycle of ATP-binding cassette transporters. *J Biol Chem* 277, 21111-21114.

10. Smith, P. C., Karpowich, N., Millen, L., Moody, J. E., Rosen, J., Thomas, P. J., and Hunt, J. F. (2002) ATP binding to the motor domain from an ABC transporter drives formation of a nucleotide sandwich dimer. *Mol Cell* 10, 139-149.

11. Verdon, G., Albers, S. V., van Oosterwijk, N., Dijkstra, B. W., Driessen, A. J., and Thunnissen, A. M. (2003) Formation of the productive ATP-Mg^{2+}-bound dimer of GlcV, an ABC-ATPase from *Sulfolobus solfataricus*. *J Mol Biol* 334, 255-267.

12. Zheng, L., Cash, V. L., Flint, D. H., and Dean, D. R. (1998) Assembly of iron-sulfur clusters. Identification of an *iscSUA-hscBA-fdx* gene cluster from *Azotobacter vinelandii*. *J Biol Chem* 273, 13264-13272.

13. Kim, J. H., Alderson, T. R., Frederick, R. O., and Markley, J. L. (2014) Nucleotide-dependent interactions within a specialized Hsp70/Hsp40 complex involved in Fe-S cluster biogenesis. *J Am Chem Soc* 136, 11586-11589.

14. Kim, J. H., Tonelli, M., Frederick, R. O., Chow, D. C., and Markley, J. L. (2012) Specialized Hsp70 chaperone (HscA) binds preferentially to the disordered form, whereas J-protein (HscB) binds preferentially to the structured form of the iron-sulfur cluster scaffold protein (IscU). *J Biol Chem* 287, 31406-31413.

15. Silberg, J. J., Tapley, T. L., Hoff, K. G., and Vickery, L. E. (2004) Regulation of the HscA ATPase reaction cycle by the co-chaperone HscB and the iron-sulfur cluster assembly protein IscU. *J Biol Chem* 279, 53924-53931.

16. Silberg, J. J., and Vickery, L. E. (2000) Kinetic characterization of the ATPase cycle of the molecular chaperone Hsc66 from *Escherichia coli*. *J Biol Chem* 275, 7779-7786.

17. Jakob, U., Gaestel, M., Engel, K., and Buchner, J. (1993) Small heat shock proteins are molecular chaperones. *J Biol Chem* 268, 1517-1520.

18. Chandramouli, K., and Johnson, M. K. (2006) HscA and HscB stimulate [2Fe-2S] cluster transfer from IscU to apoferredoxin in an ATP-dependent reaction. *Biochemistry* 45, 11087-11095.

19. Outten, F. W., Wood, M. J., Munoz, F. M., and Storz, G. (2003) The SufE protein and the SufBCD complex enhance SufS cysteine desulfurase activity as part of a sulfur transfer pathway for Fe-S cluster assembly in *Escherichia coli*. *J Biol Chem* 278, 45713-45719.

20. Layer, G., Gaddam, S. A., Ayala-Castro, C. N., Ollagnier-de Choudens, S., Lascoux, D., Fontecave, M., and Outten, F. W. (2007) SufE transfers sulfur from SufS to SufB for iron-sulfur cluster assembly. *J Biol Chem* 282, 13342-13350.

21. Beinert, H. (1983) Semi-micro methods for analysis of labile sulfide and of labile sulfide plus sulfane sulfur in unusually stable iron-sulfur proteins. *Anal Biochem* 131, 373-378.

22. Riemer, J., Hoepken, H. H., Czerwinska, H., Robinson, S. R., and Dringen, R., (2004) Colorimetric ferrozine-based assay for the quantitation of iron in cultured cells. *Anal Biochem* 331, 370-375.

23. Petrovic, A., Davis, C. T., Rangachari, K., Clough, B., Wilson, R. J., and Eccleston, J. F. (2008) Hydrodynamic characterization of the SufBC and SufCD complexes and their interaction with fluorescent adenosine nucleotides. *Protein Sci* 17, 1264-1274.

24. Saini, A., Mapolelo, D. T., Chahal, H. K., Johnson, M. K., and Outten, F. W. (2010) SufD and SufC ATPase activity are required for iron acquisition during *in vivo* Fe-S cluster formation on SufB. *Biochemistry* 49, 9402-9412.

25. Wollers, S., Layer, G., Garcia-Serres, R., Signor, L., Clemancey, M., Latour, J. M., Fontecave, M., and Ollagnier de Choudens, S. (2010) Iron-sulfur (Fe-S) cluster assembly: the SufBCD complex is a new type of Fe-S scaffold with a flavin redox cofactor. *J Biol Chem* 285, 23331-23341.

26. Chahal, H. K., Dai, Y., Saini, A., Ayala-Castro, C., and Outten, F. W. (2009) The SufBCD Fe-S scaffold complex interacts with SufA for Fe-S cluster transfer. *Biochemistry* 48, 10644-10653.

27. Chahal, H. K., and Outten, F. W. (2012) Separate Fe-S scaffold and carrier functions for $SufB_2C_2$ and SufA during *in vitro* maturation of [2Fe-2S] Fdx. *J Inorg Biochem* 116, 126-134.

28. Tian, T., He, H., and Liu, X. Q. (2013) The SufBCD protein complex is the scaffold for iron-sulfur cluster assembly in *Thermus thermophilus* HB8. *Biochem Biophys Res Commun* 443, 376-381.

29. Bolanos-Garcia, V. M., and Davies, O. R. (2006) Structural analysis and classification of native proteins from *E. coli* commonly co-purified by immobilised metal affinity chromatography. *Biochim Biophys Acta* 1760, 1304-1313.

30. Badger, J., Sauder, J. M., Adams, J. M., Antonysamy, S., Bain, K., Bergseid, M. G., Buchanan, S. G., Buchanan, M. D., Batiyenko, Y., Christopher, J. A., Emtage, S., Eroshkina, A., Feil, I., Furlong, E. B., Gajiwala, K. S., Gao, X., He, D., Hendle, J., Huber, A., Hoda, K., Kearins, P., Kissinger, C., Laubert, B., Lewis, H. A., Lin, J., Loomis, K., Lorimer, D., Louie, G., Maletic, M., Marsh, C. D., Miller, I., Molinari, J.; Muller-Dieckmann, H. J., Newman, J. M., Noland, B. W., Pagarigan, B., Park, F., Peat, T. S., Post, K. W., Radojicic, S., Ramos, A., Romero, R., Rutter, M. E., Sanderson, W. E., Schwinn, K. D., Tresser, J., Winhoven, J., Wright, T. A., Wu, L., Xu, J., and Harris, T. J. (2005) Structural analysis of a set of proteins resulting from a bacterial genomics project. *Proteins* 60, 787-796.

31. Rees, D. C., Johnson, E., and Lewinson, O. (2009) ABC transporters: the power to change. *Nat Rev Mol Cell Biol* 10, 218-227.

CHAPTER 3

Kinetic analysis of SufC ATPase in Fe-S scaffolds $SufBC_2D$ and $SufB_2C_2$ from *E. coli*

Abstract

In vivo Fe-S cluster assembly requires ATP hydrolysis. SufC is the ATPase component of the Suf Fe-S cluster assembly system. There are two proposed Fe-S scaffold complexes in *E. coli*. $SufBC_2D$ and $SufB_2C_2$ can both assemble [4Fe-4S] clusters and efficiently transfer the cluster to carrier protein SufA or directly to target Fe-S proteins. $SufBC_2D$ and $SufB_2C_2$ contain two SufC subunits, both essential for nucleotide induced dimerization necessary for ATP hydrolysis. The kinetics of the SufC ATPase have been extensively studied in other species, but there is currently no kinetic analysis of SufC or the SufBCD complexes from *E. coli*. We use an ATP-regenerating linked enzyme assay and stopped-flow fluorescence techniques to study the kinetic behavior of the ATP hydrolysis of SufC alone and within the $SufBC_2D$ and $SufB_2C_2$ complexes. Steady state ATPase measurements revealed SufC ATPase activity is enhanced in the $SufB_2C_2$ complex and even further enhanced in $SufBC_2D$. Our results suggest varying rates of ATP hydrolysis dependent on SufC being alone or associated with a respective scaffold SufBCD complex.

3.1 Introduction

The gram-negative bacterium *E. coli* encodes the *suf* operon to mobilize iron and sulfide for iron-sulfur (Fe-S) cluster assembly and transfer during iron starvation and oxidative stress conditions. The *E. coli* Suf pathway is comprised of SufA, SufB, SufC, SufD, SufS, and SufE proteins. SufS and SufE mobilize sulfide via a coupled cysteine desulfurase and sulfur transferase mechanism. SufB, SufC, and SufD are localized in the cytoplasm and interact as a stable $SufBC_2D$ complex that serves as a novel scaffold for Fe-S cluster assembly. SufA is a carrier protein that accepts and transfers intact Fe-S clusters to target apo-proteins.[1]

The *suf* operon structure varies by organism. The most conserved *suf* genes are *sufB* and *sufC* found in archaea, bacteria, plants, and parasites. Mutations in *sufC* cause increased intracellular concentrations of free iron, hypersensitivity to oxidative stress agent paraquat, and reduced virulence in *Erwinia chrysanthemi* (recently renamed *Dickeya dadantii*). Inactivation of *sufC* causes the most drastic phenotypic alterations compared to inactivation of the other *suf* genes[2], suggesting SufC plays a central role in Suf pathway function. Primary sequence analysis and structural studies of SufC reveal SufC shares limited homology (≤ 25% sequence identity) with the ATPase subunit of ATP-binding cassette (ABC) transporters. The SufC sequence possesses motifs conserved among ABC ATPases that contribute to ATP binding and hydrolysis (Walker A, Walker B, and ABC signature), dimerization (D-loop), and interaction with partner proteins (Q-loop).[3-5] Superposition of *E. coli* SufC monomer and *S. typhimurium* HisP structures reveal the structural similarities and differences in the conserved motifs (Figure

A

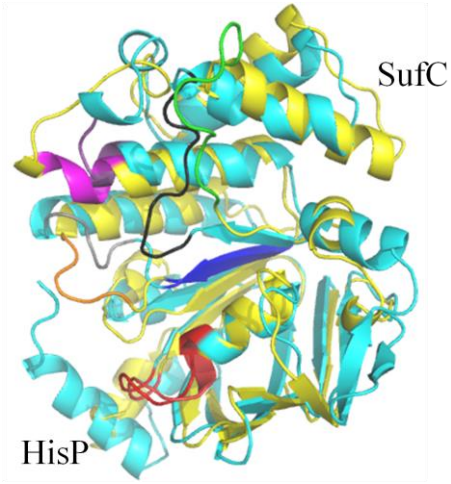

B

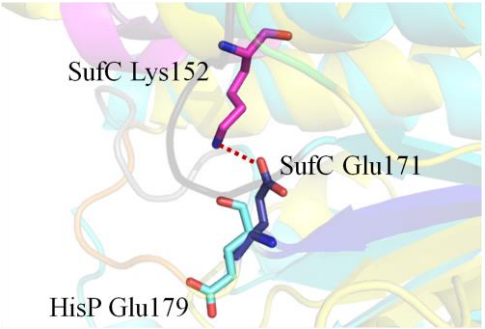

Figure 3.1 (A) Structural alignment of *E. coli* SufC monomer[3] (yellow) and *S. typhimurium* HisP (cyan) (PDB entry 1B0U)[24]. Walker A (red), Walker B (blue), ABC signature (magenta-SufC; purple-HisP), D-loop (orange-SufC; grey-HisP), and Q-loop (green-SufC; black-HisP) motifs are colored. (B) Close-up view of panel A. SufC Lys152 (magenta) and Glu171 (blue) and HisP Glu179 (cyan) residues are shown as sticks. Lys152-Glu171 salt bridge shown as red dotted line.

3.1). It has been reported that SufC has the intrinsic ability to hydrolyze ATP and that this hydrolysis is enhanced by association with SufB or SufD. Hydrodynamic characterization and thorough pre-steady state kinetic analysis of SufC from *T. maritima* indicate $SufB_2C_2$ and $SufC_2D_2$ complexes bind fluorescent analogs mantATP and mantADP more tightly than SufC alone and the cleavage step of SufC mantATP hydrolysis is accelerated.[6-9]

It has been established that *E. coli sufB* co-expressed with *sufCDSE* purifies as two separate complexes: $SufB_2C_2$ and $SufBC_2D$.[10] Both $SufB_2C_2$ and $SufBC_2D$ can assemble an Fe-S cluster and transfer the intact cluster to SufA *in vitro*. Addition of Mg-ATP to holo-$SufBC_2D$ results in inhibited cluster transfer to apo-SufA. In contrast, Mg-ATP only slightly slowed the rate of cluster transfer from holo-$SufB_2C_2$ to apo-SufA.[11] The previous studies raise the major question of the role of SufC ATP binding and hydrolysis in the cluster assembly process. Here we have characterized the SufC ATPase activity in the $SufBC_2D$ scaffold for the first time and have compared it to $SufB_2C_2$ and SufC alone. Through our biochemical analysis, we have identified two separate conformations of the $SufBC_2D$ complex that differ in their basal ATPase activity. Steady state, single-turnover, and pre-steady state stopped-flow kinetic studies using fluorescent nucleotide analogs allowed us to identify the step responsible for the observed difference in ATPase activity.

3.2 Materials and Methods

Reagents. Adenosine 5'-triphosphate (ATP) (99% purity, HPLC) was purchased from Sigma-Aldrich (A7699). ATP concentrations were determined by absorbance at

259 nm using an extinction coefficient (ε_{259}) of 15, 400 M^{-1} cm^{-1}. 2'-(or -3')-*O*-(*N*-Methylanthraniloyl) adenosine 5'-triphosphate (mantATP) (98% purity, HPLC) and 2'-(or -3')-*O*-(*N*-Methylanthraniloyl) adenosine 5'-diphosphate (mantADP) (97% purity, HPLC) were purchased from Life Technologies (M12417, M12416). Mant-nucleotide concentrations were determined using ε_{254} of 23, 300 M^{-1} cm^{-1}. All experimental measurements were made in ATPase buffer (50 mM Tris, pH 7.5, 100 mM KCl, 5 mM $MgCl_2$, and 1 mM DTT) unless otherwise noted.

Strains, growth conditions, and protein purification of recombinant Suf proteins. The over-expression plasmid pET3a (Novagen) expressing SufC was transformed into *E. coli* strain BL21(DE3).[12] 2 L cultures were grown in LB at 37°C to an OD_{600} of 0.7 then induced with 1 mM IPTG for 3 hours at 37°C. Cells were harvested and cell pellets frozen at -80°C. For purification, cells were resuspended in cold extract buffer (25 mM Tris-HCl, pH 8.0, 50 mM NaCl, 10 mM βME) containing 1 mM PMSF, lysed via sonication (Branson Digital Sonifier) on ice (power = 50%, pulse on = 2 seconds, pulse off = 18 seconds, total time = 1 minutes per 1 L culture), and centrifuged for lysate collection after treatment with 2% streptomycin sulfate. Cleared lysate was loaded onto a HiLoad 16/10 Q Sepharose High Performance column (20 mL) (GE Healthcare) equilibrated with Q buffer A (25 mM Tris-HCl, pH 8.0, 50 mM NaCl, 10 mM βME). Fractions containing SufC eluted at 30-45% Q buffer B (25 mM Tris-HCl pH 8.0, 1 M NaCl, 10 mM βME). SufC fractions were diluted 1:1 with Phenyl buffer A (25 mM Tris-HCl pH 7.5, 100 mM NaCl, 1 M $(NH_4)_2SO_4$, 10 mM βME) and loaded onto a Phenyl FF column (20 mL) (GE Healthcare). Fractions containing SufC eluted at 100% Phenyl buffer B (25 mM Tris-HCl, pH 7.5, 10 mM βME). Fractions were pooled and

concentrated then loaded onto a HiLoad 16/60 Superdex-75 column in buffer containing 50 mM Tris-HCl, pH 7.5, 200 mM NaCl, and 4 mM DTT. Fractions with pure SufC were concentrated and stored at -80°C.

The pETDuet-1 (Novagen) vector containing only the *sufBC* genes (pFWO469) was used to over-express His_6-SufBC in *E. coli* BL21 (DE3) strain.[10] 2 L cultures were grown in LB at 37°C to an OD_{600} of 0.7 and induced with 200 µM IPTG. After 18 hour induction at 18°C, cells were harvested and cell pellets frozen at -80°C. His_6-SufBC was purified as described previously[7] with modifications. Briefly, cells were resuspended in anaerobic Hisprep buffer A (25 mM Tris, pH 8.0, 300 mM NaCl, 10 mM Imidazole, 10 mM βME) containing 1 mM phenylmethanesulfonyl fluoride (PMSF), followed by anaerobic sonication (Branson Digital Sonifier) on ice (power = 50%, pulse on = 5 seconds, pulse off = 20 seconds, total time= 1.5 minutes per 1 L culture) and centrifugation (16,000 x g, 40 min, 4°C) to remove cellular debris. Cleared lysate was loaded onto a Hisprep FF (20 mL) (GE Healthcare) column equilibrated with Hisprep buffer A. After 4 column volume washes with 10% Hisprep buffer B (25 mM Tris, pH 8.0, 300 mM NaCl, 500 mM imidazole, 10 mM βME), bound proteins were eluted stepwise with 25%, 50%, and 100% Hisprep buffer B. His_6-SufBC eluted as a single peak at 25% Hisprep buffer B. Fractions were pooled and concentrated. Concentrated His_6-SufBC was then loaded onto a HiLoad 16/60 Superdex-200 column equilibrated in aerobic buffer C (25 mM Tris, pH 8.0, 150 mM NaCl, 2 mM DTT). Fractions containing pure His_6-$SufB_2C_2$ were concentrated and stored at -80°C.

The pBAD/*Myc*-His C vector (Invitrogen) containing the entire *suf* operon (pGSO164) under control of an arabinose-inducible promoter was used to over-express

sufABCDSE in *E. coli* TOP10 strain.[12, 13] 4 L cultures were grown in LB at 37°C to an OD_{600} of 0.5 and induced with 0.2% (w/v) L-arabinose. After 3 hour induction at 37°C, cells were harvested by centrifugation and cell pellets frozen at -80°C. The $SufBC_2D$ complex was purified as described *previously*[13] with modifications. Briefly, cleared lysate was loaded onto a Phenyl FF column in line with a Biologic DuoFlow FPLC system (Biorad). The column was washed with 3 column volumes of phenyl binding buffer (25 mM Tris-HCl, pH 7.5, 100 mM NaCl, 1 M ammonium sulfate, and 10 mM βME). Suf proteins were eluted with a gradient of 1-0 M ammonium sulfate. SufBCD proteins eluted at 75 – 100% phenyl buffer B (25 mM Tris-HCl, pH 7.5, 0 M ammonium sulfate, 10 mM βME). Fractions eluting between 70-100% (early) and eluting at 100% (late) phenyl buffer B were pooled separately and diluted 2.5 times with Q buffer A (25 mM Tris, pH 7.5, 10 mM βME). All subsequent purification steps were the same as previously reported.[12, 13] Iron content and acid-labile sulfide content was determined by previously reported methods.[14, 15] For all preps, purity was determined by SDS PAGE and protein concentrations were measured by Bradford assay.

Preparation of 100 mM Mg^{2+}-ATP stocks. Dissolve 1.10 g adenosine 5'-triphosphate (ATP) disodium salt hydrate (Sigma-Aldrich A7699) in 15 mL MilliQ water. Add 0.41 g $MgCl_2$ and dissolve. Adjust to pH ~7.0 with 3 M NaOH added dropwise with stirring. Add water to a final volume of 20 mL and filter the solution. Store in aliquots at -20°C. Mg-ATP stocks are stable at -20°C for six months.

Steady State ATPase activity. SufC steady state ATPase activity was measured using a ATP-regenerating, linked enzyme assay that couples ADP production to NADH oxidation.[16] Reactions (200 µL) contained 0.16 mM reduced β-nicotinamide adenine

dinucleotide (NADH) (Sigma-Aldrich N4505), 1 mM phosphoenolpyruvate (PEP) (Sigma-Aldrich P7002), 5 U pyruvate kinase (PK) (Sigma-Aldrich P1506), 10 U lactate dehydrogenase (LDH) (Sigma-Aldrich L2500), and varying amounts of Mg-ATP in reaction buffer. Each reaction mixture was incubated at room temperature for 5 min prior to initiating the hydrolysis reaction by addition of SufC, $SufB_2C_2$, or $SufBC_2D$ (2 µL). The following stepwise procedure was used to initiate all ATPase reactions. First, 2 µL of SufC, His-$SufB_2C_2$, or $SufBC_2D$ was added to an empty well of a 96-well plate. Then, 198 µL of reaction mixture was added to the protein in the well to initiate the reaction. Measurements were taken immediately following addition of the reaction mixture using a Synergy H1 hybrid reader (Biotek). NADH absorbance was measured at 340 nm and NADH concentrations were determined based on NADH ε_{340} of 4662 M^{-1} cm^{-1} (determined experimentally for 96-well plate reaction conditions). All reactions were measured at 25°C. Initial rates (v_o) were determined by linear regression analysis (ensuring the fraction of NADH oxidized did not exceed 10%). K_m and V_{max} values were determined by fitting the Michaelis Menten equation to a plot of v_o against [ATP] using GraphPad Prism 6.0 software.

ADP ANS-binding fluorescence assay. 10 mM 8-Anilinonaphthalene-1-sulfonic acid (ANS) (Sigma-Aldrich A1028) stock was prepared by dissolving 2.99 mg ANS in 10 µL DMSO then diluting to 1 mL with MilliQ water. All fluorescence measurements were conducted at 25°C in a 96-well plate using a Synergy H1 hybrid reader (Biotek) with the excitation wavelength at 380 nm and emission wavelength scan from 450-600 nm. ANS titrations contained 823 nM $SufBC_2D$ with or without 200 µM ADP (175 µL). ADP titrations contained 823 nM $SufBC_2D$ with 200 µM ANS. The steady-state

fluorescence intensities as a function of ADP concentration were fitted to a rectangular hyperbola equation (shown below) using a nonlinear regression program (GraphPad Prism 6). Assuming $SufBC_2D$ possesses a one-site specific nucleotide binding site:

$$FI = \frac{(FI_{max})\ [ADP]_F}{K_d + [ADP]_F}$$

FI is fluorescence intensity, FI_{max} is the maximum fluorescence of the ANS-bound $SufBC_2D$-ADP complex, $[ADP]_F$ is the concentration of free ADP ($[SufBC_2D] << [ADP]$, therefore $[ADP] = [ADP]_F$), and K_d is the apparent dissociation equilibrium constant for ADP binding to $SufBC_2D$.

Fluorescent nucleotide binding kinetics. Rapid kinetic measurements were performed using a stopped-flow instrument (Applied Photophysics). Experiments were initiated by mixing equal volumes of protein and fluorescent nucleotide solutions. Excitation at 280 nm was achieved through a monochromator and emission was viewed through a 399 cut-off filter. Nonlinear least-squares fitting were performed with Pro-Data SX software (Applied Photophysics). The concentrations of proteins and nucleotides reported in each figure are final concentrations after mixing.

3.3 Results

SufC from E. coli has low intrinsic ATPase activity. The ATPase activity of purified recombinant SufC was assayed using the NADH linked enzyme system (see Materials and Methods). SufC ATPase activity exhibited hyperbolic dependence on ATP concentration. Fitting the data to the Michaelis Menten equation gave a K_m value of 59.2 μM and a k_{cat} of 1.9 X 10^{-4} s^{-1} (Figure 3.2). The K_m is similar to the value reported for *T. maritima* SufC (Table 3.1), but the k_{cat} value is almost 100 times slower (0.04 s^{-1}).[6]

Michaelis Menten parameters have been reported for SufC isolated from *T. thermophilus* HB8, *E. chrysanthemi, P. falciparum,* and *T. maritima*.[8, 9, 17, 18] These SufC homologs share at least 40 % sequence identity with *E. coli* SufC: *T. thermophilus* (52%), *E. chrysanthemi* (85%), *P. falciparum* (48%), and *T. maritima* (46%). SufC K_m and k_{cat} values are summarized in Table 3.1. *E. coli* SufC has the lowest intrinsic ATPase activity among the values reported for SufC homologs.

SufC ATPase activity is enhanced in the SufBC$_2$D complex. The SufBC$_2$D complex is required for *in vivo* Fe-S cluster assembly by the Suf pathway in *E. coli*.[10-13, 19] Despite clear evidence that binding of SufC to partner proteins SufB and/or SufD enhances the rate of ATP hydrolysis by SufC[6-9], thorough kinetic analysis of the SufBC$_2$D complex has not been reported. Recent results reported by Tian et al[9] showed that the ATPase activity of SufC is doubled in the SufBC and SufCD complexes and tripled in the SufBCD complex isolated from *T. thermophilus* HB8. The ATPase activity of SufBC$_2$D isolated from *E. coli* was measured and compared to SufC alone. At 100 μM Mg-ATP, SufC (0.5-2 μM) showed no measurable ATPase activity (Figure 3.3A). In contrast, the observed rate of ATP hydrolysis by 500 nM SufBC$_2$D was 3.3 μM min^{-1}. The rate of ATP hydrolysis increased directly with increasing SufBC$_2$D concentration to 8.9 μM min^{-1} at 2 μM protein (Figure 3.3B). As reported in the previous data, *E. coli* SufC has very low intrinsic ATPase activity. This activity is enhanced more than 100-fold in SufBC$_2$D.

Steady state kinetic analysis of the SufBC$_2$D ATP hydrolysis cycle. The ATPase activity of SufBC$_2$D was assayed as a function of ATP concentration. The ATP-dependence initial velocity data did not fit well to a simple Michaelis Menten equation

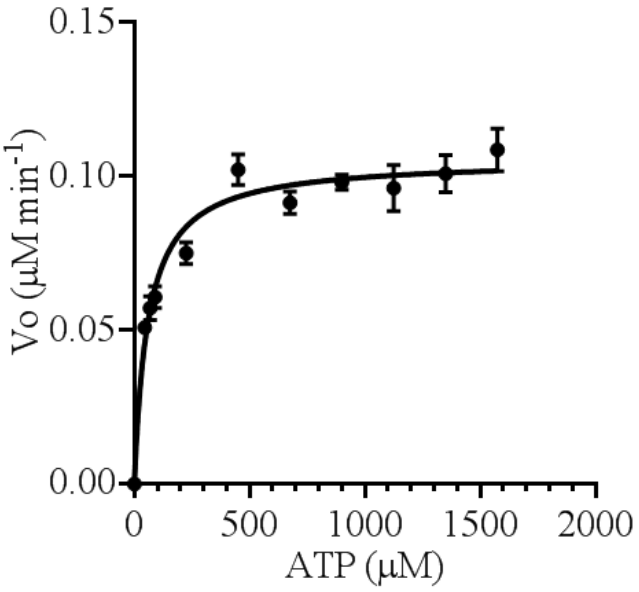

Figure 3.2. Kinetic analysis of *E. coli* SufC activity in response to varied ATP concentrations. Initial rates of ADP production (v_o) plotted as a function of ATP concentration. Reactions were initiated by the addition of 5 μM SufC. Solid line is a best fit of the data to the Michaelis Menten equation yielding a K_m of 59.2 μM and V_{max} of 0.11 μM min^{-1}. Measurements were performed in triplicate.

Table 3.1 K_m and k_{cat} values for SufC homologs

Organism	K_m (μM)	k_{cat} (s^{-1})	Temp (°C)	Protein modification	ref
E.coli[a]	59.2	1.9×10^{-4}	25	None	This study
T. thermophilus HB8[a]	17.7	1.2×10^{-3} [d]	30	None	9
P. falciparum[a,c]	226	5.4×10^{-2}	25	N-terminal His-tag	17
E. chrysanthemi[b]	290	2.9×10^{-1} [d]	37	N-terminal MBP-tag	18
T. maritima[a]	45	4.0×10^{-2}	20	C-terminal His-tag	8

[a]Measured using NADH linked enzyme assay. [b]Measured using Malachite green phosphate release assay. [c]K_m and V_{max} determined using transformed data and modified Lineweaver-Burk plot. [d]k_{cat} calculated from reported V_{max} and reported enzyme concentrations.

(Figure 3.4). The data was alternatively fit to an allosteric sigmoidal equation (modified Michaelis Menten equation) that accounts for cooperativity:

$$V_o = \quad V_{max}\,[\mathrm{ATP}]^h / K' + [\mathrm{ATP}]^h$$

,where v_o is the measured initial velocity, V_{max} is the maximum enzyme velocity, [ATP] is the concentration of added ATP, K' is related to K_m, reporting the substrate concentration that produces ½ V_{max} corrected for h, and h is the Hill constant, a measure of cooperativity. K' equals K_m when h equals 1 (i.e. an enzyme does not display cooperativity and obeys Michaelis Menten kinetics). A comparison of the goodness of fit for both Michaelis Menten and allosteric sigmoidal equations showed that the fit for the allosteric sigmoidal model was superior (p value < 0.0001). Least squares fit of the data to the allosteric sigmoidal equation yielded values of V_{max} = 26.4 µM min^{-1}, K' = 26.9 µM, and h = 0.57 ± 0.06 (Table 3.2). A Hill constant (h) less than 1 can be indicative of negative cooperativity.

To ensure the observed deviation from Michaelis Menten kinetics was not due to our assay conditions, we assayed the steady state ATPase activity of a complex consisting of only SufB and SufC proteins. His_6-$SufB_2C_2$ activity was hyperbolically dependent on ATP concentration, and the velocity data fit well to the Michaelis Menten equation (Figure 3.5). K_m and k_{cat} values obtained were 71.5 µM and 0.025 s^{-1}, respectively. Fitting the data to the allosteric sigmoidal equation yielded an h constant of 0.91. Compared to SufC alone, the rate of ATP turnover by His_6-$SufB_2C_2$ is 100-times faster. In contrast, SufC ATP turnover rate is enhanced 1000-times in the $SufBC_2D$ complex (Table 3.2).

SufB shares sequence similarities with SufD at the C-terminal α-helical region shown to participate in binding to SufC in the $SufC_2D_2$ structure.[3] However, SufB and SufD are proposed to have independent functions. Though the interaction of SufB with SufC is presumed to be similar to the SufC-SufD interaction, without direct structural characterization of a $SufBC_2D$ complex, it is difficult to make that conclusion. It is possible that the structural arrangement of the SufC nucleotide binding site differs based on which partner protein (SufB or SufD) is bound. Slight differences in the structure of the SufC active site could theoretically explain the observed negative cooperativity. Another possible explanation of the observed deviation from Michaelis Menten kinetics is the presence of a contaminating protein that also hydrolyzes ATP or a mixture of inactive and active SufC ATPase. These possibilities were investigated.

Equilibrium binding affinity of ADP to $SufBC_2D$. The equilibrium binding constant of ADP to $SufBC_2D$ was determined using the fluorescent probe 1-anilinonaphthalene-8-sulfonate (ANS). ANS is a fluorescent molecular probe used to monitor changes in protein surface hydrophobicity.[20, 21] When ANS binds a protein, the fluorescent quantum yield increases significantly. The increased fluorescence response is accompanied by a blue shift of the emission maximum wavelength. Protein structural changes induced by ligand binding can lead to displacement of ANS, causing a reduced fluorescent response. The interaction of ADP with $SufBC_2D$ was investigated by monitoring fluorescent changes of ANS-bound $SufBC_2D$. ANS bound to $SufBC_2D$ fluoresced at a maximum emission wavelength of 506 nm compared to 542 nm for free ANS in solution (Figure 3.6A). Titration curves obtained by adding increasing amounts of ANS to $SufBC_2D$ revealed a quenching of fluorescence in the presence of 200 μM

ADP (Figure 3.6B). The maximum fluorescence changes were 38% reduction in ANS protein-bound fluorescence. Though it is difficult to specifically attribute the observed reduced fluorescent responses with changes in the quantum yield, stoichiometry, or binding efficiency of ANS to $SufBC_2D$, we can conclude that the fluorescence response is specific to ADP binding to $SufBC_2D$ (Figure 3.6A). The altered fluorescent response provided a means to quantify the interaction of $SufBC_2D$ with ADP. ANS-bound $SufBC_2D$ was titrated with increasing amounts of ADP and the resulting change in ANS fluorescence was measured (Figure 3.7). The binding data was best fit to a single-site binding model and yielded an equilibrium binding constant (K_d) of 13.2 ± 3.1 μM for ADP binding to $SufBC_2D$. No cooperativity was displayed in the ADP binding step. $SufBC_2D$ equilibrium binding affinity for Mg-ATP was not determined using this approach because $SufBC_2D$ hydrolyzes Mg-ATP.

Isolation of low and high activity $SufBC_2D$. $SufBC_2D$ used for the previously described kinetic characterization was isolated from *E. coli* cells co-expressing the entire *sufABCDSE* operon. The SufB, SufC, and SufD proteins co-elute from a hydrophobic interaction column (HIC) (Phenyl FF) using a gradient of ammonium sulfate in a broad elution profile (determined by SDS PAGE) (Figure 3.8A). For the initial characterization of $SufBC_2D$ ATPase activity (shown in Figure 3.4), all fractions containing the three proteins were pooled and carried forward through the remaining purification procedure (anion exchange and size exclusion chromatography). This pooling step was previously performed to maximize the yield of $SufBC_2D$ for downstream biochemical analyses.

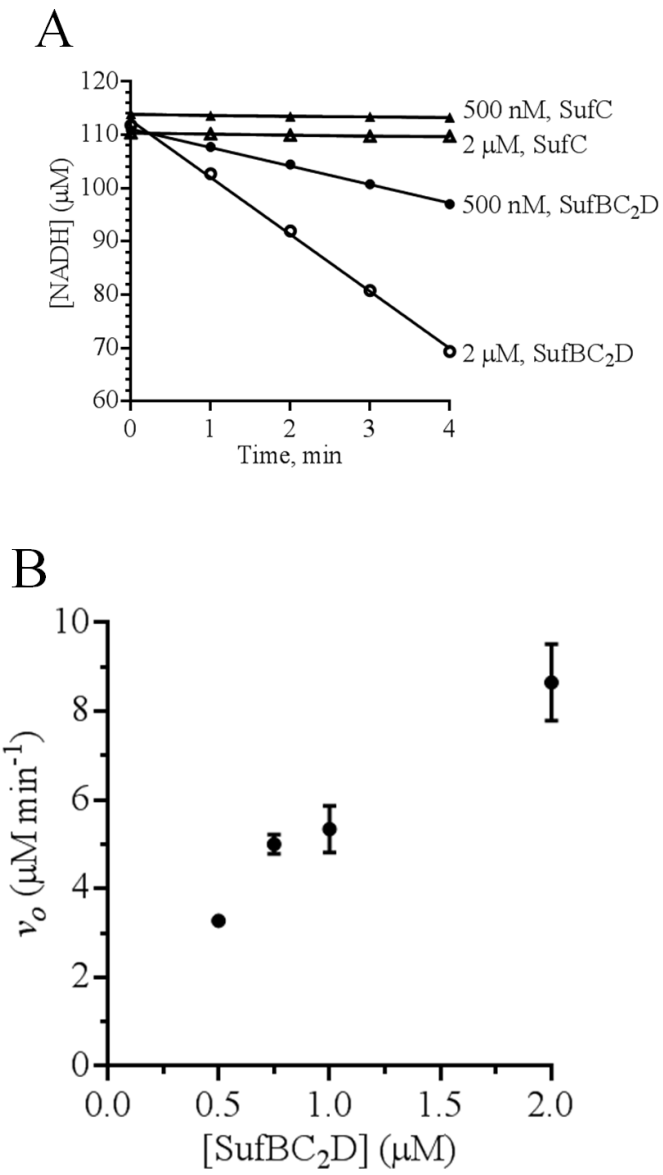

Figure 3.3 Enhanced SufC ATPase activity in $SufBC_2D$. (A) NADH consumption over time at 100 μM ATP by SufC (triangles) or $SufBC_2D$ (circles). (B) ATPase activity at increasing concentrations of $SufBC_2D$.

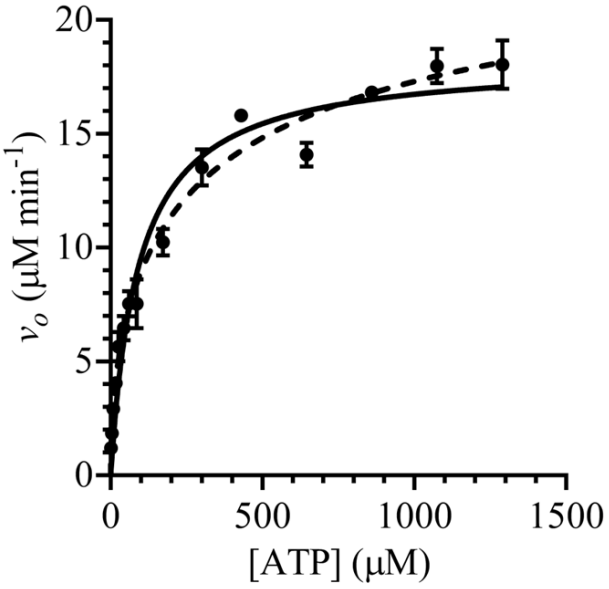

Figure 3.4 Kinetic analysis of "mixed" $SufBC_2D$ activity. Initial rates v_o plotted against ATP concentration. Reactions were initiated by the addition of 750 nM "mixed" $SufBC_2D$. Lines are best fits to Michaelis-Menten (solid) or allosteric sigmoidal (dashed) equations. Measurements were performed in triplicate. Error bars are indicated.

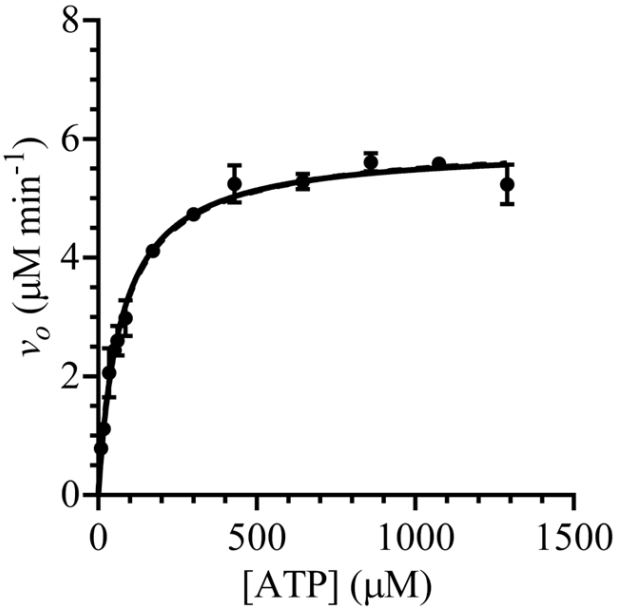

Figure 3.5 Kinetic analysis of His_6-$SufB_2C_2$ activity. Initial rates v_o plotted against ATP concentration. Reactions were initiated by the addition of 2 μM His_6-$SufB_2C_2$. Lines are best fits to Michaelis-Menten (solid) or allosteric sigmoidal (dashed) equations. Measurements were performed in triplicate. Error bars are indicated.

A

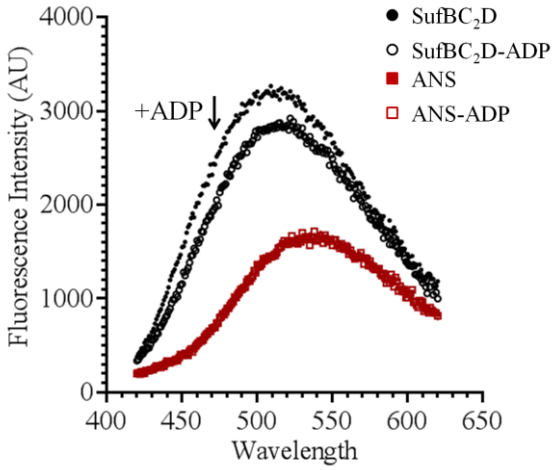

B

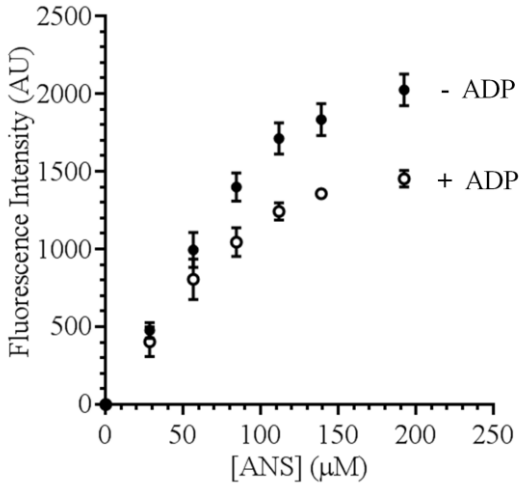

Figure 3.6 Effect of ADP on the fluorescence of ANS-bound $SufBC_2D$. (A) Emission spectra ($\lambda_{excitation}$ = 380 nm) of ANS (395 μM) in buffer (red) and ANS-bound $SufBC_2D$ (823 nM) with (black closed circle) and without (black open circle) 200 μM ADP. (B) Titration of $SufBC_2D$ (closed circle) and $SufBC_2D$-ADP (open circle) with increasing amounts of ANS. Concentrations same as (A). Fluorescence is in arbitrary units.

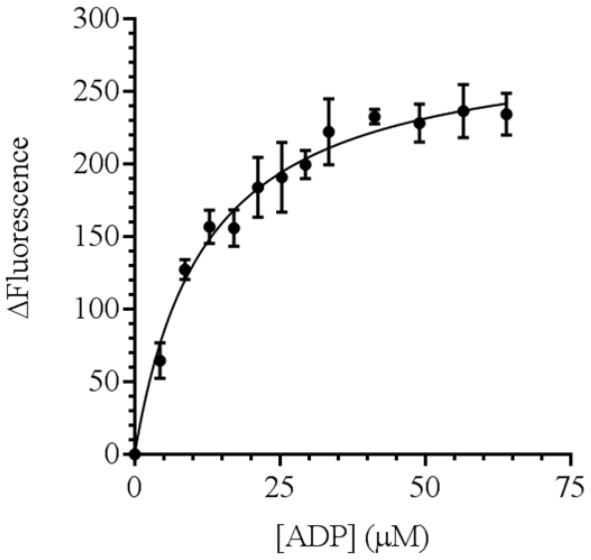

Figure 3.7 Titration of ANS-bound $SufBC_2D$ with ADP. Samples contained 823 nM $SufBC_2D$ and 200 μM ANS. Line is best fit to the one site specific binding equation obtained using GraphPad Prism. Plotted data is the average of four independent measurements.

We refer to the combined $SufBC_2D$ sample as "mixed" $SufBC_2D$ (Figure 3.4 and Table 3.2) throughout this text.

Several differences were observed among the fractions containing SufB, SufC, and SufD from the HIC column. Fractions collected from early in the elution profile were colored yellow. As an example, the UV-visible absorption spectrum of fraction 13 from this early region showed a sharp feature at 420 nm (Figure 3.8B). The cysteine desulfurase enzyme SufS binds the pyridoxal phosphate (PLP) cofactor, which is yellow in solution and has a maximum absorption at 420 nm. Indeed, SDS PAGE indicated fraction 13 also contained SufS (Figure 3.8B, inset), so we concluded the 420 nm peak was from PLP-bound SufS. Fractions collected later in the elution profile were a dark greenish-brown color. The UV-visible absorption spectrum of fraction 16 collected from this later region was more complex, showing a broad shoulder at 320 nm and features in the 420 nm and 600 nm regions (Figure 3.8B). SDS PAGE showed fraction 16 contained predominantly the SufB, SufC, and SufD proteins with little to no SufS (Figure 3.8B, inset). The spectrum was similar to the spectrum for His_6-$SufBC_2D$ isolated from *E. coli* cells co-expressing *sufBCD* and *sufSE*.[10] The spectrum is consistent with sub-stoichiometric amounts of Fe-S cluster or partially degraded Fe-S cluster due to the aerobic purification technique.

As a result of our interest in the complex kinetics observed for the "mixed" $SufBC_2D$ complex, we separately measured the ATPase activity of each HIC fraction containing SufB, SufC, and SufD before pooling any fractions for further purification (Figure 3.9A). Equal volumes of each fraction were added to initiate the ATPase reaction. Higher rates of ATPase activity were observed in the fractions containing SufB,

SufC, and SufD that eluted later in the elution profile. Although the Suf proteins were not completely pure at this first column step, the approximate amounts of SufB, SufC, and SufD proteins in each fraction were similar (Figure 3.8A). For example, immunoblots indicated similar SufC protein levels in fractions 13 and 16 (data not shown), but the ATPase activity of fraction 16 (18.3 μM min^{-1}) was ten times higher than that of fraction 13 (1.7 μM min^{-1}) (Figure 3.9A).

Chemical analysis of HIC fractions revealed higher levels of both iron and acid-labile sulfide in fractions from later in the elution profile (Figure 3.9B). We note that the increased iron and sulfide levels correlate with the increased ATPase activity of the later fractions (compare Figures 3.9A and 3.9B). The unusual *h* constant we observed in Figure 3.4 could be due to a mixture of active and inactive $SufBC_2D$, so the fractions from the different regions of the elution profile were pooled separately and purified in parallel. SufB, SufC, and SufD from each HIC pooled sample subsequently co-eluted from the anion exchange column (Q Sepharose) at identical salt concentrations (Figure 3.10A). Analytical size exclusion analysis showed the SufB, SufC, and SufD proteins from the two separate pools eluted at identical apparent molecular weights (Figure 3.10B). The molecular masses were consistent with a $SufBC_2D$ complex. For final yields, early fractions from the HIC column accounted for approximately 76% of total $SufBC_2D$ isolated; while later fractions contained approximately 24% of total $SufBC_2D$. The iron content of $SufBC_2D$ purified to homogeneity varied from prep to prep, however $SufBC_2D$ with the lower ATPase activity (< 0.07 Fe per complex) consistently retained less iron than $SufBC_2D$ with the higher ATPase activity (0.1 - 0.3 Fe per complex). Upon completion of the final steps of the purification, each $SufBC_2D$ complex was

largely colorless. By SDS PAGE, each $SufBC_2D$ complex showed equal levels of purity after the final steps (Figure 3.10B). In summary, ATPase activity measurements, UV-Vis absorption spectroscopy, and chemical analysis indicate the potential isolation of two separate $SufBC_2D$ complexes at the first step of purification (HIC).

The steady state ATPase activity of each isolated $SufBC_2D$ complex was then measured separately to ensure the initial difference in ATPase activity observed at the HIC column step was maintained throughout the purification. $SufBC_2D$ isolated from early HIC fractions had an ATPase activity hyperbolically dependent on ATP concentration. Fitting the data to the Michaelis Menten equation gave a K_m of 133 µM and a k_{cat} of 0.043 s^{-1}. This k_{cat} value is four times faster than the k_{cat} value of His_6-$SufB_2C_2$ but fifty times slower than the ATP turnover rate by "mixed" $SufBC_2D$ (Table 3.2). $SufBC_2D$ isolated from the early HIC fractions will be referred to as "low activity" $SufBC_2D$ throughout the remainder of this text. $SufBC_2D$ isolated from later HIC fractions also exhibited Michaelis Menten behavior and yielded a K_m of 133.1 µM and k_{cat} of 1.72 s^{-1}. $SufBC_2D$ isolated from the later HIC fractions will be referred to as "high activity" $SufBC_2D$. The k_{cat} of "mixed" $SufBC_2D$ is approximately 20% the k_{cat} of "high activity" $SufBC_2D$, which roughly correlates with our observation that high activity $SufBC_2D$ only accounts for 24% of total $SufBC_2D$ protein isolated in a normal prep. Our data supports that a $SufBC_2D$ complex with impaired ATPase activity was the reason for "mixed" $SufBC_2D$ deviation from Michaelis Menten kinetics and not negative cooperativity.

A

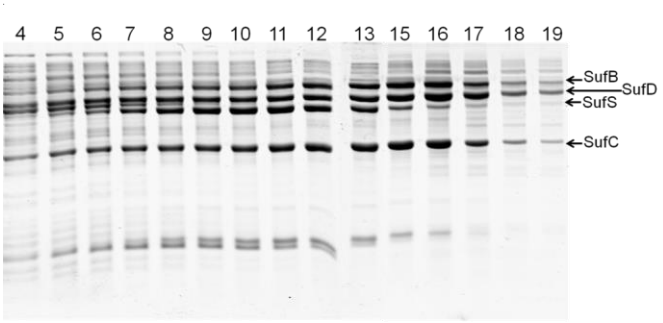

B

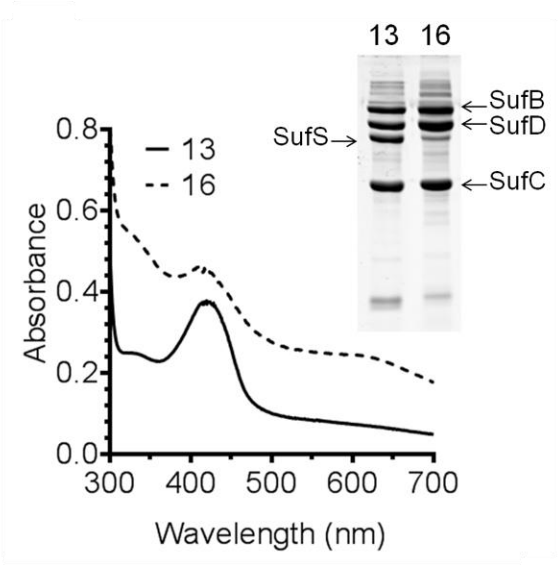

Figure 3.8 (A) SDS PAGE of HIC fractions containing SufB, SufC, and SufD proteins. (B) UV-visible absorption spectra of fractions 13 (solid) and 16 (dashed) from HIC column, representative of low activity and high activity $SufBC_2D$ samples, respectively. *Inset*, SDS PAGE (15%) of HIC fractions 13 and 16.

A

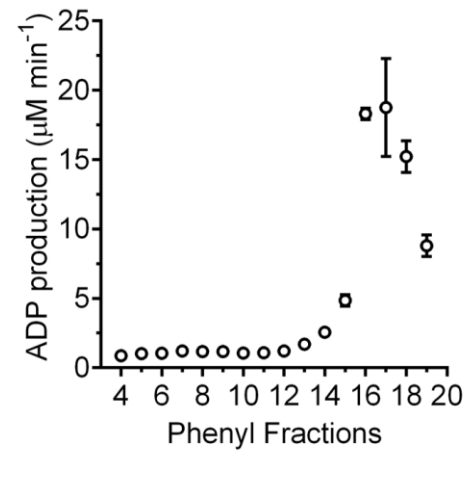

B

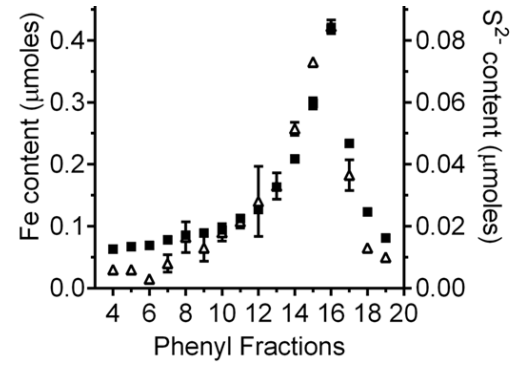

Figure 3.9 (A) Steady state rate of ADP production at 1mM ATP of each HIC fraction. 2μL of each fraction added to initiate the reaction. (B) Average iron (closed square) and acid-labile sulfide (open triangle) content of each HIC fraction (in μmoles). Absolute amounts varied from prep to prep, but the trend is reproducible.

A

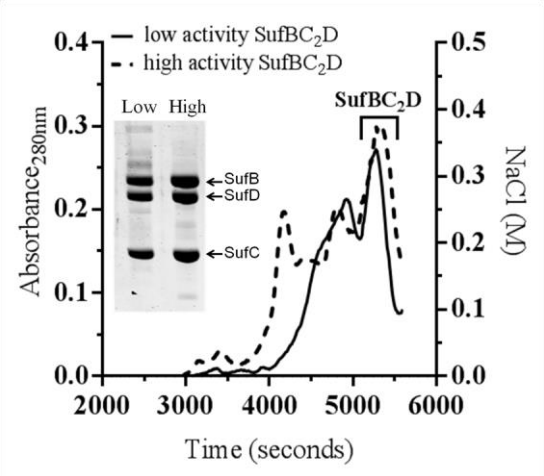

B

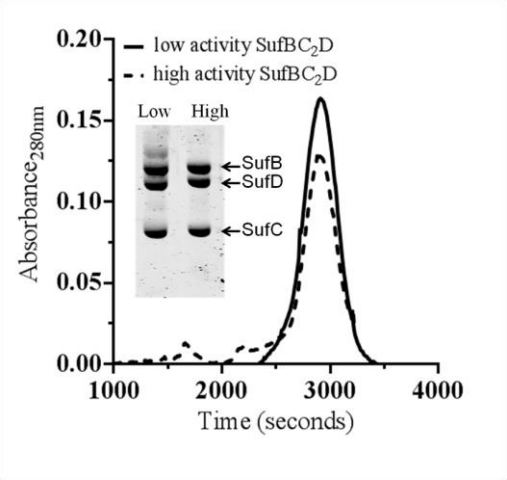

Figure 3.10 Isolation of $SufBC_2D$ complexes. (A) Anion exchange elution profile of low activity (solid) and high activity (dashed) $SufBC_2D$. *Inset*, SDS PAGE analysis of $SufBC_2D$ from Q Sepharose column. (B) Size exclusion elution profile of low activity (solid) and high activity (dashed) $SufBC_2D$. *Inset*, SDS PAGE of final $SufBC_2D$ complexes.

Table 3.2 Kinetic parameters of SufC, $SufB_2C_2$, and $SufBC_2D$

Protein	K_m (μM)	k_{cat} (s^{-1})
SufC[a]	59.2 ± 5.9	1.9 X 10^{-4}
His_6-$SufB_2C_2$[b]	71.5 ± 4.1	2.5 X 10^{-2}
Mixed $SufBC_2D$[c]	26.9 ± 0.3[f]	0.29[f]
Low $SufBC_2D$[d]	133 ± 10	4.3 X 10^{-2}
High $SufBC_2D$[e]	133 ± 11	1.72

[a]5 μM SufC per reaction. [b]2 μM His_6-$SufB_2C_2$ per reaction. [c]750 nM mixed $SufBC_2D$ per reaction. [d]1 μM low activity $SufBC_2D$ per reaction. [e]100 nM high activity $SufBC_2D$ per reaction. [f]Values based on *K'* and V_{max} determined from fitting data to allosteric sigmoidal equation.

Interaction of His_6-$SufB_2C_2$ and the $SufBC_2D$ complexes with mant-nucleotides. Many ATP derivatives have been synthesized to probe the mechanism of the ATP cycle in biosystems.[22, 23] The structure of ATP contains multiple aromatic systems and thus absorbs strongly in the UV region (259 nm) (Figure 3.11A). Substitution of an aromatic ring (mant- group) at the ribose group of ATP generates a fluorescent ATP derivative that serves as a more-sensitive probe for spectroscopic studies (Figure 3.11B). Fluorescent analogues 2' or 3' – *O* – (N-methylanthraniloyl)- (mant) ATP and mantADP were designed to report on the action of ATP with minimal effect on its properties.[23] The pre-steady state kinetics of SufC and SufBC and SufCD complexes from *T. maritima* have been studied using fluorescent mantATP and mantADP. Petrovic et al reported SufBC and SufCD complexes bind mantATP and mantADP more tightly than SufC alone.[6-8] Here mant-nucleotides were employed to determine which step in the ATP hydrolysis cycle may be impaired in low activity $SufBC_2D$. Binding of His_6-$SufB_2C_2$ and $SufBC_2D$ with mant-nucleotides was investigated by kinetic methods. Experiments were performed under pseudo-first order conditions with excess nucleotide. The presence of one Trp residue on SufC, seven Trp residues on SufB, and three Trp residues on SufD allowed us to monitor mant-nucleotide binding by fluorescence resonance energy transfer (FRET). In this method, Trp residues are excited at 280 nm and the emission from resonance energy transfer to the mant-group on the nucleotide is measured by an increase in fluorescence intensity.

Pre-steady state kinetics of mantATP binding to His_6-$SufB_2C_2$ and $SufBC_2D$ complexes. His_6-$SufB_2C_2$ was mixed with 10-50 μM mantATP in a stopped-flow instrument. A time-dependent increase in fluorescence intensity showed deviation from a

single exponential fit (Figure 3.12). The data was best fit to a double exponential to account for a slow second phase that was well resolved from the fast initial phase in rate constant and amplitude. Under pseudo-first order conditions, the observed rate constants (k_{obs}) of the fast phase were linearly dependent on mantATP concentration:

$$k_{obs} = k_{on}[\text{mantATP}] + k_{off}$$

The second order association rate constant (k_{on}) for His_6-$SufB_2C_2$-mantATP determined from the slope was 1.78 X 10^5 M^{-1} s^{-1} (Figure 3.13A). The dissociation rate constant (k_{off}) determined from the y-intercept was 7.9 s^{-1}. His_6-$SufB_2C_2$ binding affinity for mantATP determined from the ratio of dissociation and association rate constants (K_d = k_{off} / k_{on}) was 45.2 µM. The k_{obs} of the slow phase (~0.10 s^{-1}) was not dependent on mantATP concentration (Figure 3.13B). We propose that the second phase represents a conformational change in His_6-$SufB_2C_2$ as a result of mantATP binding at the active site in SufC. These results are consistent with affinity chromatography data that shows that the presence of nucleotide (Mg-ATP or ADP) enhances an otherwise unstable interaction between SufC and His-SufB (Chapter 2 of this study).

For high and low activity $SufBC_2D$, the data were best fit to a single exponential (Figure 3.12). The k_{on} values for low and high activity $SufBC_2D$ were similar, 4.39 X 10^5 M^{-1} s^{-1} and 4.02 X 10^5 M^{-1} s^{-1}, respectively. The k_{off} value for low activity $SufBC_2D$ determined from the y-intercept was 5.8 s^{-1}, giving a K_d of 13.3 µM. High activity $SufBC_2D$ k_{off} was 5.4 s^{-1}, and the calculated binding affinity for mantATP was 13.4 µM (Figure 3.13A). Our results reveal the observed difference in ATPase activities between high and low activity $SufBC_2D$ is not due to a difference in the ATP binding step of the ATP hydrolysis cycle. We also determined mantATP binds more tightly to $SufBC_2D$

than to His_6-$SufB_2C_2$, which may partially explain the greater ATPase activity of $SufBC_2D$ compared to His_6-$SufB_2C_2$ (Table 3.2).

Pre-steady state kinetics of mantADP binding to His_6-$SufB_2C_2$ and $SufBC_2D$ complexes. The kinetics of mantADP binding was investigated as described for mantATP. In this case, His_6-$SufB_2C_2$ data followed a single exponential process at all mantADP concentrations (Figure 3.14A). The second order association rate constant for His_6-$SufB_2C_2$ was 1.37 X 10^6 M^{-1} s^{-1}. The y-intercept value, corresponding to the dissociation rate constant, was 9.3 s^{-1}. The calculated K_d of mantADP binding was 6.79 μM. Time courses of mantADP binding to both $SufBC_2D$ complexes followed single exponentials with k_{obs} values that were linearly dependent on mantADP concentration (Figure 3.14A). Using the association (1.60 X 10^6 M^{-1} s^{-1}) and dissociation (3.6 s^{-1}) rate constants determined from the slope and y-intercept, respectively, the K_d of mantADP binding to low activity $SufBC_2D$ was calculated to be 2.24 μM. High activity $SufBC_2D$ had similar rate constants and binding affinity for mantADP (k_{on} = 1.34 X 10^6 M^{-1} s^{-1}, k_{off} = 7.5 s^{-1}, K_d = 5.61 μM).

In the previous section, to determine mant-ADP dissociation rate constants from His_6-$SufB_2C_2$ and $SufBC_2D$, we used the dissociation rate constant obtained from the y-intercept values of the second-order plot (Figure 3.14A). To determine the accuracy of the y-intercept values, we directly measured the rate of mantADP dissociation from His_6-$SufB_2C_2$ and $SufBC_2D$ using unlabeled ADP. The dissociation of mantADP from His_6-$SufB_2C_2$ and $SufBC_2D$ was measured by mixing 1 mM unlabeled ADP with a pre-formed protein-mantADP complex. Unlabeled ADP should displace mantADP from the nucleotide binding site in SufC. The time course of mantADP dissociation from all

SufBCD complexes followed a single exponential with similar rate constants (3.69 s^{-1}, 5.18 s^{-1}, and 5.14 s^{-1}) (Figure 3.14B). These values are in agreement with the values estimated from the y-intercept values from the mantADP association kinetics (Figure 3.14A). The mantADP binding affinities determined from the ratio of association and experimentally measured dissociation rate constants were 2.69 μM for His_6-$SufB_2C_2$, 3.24 μM for low activity $SufBC_2D$, and 3.84 μM for high activity $SufBC_2D$. The results show His_6-$SufB_2C_2$ and both $SufBC_2D$ complexes bind and release mantADP similarly. The results suggest a slower ADP release step does not contribute to the diminished ATPase activity observed in low activity $SufBC_2D$.

We attempted to activate the ATPase activity of "low activity" $SufBC_2D$. We proposed a modification of the enzyme contributes to the observed impaired activity. A common modification is disulfide bond formation between Cys residues. TCEP is a strong reductant that irreversibly cleaves disulfide bonds. The ATPase activity of "low activity" $SufBC_2D$ was measured after reduction with TCEP compared to DTT (Figure 3.15A). Bacterioferritin (Bfr) is a proposed *in vivo* iron donor for the Suf pathway. We tested if Fe-loaded Bfr could enhance the activity of "low activity" $SufBC_2D$ (Figure 3.15B). Finally, we attempted to activate "low activity" $SufBC_2D$ with different iron sources. Equimolar amounts of Fe-S-bound SufA (holo-SufA) and Apo-SufA alone and with iron salts ferrous ammonium sulfate (FAS) and iron chloride ($FeCl_3$) were incubated with $SufBC_2D$ and ATPase activity measured. Results are summarized in Table 3.3. Attempts to enhance "low activity" $SufBC_2D$ activity were unsuccessful.

A

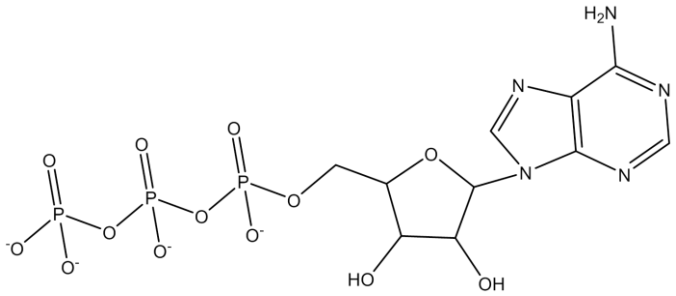

B

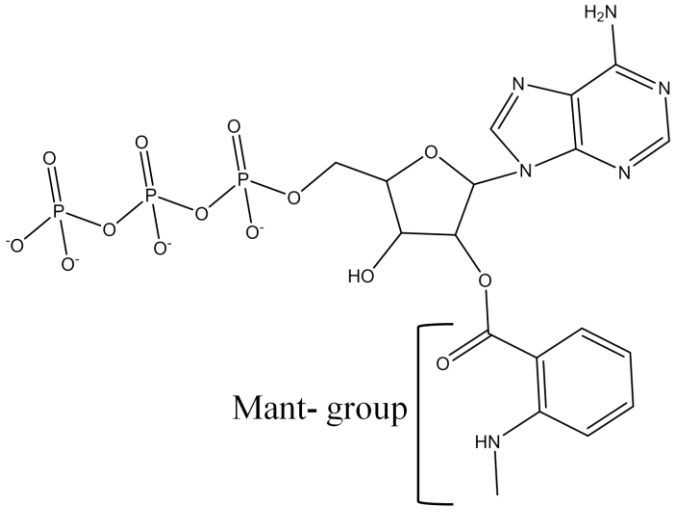

Figure 3.11 (A) Structure of ATP molecule. (B) Structure of mantATP molecule. Mant group substitutes a OH group on the ribose moiety of ATP.

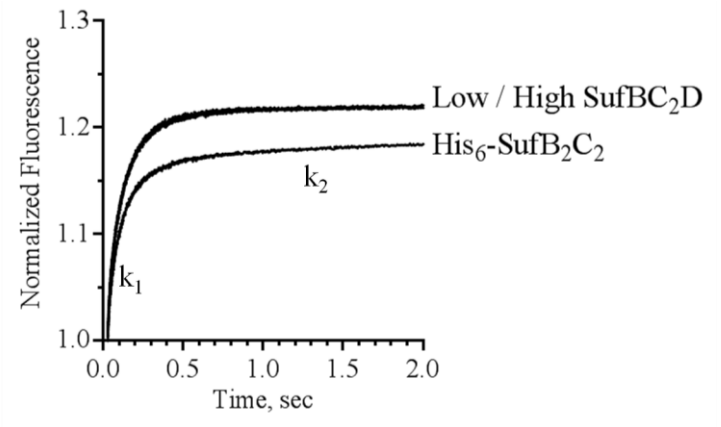

Figure 3.12 Interaction of His_6-$SufB_2C_2$ and $SufBC_2D$ complexes with mantATP. Stopped-flow fluorescence intensity recorded upon mixing 1 µM His_6-$SufB_2C_2$ or $SufBC_2D$ with 10 µM mantATP. k_1 is the rate of the fast mantATP binding process. k_2 is the rate of a slow second exponential process observed only in His_6-$SufB_2C_2$ binding data.

A

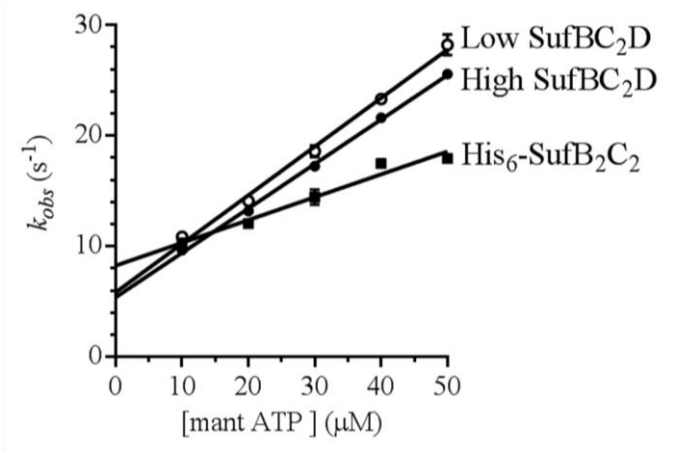

B

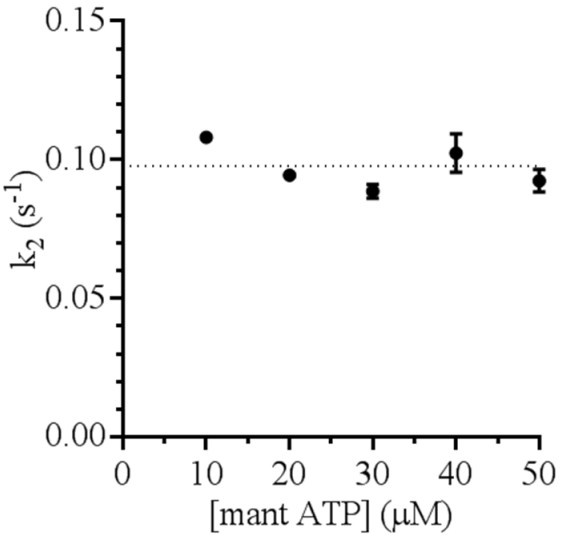

Figure 3.13 Interaction of His_6-$SufB_2C_2$ and $SufBC_2D$ complexes with mantATP. (A) Rate constant of fast phase (k_1) plotted against mantATP concentrations. Solid line is the best linear fit to the data. (B) Plot of k_2 from His_6-$SufB_2C_2$ binding data plotted against mantATP concentrations. The *dotted line* represents the average value obtained for k_2, 0.10 s^{-1}.

A

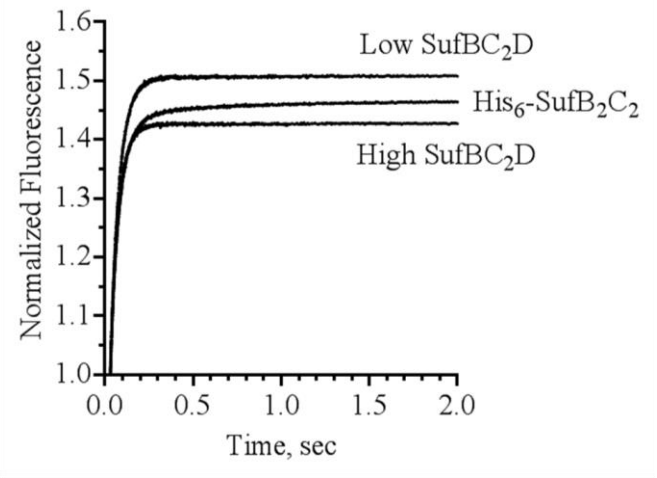

B

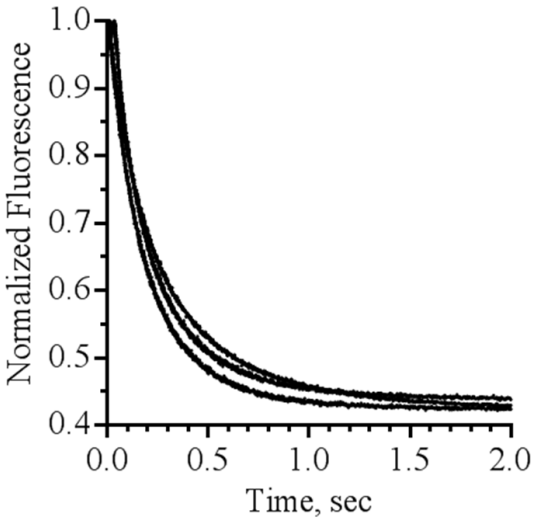

Figure 3.14 Interaction of His_6-$SufB_2C_2$ and $SufBC_2D$ complexes with mantADP. (A) Stopped-flow fluorescence intensity recorded upon mixing 1 µM His_6-$SufB_2C_2$ or $SufBC_2D$ with 10 µM mantADP. (B) Displacement of mantADP from His_6-$SufB_2C_2$ or $SufBC_2D$ by unlabeled ADP. Stopped-flow fluorescence intensity recorded upon mixing 1 mM ADP with a pre-incubated mixture of 750 nM protein and 30 µM mantADP.

A

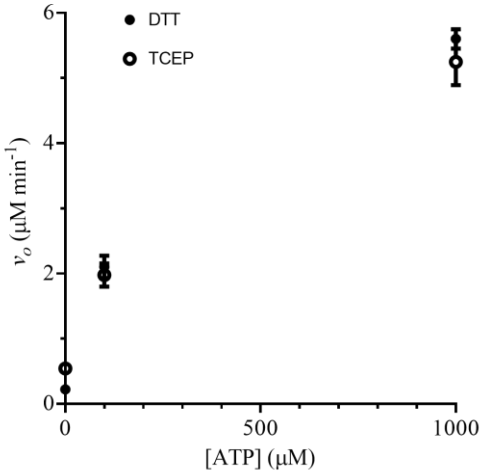

B

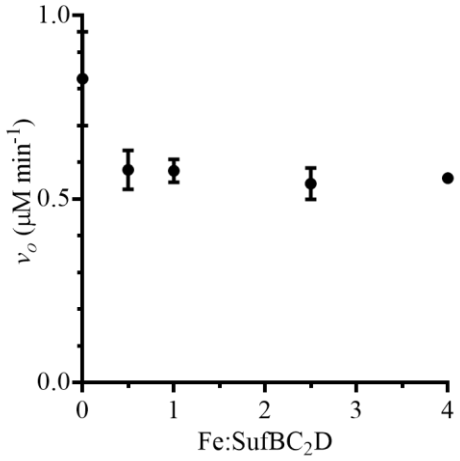

Figure 3.15 Attempts to activate "low activity" SufBC$_2$D. (A) SufBC2D ATPase activity at 0, 0.1, and 1 mM Mg^{2+}-ATP. "Low activity" SufBC$_2$D treated with 2mM DTT (closed) and TCEP (open) for 30 minutes prior to measurements. (B) "Low activity" SufBC$_2$D ATPase activity at increasing concentrations of Fe-bound Bfr. Measurements performed in triplicate. Error bars are indicated.

Table 3.3 "Low activity" $SufBC_2D$ ATPase activity in the presence of Fe sources

Protein	Fe sources added									
$SufBC_2D$[a]	+	+	+	+	+	+	+	+	+	+
Apo-SufA		+					+	+	+	+
Holo-SufA[b]			+							
Fe-Bfr[c]				+						
Fe source										
FAS[d]					+		+		+[e]	
$FeCl_3$						+		+		+[e]
v_o (μM min^{-1})[f]	4.8	5.1	4.8	5.0	4.5	4.8	4.8	4.7	4.3	5.0

[a]Equimolar amounts of protein used in each experiment. [b]Holo-SufA is Fe-S-bound SufA. [c]90 Fe per Bfr. [d]FAS is ferrous ammonium sulfate. [e]Four times more FAS or $FeCl_3$. [f]Values are the average of three experiments.

3.4 Discussion

In this study, we investigate the steady state and transient kinetics of the SufC ATPase from *E. coli*. The kinetic properties of SufC alone are compared to the Fe-S scaffold complexes $SufBC_2D$ and His_6-$SufB_2C_2$. Kinetics of SufBC, SufCD, and SufBCD complexes from *T. maritima*[7] and *T. thermophilus* HB8[9], respectively, have been studied, but there is currently no kinetic characterization of the SufBCD complexes isolated from *E. coli*. This is the first kinetic analysis of ATP binding and hydrolysis of $SufBC_2D$.

In agreement with SufC structural characterization and kinetic studies of SufC homologs,[3, 5, 6, 8, 9, 17, 18] *E. coli* SufC possesses very low intrinsic ATPase activity. The k_{cat} value for *E. coli* SufC is lower than the reported activities of SufC homologs. For example, SufC from *E. coli* turns over ATP six times slower than SufC isolated from *T. thermophilus* HB8 and two hundred times slower than SufC from *T. maritima* and *P. falciparum*. SufC from *E. coli* and *T. thermophilus* HB8 share 52% sequence identity and have similar tertiary structures according to the published crystal structures.[3, 5] However, major differences are observed at the D-loop structures (Figure 3.16). The D-loop in *E. coli* SufC is a flexible loop. In contrast, the D-loop in *T. thermophilus* HB8 SufC is a rigid 3_{10} helix stabilized by hydrogen bonds. This structural difference suggests a difference in the mechanism of ATP hydrolysis by SufC. It is difficult to explain the differences in ATPase activity observed among the SufC homologs without structures of the other SufC homologs. The structure of SufC monomer reveals that the proposed catalytic base Glu171 is rotated away from the active site and engaged in a salt-bridge with Lys152.[3] The Glu171-Lys152 salt-bridge in the SufC monomer structure explains

the low ATPase activity of SufC. The SufC active site is not in an optimal state to efficiently bind ATP or catalyze ATP hydrolysis.

The precise role of SufC ATP hydrolysis during Suf Fe-S cluster assembly is still unclear. We have established that ATP hydrolysis depends on SufC association with SufB and SufD in a $SufB_2C_2$ or $SufBC_2D$ complex. The rate of ATP turnover by His_6-$SufB_2C_2$ is 100-times faster than SufC yet 10-times slower than $SufBC_2D$, suggesting independent roles or mechanisms of ATP hydrolysis. Why the rate of ATP turnover is doubled in low activity $SufBC_2D$ and 70-times greater in high activity $SufBC_2D$ compared to His_6-$SufB_2C_2$ remains unclear in the absence of resolved structures. Fluorescent mant-adenine nucleotide analogs are commonly used to study the binding kinetics of ATPases.[22, 23] We used a similar methodology to study the mechanism of the ATP cycle in His_6-$SufB_2C_2$ and $SufBC_2D$ complexes. A major finding was that the initial binding of mantATP was much tighter to $SufBC_2D$ than to His_6-$SufB_2C_2$. This was a result of doubled association rate constants and slightly slower dissociation constants for both $SufBC_2D$ complexes compared to His_6-$SufB_2C_2$. Following the initial exponential increase in fluorescence measuring the rate of mantATP binding to His_6-$SufB_2C_2$, there was a subtle increase of fluorescence over the next 60 seconds. This second exponential increase over time was not observed in the $SufBC_2D$ complexes. The rate of the second phase was more than 100-times slower than the rate of the first phase and was not dependent on mantATP concentration. We attribute this second process to a nucleotide-induced structural change in SufC that allows better binding to His_6-SufB in the absence of SufD. We recently determined that SufC has a weaker affinity for SufB when SufD is not present (Figure 2.4), but SufC binds SufB more tightly in the presence

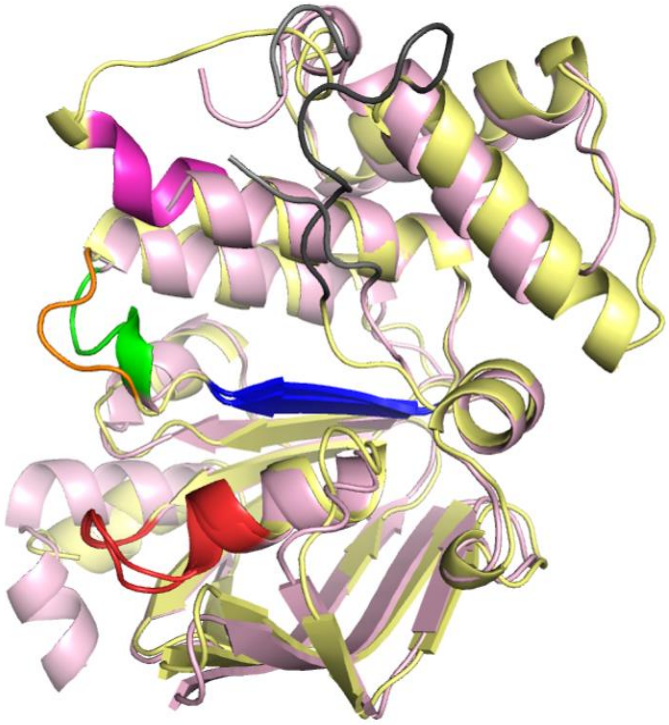

Figure 3.16 Structural alignment of SufC monomer from *E. coli* (yellow)[3] and *T. thermophilus* HB8 (pink).[5] Walker A (red), Walker B (blue), ABC signature (magenta), and Q-loop (grey) motifs are colored. D-loops of SufC from *E. coli* and *T. thermophilus* HB8 are colored orange and green, respectively.

of ATP or ADP. The affinity of SufC for SufB appears to be stronger in the $SufBC_2D$ complex. We proposed that His_6-$SufB_2C_2$ is a transient complex that is maintained for Suf function only when SufC accesses ATP. The observed second exponential phase could be detecting structural changes occurring in SufC to accommodate the mantATP and/ or structural changes occurring in SufB as a result of its association with mantATP-bound SufC.

The SufC subunits are spatially separated in the crystal structure of $SufC_2D_2$.[4] Crosslinking experiments provide evidence that the SufC subunits form a dimer in the presence of Mg-ATP.[4] ATP binding likely induces SufC dimerization prior to ATP hydrolysis as reported for the ATPase domains of ABC transporters. The second exponential process could also be detecting dimerization of the SufC subunits in His_6-$SufB_2C_2$. A similar process would need to occur in $SufBC_2D$ to initiate ATP hydrolysis. Our results suggest a structural change in His_6-$SufB_2C_2$ caused by mantATP binding that is slow and thus detectable under our experimental conditions. Any mantATP induced structural changes that occur in the $SufBC_2D$ complexes are probably very rapid and stable under identical experimental conditions. Binding of mantADP to His_6-$SufB_2C_2$ and $SufBC_2D$ was also a second-order process. The similar association and dissociation rate constants indicate each SufBCD complex has comparable binding affinities for ADP.

The role of the two conformations of $SufBC_2D$ is still under investigation. Both conformations have identical K_m values for Mg-ATP and similar binding affinities for mantATP and mantADP, yet the k_{cat} value was forty times faster for high activity $SufBC_2D$ compared to low activity $SufBC_2D$. The basic ATP hydrolysis cycle involves three steps: ATP binding, ATP hydrolysis, and ADP and inorganic phosphate release.

Nucleotide-bound enzyme intermediates may also be a part of the ATP hydrolysis mechanism. We are currently optimizing a molybdate colorimetric assay that monitors phosphate in solution to directly measure the rate of the ATP cleavage step by SufC and the aforementioned SufBCD complexes. We expect rates of ATP cleavage to be comparable between His_6-$SufB_2C_2$ and low activity $SufBC_2D$ but accelerated in high activity $SufBC_2D$.

In this study, we determined that two conformations of $SufBC_2D$ can be isolated from *E. coli* cells over-expressing the *sufABCDSE* genes. Low activity $SufBC_2D$ does not bind the HIC column as tightly as high activity $SufBC_2D$, and high activity $SufBC_2D$ is isolated with higher levels of iron and sulfide. Due to the diminished iron and sulfide levels, low activity $SufBC_2D$ is considered an apo-form of $SufBC_2D$ that has either not performed Fe-S cluster assembly yet or has already transferred its cluster to target proteins at the time of cell harvesting. High activity $SufBC_2D$ is considered a holo-form of $SufBC_2D$ that is trapped in the process of assembling an Fe-S cluster at the time of cell harvesting. The ATPase MalK shows enhanced activity when the maltose-bound maltose binding protein (MBP) binds the $MalFGK_2$ ABC transporter for maltose cellular import.[25] We propose a structural modification to one of the $SufBC_2D$ conformations prior to or during Fe-S cluster assembly that impairs or stimulates ATP hydrolysis, respectively. Thorough structural analysis is needed to understand why the ATPase activity is much greater in one $SufBC_2D$ conformation compared to the other.

3.5 References

1. Ayala-Castro, C., Saini, A., and Outten, F. W. (2008) Fe-S cluster assembly pathways in bacteria. *Microbiol Mol Biol Rev* 72, 110-125.

2. Nachin, L., El Hassouni, M., Loiseau, L., Expert, D., and Barras, F. (2001) SoxR-dependent response to oxidative stress and virulence of *Erwinia chrysanthemi*: the key role of SufC, an orphan ABC ATPase. *Mol Microbiol* 39, 960-972.

3. Kitaoka, S., Wada, K., Hasegawa, Y., Minami, Y., Fukuyama, K., and Takahashi, Y. (2006) Crystal structure of *Escherichia coli* SufC, an ABC-type ATPase component of the SUF iron-sulfur cluster assembly machinery. *FEBS Lett* 580, 137-143.

4. Wada, K., Sumi, N., Nagai, R., Iwasaki, K., Sato, T., Suzuki, K., Hasegawa, Y., Kitaoka, S., Minami, Y., Outten, F. W., Takahashi, Y., and Fukuyama, K. (2009) Molecular dynamism of Fe-S cluster biosynthesis implicated by the structure of the $SufC_2$-$SufD_2$ complex. *J Mol Biol* 387, 245-258.

5. Watanabe, S., Kita, A., and Miki, K. (2005) Crystal structure of atypical cytoplasmic ABC-ATPase SufC from *Thermus thermophilus* HB8. *J Mol Biol* 353, 1043-1054.

6. Eccleston, J. F., Petrovic, A., Davis, C. T., Rangachari, K., and Wilson, R. J. (2006) The kinetic mechanism of the SufC ATPase: the cleavage step is accelerated by SufB. *J Biol Chem* 281, 8371-8378.

7. Petrovic, A., Davis, C. T., Rangachari, K., Clough, B., Wilson, R. J., and Eccleston, J. F. (2008) Hydrodynamic characterization of the SufBC and SufCD complexes and their interaction with fluorescent adenosine nucleotides. *Protein Sci* 17, 1264-1274.

8. Rangachari, K., Davis, C. T., Eccleston, J. F., Hirst, E. M., Saldanha, J. W., Strath, M., and Wilson, R. J. (2002) SufC hydrolyzes ATP and interacts with SufB from *Thermotoga maritima*. *FEBS Lett* 514, 225-228.

9. Tian, T., He, H., and Liu, X. Q. (2013) The SufBCD protein complex is the scaffold for iron-sulfur cluster assembly in *Thermus thermophilus* HB8. *Biochem Biophys Res Commun* 443, 376-381.

10. Saini, A., Mapolelo, D. T., Chahal, H. K., Johnson, M. K., and Outten, F. W. (2010) SufD and SufC ATPase activity are required for iron acquisition during *in vivo* Fe-S cluster formation on SufB. *Biochemistry* 49, 9402-9412.

11. Chahal, H. K., and Outten, F. W. (2012) Separate Fe-S scaffold and carrier functions for $SufB_2C_2$ and SufA during *in vitro* maturation of [2Fe-2S] Fdx. *J Inorg Biochem* 116, 126-134.

12. Layer, G., Gaddam, S. A., Ayala-Castro, C. N., Ollagnier-de Choudens, S., Lascoux, D., Fontecave, M., and Outten, F. W. (2007) SufE transfers sulfur from SufS to SufB for iron-sulfur cluster assembly. *J Biol Chem* 282, 13342-13350.

13. Outten, F. W., Wood, M. J., Munoz, F. M., and Storz, G. (2003) The SufE protein and the SufBCD complex enhance SufS cysteine desulfurase activity as part of a sulfur transfer pathway for Fe-S cluster assembly in *Escherichia coli*. *J Biol Chem* 278, 45713-45719.

14. Beinert, H. (1983) Semi-micro methods for analysis of labile sulfide and of labile sulfide plus sulfane sulfur in unusually stable iron-sulfur proteins. *Anal Biochem* 131, 373-378.

15. Riemer, J., Hoepken, H. H., Czerwinska, H., Robinson, S. R., and Dringen, R. (2004) Colorimetric ferrozine-based assay for the quantitation of iron in cultured cells. *Anal Biochem* 331, 370-375.

16. Monk, B. C., and Kellerman, G. M. (1976) A rapid method for the assay of mitochondrial ATPase activity. *Anal Biochem* 73, 187-191.

17. Kumar, B., Chaubey, S., Shah, P., Tanveer, A., Charan, M., Siddiqi, M. I., and Habib, S. (2012) Interaction between sulphur mobilisation proteins SufB and SufC: evidence for an iron-sulphur cluster biogenesis pathway in the apicoplast of *Plasmodium falciparum*. *Int J Parasitol* 41, 991-999.

18. Nachin, L., Loiseau, L., Expert, D., and Barras, F. (2003) SufC: an unorthodox cytoplasmic ABC/ATPase required for [Fe-S] biogenesis under oxidative stress. *Embo J* 22, 427-437.

19. Wollers, S., Layer, G., Garcia-Serres, R., Signor, L., Clemancey, M., Latour, J. M., Fontecave, M., and Ollagnier de Choudens, S. (2010) Iron-sulfur (Fe-S) cluster assembly: the SufBCD complex is a new type of Fe-S scaffold with a flavin redox cofactor. *J Biol Chem* 285, 23331-23341.

20. Brand, L., and Gohlke, J. R. (1972) Fluorescence probes for structure. *Annu Rev Biochem* 41, 843-868.

21. Cardamone, M., and Puri, N. K. (1992) Spectrofluorimetric assessment of the surface hydrophobicity of proteins. *Biochem J* 282 589-593.

22. Bagshaw, C. (2001) ATP analogues at a glance. *J Cell Sci* 114, 459-460.

23. Jameson, D. M., and Eccleston, J. F. (1997) Fluorescent nucleotide analogs: synthesis and applications. *Methods Enzymol* 278, 363-390.

24. Hung, L. W., Wang, I. X., Nikaido, K., Liu, P. Q., Ames, G. F., and Kim, S. H. (1998) Crystal structure of the ATP-binding subunit of an ABC transporter. *Nature* 396, 703-707.

25. Gould, A. D., Telmer, P. G., and Shilton, B. H. (2009) Stimulation of the Maltose Transporter ATPase by Unliganded Maltose Binding Protein. *Biochem* 48, 8051-8061.

CHAPTER 4

Suf post-translational regulation in *Escherichia coli*

Abstract

In *Escherichia coli*, the *sufABCDSE* operon is activated to build Fe-S clusters under iron starvation and oxidative stress, conditions that can perturb iron and sulfur homeostasis. Immunoblot analysis of cell lysates isolated from *E. coli* cells grown under normal conditions showed SufC and SufD are present. Under normal growth conditions, the housekeeping Isc pathway is the predominant Fe-S cluster assembly system. In our study, we examine the post-translational regulation of SufC and SufD proteins in response to variable growth conditions. Mass spectrometry analysis of recombinant SufC identified a phosphorylation site at residue Tyr241. Using phosphomimetic and nonphosphorylatable mutations, we investigate the effect of phosphorylation at Tyr241 on Suf function *in vivo* and *in vitro*. We also identify a phosphorylation site at Ser residue on native SufC isolated from *E. coli* cells grown under normal conditions. These results provide evidence that phosphorylation is a mode of regulation for Suf at the protein level.

4.1 Introduction

E. coli encodes operons for two distinct Fe-S cluster assembly pathways: *iscRSUA-hscBA-fdx* and *sufABCDSE*. The *isc* operon encodes the main Fe-S cluster assembly machinery. The *suf* genes encode a stress-responsive pathway induced by oxidative stress and iron starvation.[1] Transcriptional regulation of the *isc* and *suf* genes has been well characterized in *E. coli*. Transcription of the *isc* operon is mediated by IscR. Regulation of the *suf* operon is much more complex, requiring OxyR, integration host factor (IHF), and IscR for oxidative stress response and Fur in response to iron deprivation. In unstressed cells, basal *suf* transcripts are maintained at low levels due to repression of transcription by Ferric uptake regulator (Fur). Demetallation of the iron sensing Fur in iron limiting conditions causes derepression of *suf* while oxidized OxyR and apo-IscR up-regulate the transcription of the *suf* genes in oxidative stress conditions.[2-7]

Comparison of intracellular SufC and SufD protein levels in normal and oxidative stress or iron starvation conditions establishes Suf proteins are present in the cell even without exposure to stress. This finding is consistent with the previously reported measurable basal levels of the *suf* transcript. We propose that Suf is present in the cell but turned "off" when Isc is the preferred Fe-S cluster assembly pathway. This led us to explore the possible regulation of the Suf proteins at the protein level. Phosphorylation is one of the most common covalent modifications used to regulate protein levels and activity. Regulation of Fe-S cluster assembly and/or stability via phosphorylation has been observed in the Fe-S cluster dependent iron regulatory protein 1 (IRP1).[8, 9] IRP1 is a Fe-S cluster dependent protein with cytosolic aconitase activity that is also capable of

binding RNA. Increased intracellular iron levels promote [4Fe-4S] cluster assembly on IRP1. Brown et al reports that substitution of phosphosite Ser138 with phospho-mimetic mutation Glu contributes to increased susceptibility of the Fe-S cluster to oxygen.[10, 11] Substitution of phosphosite Ser711 with phosphomimetic Glu functionally inactivates IRP1, completely abolishing its aconitase and RNA-binding activities.[12]

$SufBC_2D$ is a novel [4Fe-4S] cluster assembly scaffold protein complex for the Suf pathway.[13-17] Multiple phosphorylation sites were mapped and confirmed by mass spectrometry on over-expressed recombinant SufBCD proteins purified from *E. coli*. Phosphorylated residues were identified in the recombinant SufB at Ser428, SufC at Tyr241 and Ser141, and SufD at Tyr374 (A. Saini and F. W. Outten, unpublished data). We recently identified a phosphorylated residue on chromosomally encoded SufC purified from endogenous expression, providing evidence that SufC is phosphorylated *in vivo* (this study). The phosphorylated residues found in *E. coli* SufC and SufD are conserved in the pathogenic *Mycobacterium tuberculosis* and other Suf homologues. Tyrosine phosphorylation of *E. coli* native SufD has also been observed under normal growth conditions. Levels of phosphorylation on SufD diminish under oxidative stress conditions where the Suf system is required for growth. The results suggest phosphorylation may be used to keep SufD inactive until it is needed for stress-responsive cluster assembly. In this study, we investigate the role of phosphorylation on SufC as a mechanism to regulate Fe-S cluster assembly by the Suf pathway in *E. coli*. Using site-directed mutagenesis of previously identified $SufBC_2D$ phosphorylation sites and enrichment of native Suf levels for phosphoprotein analysis by mass spectrometry,

we investigate the role of phosphorylation as a mechanism to regulate Fe-S cluster assembly by the Suf pathway in *E. coli*.

4.2 Materials and Methods

Site-directed mutagenesis. Site-directed mutagenesis of SufC Tyr241 (Y241) was done on the pBAD/*Myc*-His C vector (Invitrogen) co-expressing *sufABCDSE*.[16] The Tyr241 point mutation to Asp (D) used the following primers: upstream (5'-AAACAACTGGAGGAGCAGGGTGATGGCTGGCTTACCGAACAGCAG-3') and downstream (5'-CTGCTGTTCGGTAAGCCAGCCATCACCCTGCTCCTCCAGTTG TTT-3'). Tyr241 point mutation to Phe (F) used the following primers: upstream (5'-AAACAACTGGAGGAGCAGGGTTTTGGCTGGCTTACCGAACAGCA G-3') and downstream (5'- CTGCTGTTCGGTAAGCCAGCCAAAACCCTGCTCCTCCAGTTG TTT-3'). Each 50 µL PCR reaction contained 1 µL (50 ng) vector template, 5 µL 10 X *Pfu* ultra reaction buffer, 2 µL 10 mM dNTP mix, 1 µL 10 µM of each primer, and 0.5 µL *Pfu* DNA polymerase in sterile water. PCR conditions were the following:

Initial denaturation		95°C	3 minutes
Denaturation	(1)	95°C	30 seconds
Annealing	(2)	55°C	30 seconds
Extension	(3)	68°C	24 minutes
Repeat steps 1-3 (15 times)			
Final Extension		68°C	10 minutes

PCR products were treated with *DpnI* restriction enzyme at 37°C for 2 hours then purified using phenol: chloroform extraction and ethanol precipitation. Plasmids

containing SufC mutations were transformed into DH5α competent cells and the mutation was confirmed by DNA sequencing. The resulting plasmids were over-expressed in *E. coli* Top10 cells, and mutant $SufBC_2D$ complexes containing SufC Y241D and SufC Y241F mutations were purified similarly to WT proteins. The $SufBC_2D$ complex was purified as described previously.[15] Iron content of proteins was determined colorimetrically using ferrozine as described previously.[18] Acid-labile sulfide content was determined by a previously reported method.[19] Protein purity was determined by SDS PAGE.

Oxidative stress and iron starvation treatments. 1 mL of overnight culture of *E. coli* MG1655 was diluted in 100 mL of fresh LB and grown at 37°C to mid-log phase. 25 mL of the culture was harvested and saved on ice; the rest of the culture was treated with 200 µM H_2O_2 (hydrogen peroxide stress) or 200 µM 2, 2'-dipyridyl (iron starvation) for 15 minutes. Cells were then harvested, washed with cold sterile 1 X PBS (20 mM Phosphate, pH 7.4, 150 mM NaCl) and stored at -80°C until use.

Strains for 2, 2'-dipyridyl and phenazine methosulfate (PMS) treatments were each initially grown in LB at 37°C overnight. The absorbance at 600 nm (OD_{600}) was measured then adjusted to 2.0 in 3 mL gluconate minimal media (1 X M9 minimal media, 0.2% gluconate, 0.02% $MgSO_4$, 0.1 mM $CaCl_2$, 0.0005% thiamine). 1 mL of cells was added to 100 mL gluconate minimal media without stress. 1 mL of cells was also added to 100 mL gluconate minimal media containing 125 µM 2, 2'-dipyridyl (iron starvation) or 3.5 µM PMS (superoxide stress). Cells were harvested after 18 hour growth at 37°C and washed with cold sterile 1 X PBS. Cell pellets were stored at -80°C until use.

Cell pellets were lysed with B-Per reagent (Bacterial Protein Extraction Reagent) (Thermo Scientific) and total protein concentrations of the lysates were measured using Bradford assay. Equal amounts of total protein (15-30 µg) were loaded for SDS PAGE and immunoblot analysis. SufC and SufD protein levels were detected using α-SufC (1:3000) and α-SufD (1:5000) antibodies.

In vivo growth assay. Strains were each grown in LB at 37°C overnight. Absorbance at 600 nm (OD_{600}) was measured then adjusted to 2.0 in 1mL gluconate minimal media. 20 µL of cells were added to 2 mL (1:100 dilution) of gluconate minimal media with increasing concentrations of 2, 2'-dipyridyl (0, 100, 150, 200, 250 µM) or phenazine methosulfate (0, 1, 2, 5, 10 µM). Final absorbance at 600 nm was measured after an 18 hour growth at 37°C. Growth assays were performed in triplicate.

In vitro Fe-S reconstitution. 150 µM pure WT and SufC Y241D mutant $SufBC_2D$ proteins were incubated in an anaerobic glove box (Coy) in 250 µL reconstitution buffer (25 mM Tris, pH 7.5, 150 mM NaCl) with 4 mM DTT for 1 hr. 0.6 µM SufSE, 6-fold excess ferrous ammonium sulfate (FAS), and 10-fold excess L-cysteine were added to initiate the reaction. Fe-S cluster formation was monitored by UV-Vis during the reconstitution.

Phosphotyrosine immunoprecipitation. Overnight cultures of MG1655 and MG1655*ΔsufABCDSE* were diluted 1:100 in fresh LB and grown at 37°C to mid-log phase. At OD_{600} = 0.5, cells were either harvested and stored at -80°C or treated with 1 mM H_2O_2 for 20 min. H_2O_2 stressed cells were then harvested. Half the cells were washed with cold 1 X PBS and stored at -80°C. The remaining half was washed twice with fresh LB and added to 100 mL fresh LB and grown for 20 additional minutes. Cells

were then harvested and stored at -80°C. Cell pellets were resuspended in cell lysis buffer (20 mM Tris-HCl, pH 7.5, 150 mM NaCl, 1 mM EDTA, 1 mM EGTA, 1% Triton X-100) containing 1 tablet protease inhibitor and 1 mM sodium orthovanadate (Na_3VO_4) and lysed by sonication on ice (power = 50%, pulse on = 1 sec, pulse off = 10 seconds, total time = 1 min). Total protein concentration of cleared lysates was measured by Bradford assay. 500 µg total protein was incubated with 25 µl immobilized α-phosphotyrosine antibody (Cell Signaling Technology) with gentle rocking at 4°C overnight. Lysate-beads mix was centrifuged and washed 5 times with cold cell lysis buffer. Washed bead pellets were resuspended in SDS sample buffer and boiled for 5 minutes at 95ºC. Samples were centrifuged at maximum speed for 1 min then the supernatant was removed and collected for SDS PAGE and immunoblot analysis. SufD protein levels were detected using α-SufD (1:4000) antibody.

Enrichment of $SufC_{His}$ and mass spectrometry. MG1655*$sufC_{His}$sufD* strain was constructed as described in Appendix A (this study). MG1655*$sufC_{His}$sufD* was grown in 8 Liters of LB at 37°C to an OD_{600} of 0.5 and harvested or induced with 300 µM H_2O_2 for 10 minutes. Cells were washed twice with 1 X TBS (50 mM Tris-HCl, pH 8.0, 150 mM NaCl), resuspended in 20 mL cold extract buffer (50 mM Tris-HCl, pH 8.0, 50 mM NaCl, 5 mM βME) with 1 mM PMSF, and lysed via sonication on ice (power = 50%, pulse on = 2 seconds, pulse off = 18 seconds, total time = 1 min per 1 L culture). The lysate was collected by spinning at 16,000 x g for 25 min at 4°C. Cleared lysate was loaded onto a Phenyl FF column (20 mL) (GE Healthcare) in line with a Biologic DuoFlow FPLC system. After a two column volume wash with buffer containing 50 mM Tris-HCl, pH 7.5, 100mM NaCl, 1M ammonium sulfate, 10 mM βME, $SufC_{His}$ eluted

with a decreasing gradient of 1-0 M ammonium sulfate. Pooled fractions were diluted with Hisprep Buffer A (25 mM Tris-HCl, pH 8.0, 300 mM NaCl, 2 mM imidazole) and loaded onto a Hisprep FF column (20mL) (GE Healthcare). After 4 column volume washes with 10% Hisprep Buffer B (Hisprep Buffer A + 500 mM imidazole), bound proteins were eluted stepwise with 25%, 50%, and 100% Buffer B. $SufC_{His}$ eluted at 25% Buffer B. Fractions were pooled and concentrated in 50-kDa MWCO filters. Sample purity was determined by SDS PAGE.

Each protein of interest was excised from the SDS PAGE gel and sent to Jennifer Bethard-Rutherford at the Mass Spectrometry Facility at Medical University of South Carolina (MUSC) for phosphopeptides analysis. Briefly, each sample was enzymatically digested with trypsin, enriched for phosphopeptides using immobilized titanium dioxide (TiO_2), and analyzed via liquid chromatography (LC)-electrospray ionization (ESI) - tandem mass spectrometry (MS/MS) on a linear ion trap mass spectrometer (LTQ XL, Thermo Finnigan) coupled to a Dionex Ultimate 3000 nano LC system. A 75 micron C-18 reversed phase LC column (Waters YMC, ODS AQ C18) was utilized with a 120 minute gradient in 0.2% formic acid from 2% acetonitrile to 60% acetonitrile. An 80 Dalton mass increase indicates a peptide is phosphorylated. A phosphopeptide was confirmed by searching MS/MS data against an *E. coli* protein identification database (Thermo Finnigan Bioworks 3.3.1 software). All peptide and phosphorylation site identifications were confirmed by manual inspection of the data.

4.3 Results

Significant intracellular Suf protein levels in unstressed cells. Transcription of the *suf* genes in *E. coli* is induced by oxidative stress and iron starvation. Genome-wide transcriptional analysis of *E. coli* cells treated with 1 mM H_2O_2 identify *sufB* (16-fold) and *sufC* (12-fold) as two of thirty genes strongly induced in response to H_2O_2 stress. Lee et al. report *sufA* is induced 11-fold in cells treated with 200 μM 2, 2'-dipyridyl.[3] The *suf* genes are also expressed at lower levels in unstressed conditions.[1] Immunoblot analysis of Suf protein levels in unstressed cells, H_2O_2 stressed cells (200 μM H_2O_2), and iron deprived cells (200 μM 2, 2'-dipyridyl) indicated significant intracellular levels of SufC and SufD prior to stress induction (Figure 4.1). Both SufC and SufD protein levels were doubled in dipyridyl treated cells. Protein levels increased more than 4-fold in response to H_2O_2 stress. Based on this result, we investigated if the Suf proteins are post-translationally modified to down-regulate Suf's function in the absence of stress.

Recombinant SufC from SufBC$_2$D is phosphorylated at Tyr241. NetPhos 2.0 and NetPhosBac 1.0 servers can be used to predict phosphorylation sites in proteins.[20-22] 23 tyrosine and serine residues are predicted sites of phosphorylation in SufB, SufC, and SufD. To determine if these predicted sites were actual phosphorylation sites, we used tandem mass spectrometry to map phosphorylation sites on purified recombinant SufBC$_2$D. Predicted residue Tyr241 in SufC was identified as a phosphorylation site by mass spectrometry. A SufC peptide containing residues Gln235 to Gln248 ionized with fragments 928.3 m/z (b ion) and 1104.44 m/z (y ion), each reporting an 80 Dalton increase in fragment mass compared to unmodified peptide (Figure 4.2A). This tyrosine residue (Tyr241) is highly conserved among SufC homologues in various species (Figure

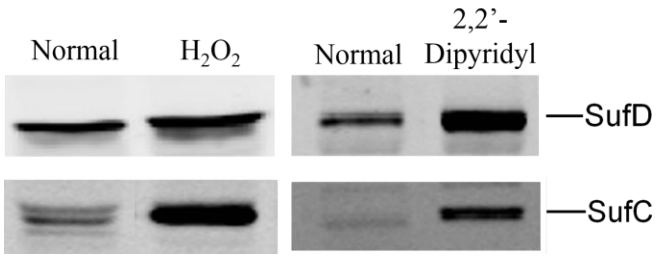

Figure 4.1 Immunoblot detection of SufD (top) and SufC (bottom) protein levels in normal cells and cells treated with 200 µM H_2O_2 or 200 µM 2, 2'-dipyridyl.

4.2B). Two other predicted phosphorylation sites were confirmed by LC-MS/MS: SufB Ser428 and SufC Ser141. (A. Saini and F.W. Outten, unpublished data)

We initially investigated how phosphorylation at SufC Tyr241 affects Suf function *in vivo.* Tyr241 was mutated to Asp (phosphomimetic mutation) and Phe (non-phosphorylatable mutation) in a plasmid expressing the *sufABCDSE* genes. The Asp mutation imparts a strong negative charge at the site to mimic constitutive phosphorylation of that residue. In contrast, the Phe mutation prevents phosphorylation due to lack of an available hydroxyl moiety.

WT and mutant plasmids (SufC Y241D and Y241F) were transformed into a *ΔsufABCDSE* strain and grown in gluconate minimal media containing increasing concentrations of the intracellular iron chelator 2, 2'-dipyridyl. 2, 2'-dipyridyl sequesters intracellular iron to generate cellular iron starvation conditions. Deletion of the *suf* operon in the Δ*sufABCDSE* strain causes decreased growth at higher levels of dipyridyl due to failure to assemble Fe-S clusters *in vivo*. Presence of *sufABCDSE* on a plasmid rescues growth of the *ΔsufABCDSE* strain.[1, 23] At dipyridyl concentrations over 150 µM, the Suf plasmid carrying the SufC Y241D mutation failed to rescue growth of the Δ*sufABCDSE* strain while a Suf plasmid with the SufC Y241F mutation still provided growth rescue (Figure 4.3). The ability to rescue the *ΔsufABCDSE* mutant phenotype was also tested under oxidative stress conditions in gluconate minimal media containing increasing concentrations of the superoxide generating phenazine methosulfate (PMS). At 5 µM PMS, the *sufABCDSE* plasmid containing the SufC Y241D mutation was no longer able to rescue the growth of *ΔsufABCDSE*. In contrast, the *sufABCDSE* plasmid containing the SufC Y241F mutation grew similarly to WT (Figure 4.4). These results

suggest phosphorylation at SufC Tyr241 prevents the proper functioning of the Suf pathway under iron starvation or oxidative stress conditions. The observed decrease in growth was not due to decreased Suf protein levels as confirmed by immunoblot analysis using α-SufC antibody. SufC Y241D protein levels were similar to WT and SufC Y241F protein levels in unstressed cells and cells treated with 125 μM dipyridyl or 3.5 μM PMS for 18 hrs at 37ºC (Figure 4.5). The cells for each condition grew to a similar OD_{600} as those observed in the growth phenotype studies. Interestingly, the phosphomimetic Asp mutation caused SufC to migrate differently by SDS PAGE. With the Asp substitution, SufC should have a theoretical molecular weight 100 Daltons smaller than WT SufC. However, immunoblots revealed the Y241D mutant SufC migrated at a slightly higher molecular weight than WT and Y241F SufC. This suggests the additional negative charge from Asp substitution at SufC residue 241 causes some structural modification or an interaction with a small molecule or protein that is not disrupted by SDS. SufD protein levels were also detected to determine if the Y241D mutation affected other Suf proteins. SufD protein levels were not affected.

Phosphomimetic mutation at SufC Tyr241 disrupts Fe-S cluster assembly on $SufBC_2D$ in vivo. To test if the Asp mutation at SufC alters Suf protein interactions, WT and SufC Y241D mutant $SufBC_2D$ complexes were purified for comparison. WT SufB, SufC, and SufD proteins co-elute as a stable $SufBC_2D$ complex from cells co-expressing the entire *suf* operon. $SufBC_2D$ formation is monitored by hydrophobic interaction chromatography (HIC) and ion exchange chromatography followed by gel filtration and SDS PAGE analysis.[15] Distinct differences were observed between the WT and SufC Y241D mutant on the HIC column. Fractions containing the majority of SufB, SufC, and

SufD (Fractions 14-17) from WT were dark greenish-brown due to accumulation of iron sulfides within the cell. The same fractions from the Y241D mutant were pale yellow yet contained similar amounts of protein (Figure 4.6A). Chemical analysis of HIC fractions 14-17 revealed decreased levels of both iron and acid-labile sulfide in fractions from Y241D mutant $SufBC_2D$ prep compared to WT $SufBC_2D$ (Figure 4.6B). The decreased iron and sulfide amounts suggest phosphomimetic substitution of Tyr241 disrupts *in vivo* Fe-S cluster assembly. Y241F mutant $SufBC_2D$ was isolated to ensure substitution of the Tyr residue did not contribute to the diminished iron and sulfide amounts observed in the Y241D mutant. Chemical analysis of HIC fractions revealed the $SufBC_2D$ Y241F mutant complex showed only a slight decrease in iron levels (Figure 4.6B). These results coincide with the previously mentioned growth studies and led us to propose that the active form of SufC is not phosphorylated. The resting state of SufC is phosphorylated but SufC must be unphosphorylated for efficient Fe-S cluster assembly. WT and Y241D $SufBC_2D$ eluted similarly from anion exchange (not shown) and size exclusion (Figure 4.7A) columns. Phosphomimetic substitution of SufC Tyr241 with Asp did not alter $SufBC_2D$ complex formation, revealing phosphorylation would not disrupt interactions between SufB, SufC, and SufD proteins. SDS PAGE analysis of final pure $SufBC_2D$ (Figure 4.7B) showed SufC containing the Y241D mutation migrated at a slightly higher molecular weight as observed in the immunoblots from the growth studies (Figure 4.5). The presence of an interacting small protein was not detectable via size exclusion chromatography and was not further investigated. These results suggest the inability of the *sufABCDSE* plasmid containing the SufC Y241D mutation to rescue *ΔsufABCDSE*

growth in iron starvation and oxidative stress conditions was due to disrupted Fe-S cluster assembly.

SufC Y241D mutant SufBC$_2$D reconstitutes an Fe-S cluster in vitro. To gain further insight into the effect of phosphorylation at Tyr241 on Fe-S cluster assembly, we performed anaerobic Fe-S reconstitution on purified WT and SufC Y241D mutant SufBC$_2$D complexes. After 2 hr reconstitution, the Y241D mutant SufBC$_2$D displayed the characteristic UV-visible spectrum of a [4Fe-4S cluster] and assembled the cluster at a rate similar to WT SufBC$_2$D (Figure 4.8). Our data suggests the Y241D mutation does not disrupt Fe-S cluster assembly when SufBC$_2$D is enzymatically reconstituted *in vitro*. The complexes were not purified to remove excess FAS and L-cysteine after the 2 hr reconstitution. Therefore, we cannot conclude that the SufC Y241D mutant SufBC$_2$D complex assembles a stable cluster similarly to WT SufBC$_2$D. It is possible that the Y241D mutation does not affect anaerobic Fe-S cluster reconstitution but causes conformational changes in SufBC$_2$D that expose the cluster, making it more sensitive to oxygen exposure. Also, ferrous ammonium sulfate (FAS) is an easily accessible iron source used for *in vitro* reconstitutions. Intracellular iron is not so readily available. It is possible that phosphorylation of SufC causes a subtle change in conformation of SufBC$_2$D that makes it unable to acquire iron from an unknown *in vivo* iron source. These hypotheses were not tested in this study.

Native SufD is phosphorylated at tyrosine residue(s). Since the phosphorylation sites identified via mass spectrometry analysis were from recombinant protein, we wanted to ensure that chromosomally expressed Suf proteins are also phosphorylated and to identify any *in vivo* phosphorylation sites. We investigated the possible *in vivo*

A

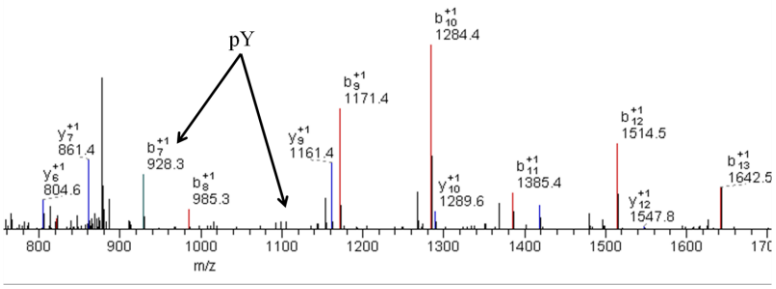

B

E. coli	.....SGDFTLVKQLEEQGYGWLTEQQ
B. subtilis	.....AELAQRLEAEGYDWIKQELGIEDETVDQEA
M. tuberculosis	.....GGSELADELDQNGYVRFSPASGRYPHQPAPTGA
T. thermophilis	.....GGPELALELEAKGYEWLKEKVKEGA

Figure 4.2 (A) LC-MS/MS spectra for SufC peptide Q235-Q248 mapping phosphosite Tyr241. (B) Sequence alignment of conserved SufC Tyr241 residue in Suf homologues.

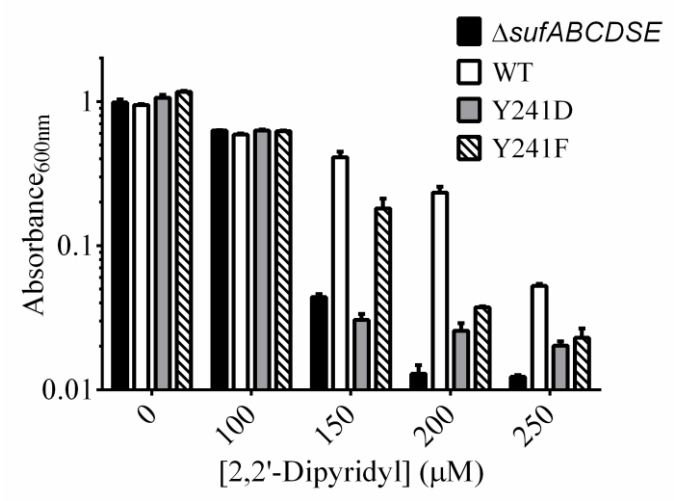

Figure 4.3 *In vivo* growth assay measuring sensitivity of SufC Tyr241 mutants to iron starvation. 18 hour growth of *ΔsufABCDSE* in increasing amounts of iron chelator 2, 2'-dipyridyl. *ΔsufABCDSE* strain contains empty plasmid (black), *sufABCDSE* on a plasmid (white), *sufABCDSE* plasmid with SufC Y241D mutation (gray), or *sufABCDSE* plasmid with SufC Y241F mutation (striped).

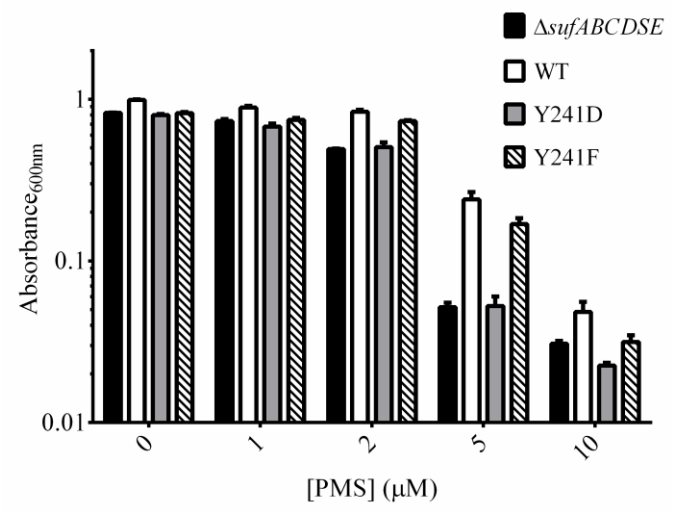

Figure 4.4 *In vivo* growth assay measuring sensitivity of SufC Tyr241 mutants to oxidative stress. 18 hour growth of *ΔsufABCDSE* in increasing amounts of superoxide stress inductant phenazine methosulfate (PMS). *ΔsufABCDSE* strain contains empty plasmid (black), *sufABCDSE* on a plasmid (white), *sufABCDSE* plasmid with SufC Y241D mutation (gray), or *sufABCDSE* plasmid with SufC Y241F mutation (striped).

A

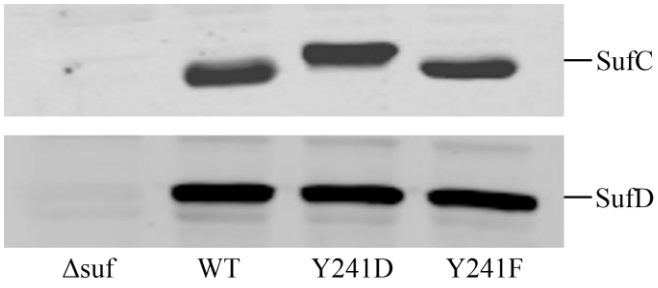

B

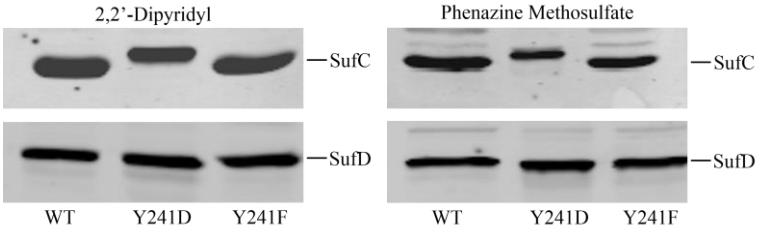

Figure 4.5 Immunoblot detection of SufC (top) and SufD (bottom) protein levels of WT and SufC Tyr241 mutant proteins during (A) normal growth and (B) iron starvation (125 μM 2,2'-dipyridyl) or superoxide stress (3.5 μM PMS). *ΔsufABCDSE* strain contains empty plasmid (lane 1), *sufABCDSE* on a plasmid (lane 2), *sufABCDSE* plasmid with SufC Y241D mutation (lane 3), or *sufABCDSE* plasmid with SufC Y241F mutation (lane 4).

A

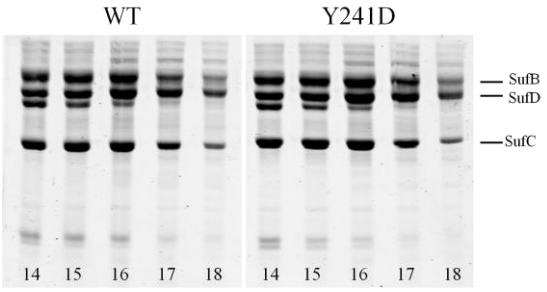

B

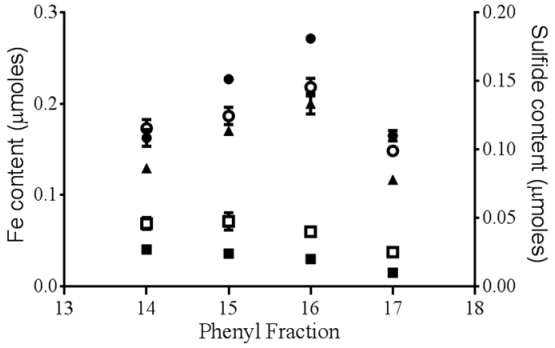

Figure 4.6 Purification of SufC Y241D mutant $SufBC_2D$. (A) Equal volumes (2.5 µL) of fractions 14-17 from HIC column separated via SDS PAGE and stained with Coomassie blue stain. (B) Iron (closed) and sulfide (open) content (in µmoles) of HIC fractions from WT (circle), SufC Y241D (square), and SufC Y241F (triangle) $SufBC_2D$ preps. Equal volumes of HIC fractions analyzed for iron and sulfide content. Measurements performed in duplicate.

A

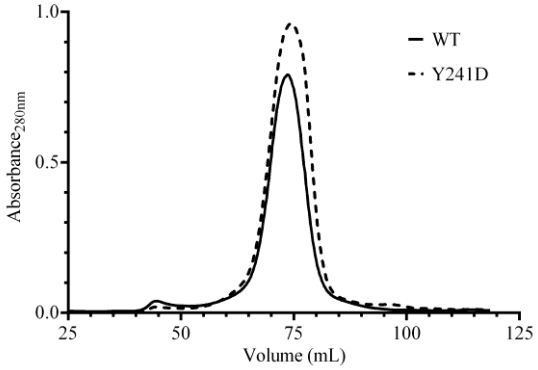

B

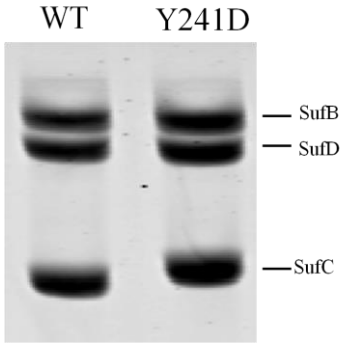

Figure 4.7 Purification of SufC Y241D mutant $SufBC_2D$. (A) Size exclusion column elution profile of WT (solid) and SufC Y241D (dashed) $SufBC_2D$. (B) SDS PAGE analysis of purified $SufBC_2D$ complexes.

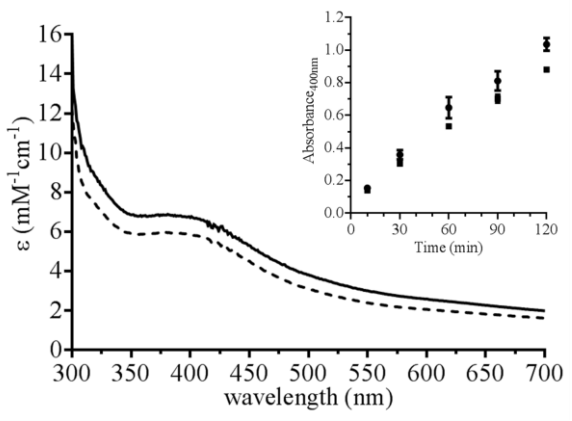

Figure 4.8 *In vitro* anaerobic Fe-S cluster reconstitution of SufC Y241D mutant $SufBC_2D$. UV-visible absorption spectrum of WT (solid) and Y241D mutant (dashed) $SufBC_2D$ after 120 minutes during reconstitution. *Inset*, Absorbance at 400 nm during reconstitution of WT (circle) and Y241D mutant (square) $SufBC_2D$.

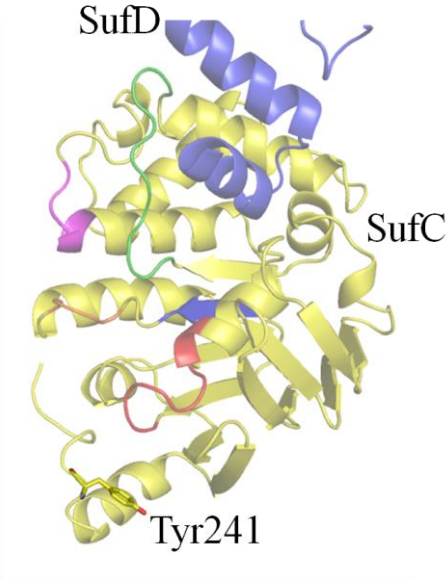

Figure 4.9 SufC (yellow) and C-terminus of SufD (blue) from $SufC_2D_2$ structure.[24] SufC conserved motifs are colored: Walker A (red), Walker B (blue), ABC signature (magenta), Q loop (green), and D loop (orange). Phosphosite Tyr241 is labeled and shown as a stick.

modification of the Suf proteins by phosphorylation at tyrosine residues. Cell lysates from normal and H_2O_2 stressed cells were incubated with immobilized phospho-tyrosine antibody for the immunoprecipitation of Suf proteins phosphorylated at tyrosine residues. Immunoblot analysis of the pull-down samples from the immobilized phosphotyrosine antibody treatment detected SufD protein levels only in the lysate from unstressed cells (Figure 4.10). Immunoblot analysis of whole cell extracts confirmed SufD is present in the cell prior to and after H_2O_2 treatment. This observation suggests SufD is phosphorylated *in vivo* under growth conditions when Suf is not the main Fe-S cluster assembly pathway and that SufD phosphorylation levels decrease under stress conditions when the Suf system is active.

$SufC_{His}$ is phosphorylated in vivo. Intracellular levels of Suf proteins are low. Isolating enough SufC for mass spectrometry required an enrichment technique. Using our newly constructed *$sufC_{His}sufD$* strain with a polyhistidine tag engineered at the C-terminus of *sufC* in the *suf* operon (this study), we partially enriched for native levels of $SufC_{His}$ via anion exchange and affinity chromatography. Through this approach, we successfully enriched $SufC_{His}$ and SufD protein levels enough to be visualized by SDS PAGE (Figure 4.11). Analysis of $SufC_{His}$ (from unstressed cells) by LC-MS/MS identified a site of phosphorylation at Ser10 (Figure 4.12). Ser10 is conserved among SufC homologues. This residue is located adjacent to Val11 in the SufC sequence. Val11 is proposed to interact with ATP in the SufC nucleotide binding site via a hydrophobic interaction, contributing to ATP stability. Based on the $SufC_2D_2$ structure, phosphorylation at residue Ser10 in SufC is predicted to destabilize ATP in the binding

site by interrupting this hydrophobic interaction (Figure 4.13). SufC Tyr241 residue was not observed to be phosphorylated using this approach.

4.4 Discussion

Phosphoanalysis of recombinant and native Suf proteins by mass spectrometry provided evidence of modification of the Suf proteins via phosphorylation. It was an important finding that measureable Suf protein levels are present in the cell even in the absence of stress. *E. coli* encodes multiple Fe-S cluster assembly pathways: the Isc pathway and the Suf pathway. Isc is the main Fe-S cluster assembly machinery under normal growth conditions. It has already been reported that basal levels of *suf* transcript are lower than *isc* transcript levels under normal growth conditions.[1] Since the Suf pathway is a stress-responsive pathway, post-translational regulation could be used to maintain specific levels of inactive Suf proteins when Isc is the preferred cluster assembly pathway. We report SufC and SufD are phosphorylated in unstressed cells. Comparison of phosphorylation levels at various stress conditions would better explain if phosphorylation correlates with Isc function conditions.

In this study, we report phosphorylated residues on SufC and SufD. We are yet to determine if other Suf proteins are phosphorylated *in vivo*. Saini et al. reported SufD and SufC ATP hydrolysis are essential for iron acquisition and *in vivo* Fe-S cluster formation in SufB.[23] If phosphorylation is specific to SufC and SufD, it could suggest phosphorylation regulates Suf's ability to acquire iron in some way. Our results show the SufC Asp mutation, which mimics the negative charge effect of phosphorylation, results in inactivation of Suf Fe-S cluster assembly *in vivo.* The Phe mutation does not affect

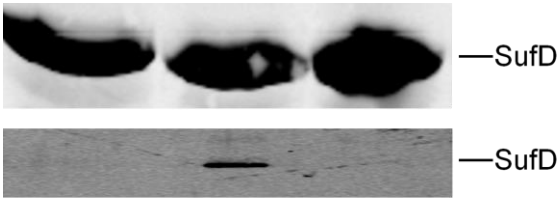

Figure 4.10 (Top) Immunoblot detection of SufD protein levels in whole cell extracts from cells harvested (lane 1) during, (lane 2) before, and (lane 3) 20 minutes after removal of 1 mM H_2O_2 stress. (Bottom) Proteins phosphorylated at tyrosine residues were immunoprecipitated with immobilized phosphotyrosine antibody. SufD was detected via immunoblot with α-SufD antibody.

Figure 4.11 SDS PAGE of enriched $SufC_{His}$ and interacting Suf proteins from unstressed (lane 1) or H_2O_2 stressed (lane 2) cells.

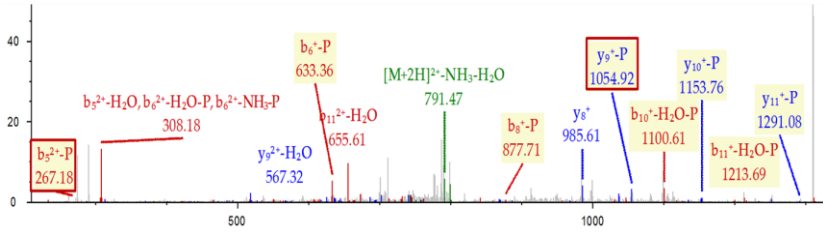

Figure 4.12 LC-MS/MS spectra for SufC peptide D6-R18 identifying phosphosite Ser10 on $SufC_{His}$.

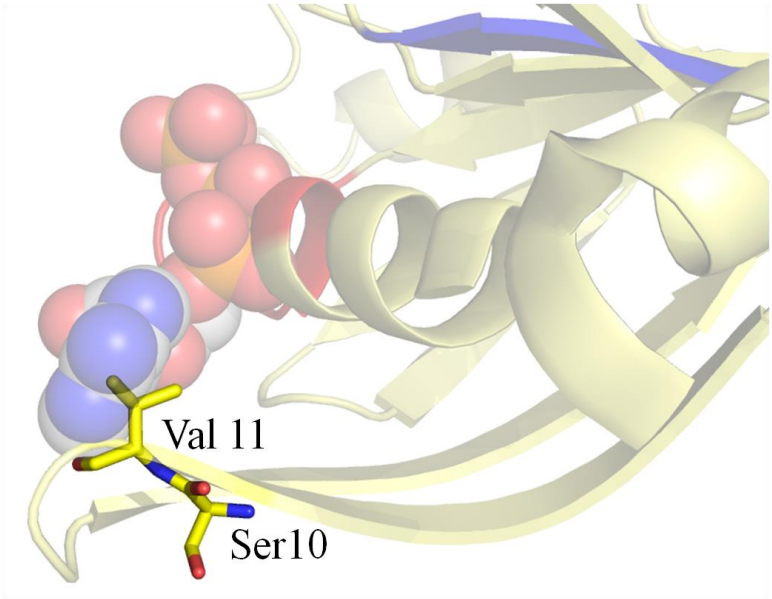

Figure 4.13 Nucleotide binding site of SufC from $SufC_2D_2$ structure.[24] Walker A (red) and Walker B (blue) motifs are shown. Phosphosite Ser10 and adjacent residue Val11 are labeled and shown as sticks.

Suf function *in vivo*, suggesting the active form of SufC is not phosphorylated. An Fe-S cluster can be anaerobically reconstituted on Y241D mutant $SufBC_2D$ with ferrous ammonium sulfate as the iron source. It is possible that phosphorylation at SufC affects its interaction with an unknown *in vivo* iron source or causes changes in $SufBC_2D$ that do not allow efficient iron acquisition *in vivo*. The crystal structure of $SufC_2D_2$ indicates Tyr241 is an exposed residue at the C-terminus of SufC.[24] This Tyr residue is not near any critical ATP binding motifs or close to the site of interaction with SufD (Figure 4.10). Therefore, as expected, the Asp mutation does not affect $SufBC_2D$ complex formation; however, altered interactions with an unknown protein are possible.

Phosphorylation may have different roles as seen with serine phosphorylation on IRP1. We identified a phosphorylated serine residue on native $SufC_{His}$ protein. Ser10 is near the Walker A motif and is adjacent to a Val residue proposed to participate in ATP binding in SufC (Figure 4.13). Based on its location, phosphorylation at Ser10 could regulate SufC's ability to bind or hydrolyze ATP. Identification of phosphorylation site Ser10 on $SufC_{His}$ isolated from unstressed cells agrees with the SufC Tyr241 mutant data that suggests Suf phosphorylation negatively regulates Suf function in the absence of stress.

We have not determined if Tyr241 is phosphorylated *in vivo.* The transient nature of phosphorylation makes it challenging to capture the modification. Additionally, phosphorylation at tyrosine residues accounts for only 0.01% of all phosphorylated amino acids on proteins.[25] Although the samples were enriched for phosphorylated peptides prior to phosphoanalysis, phosphopeptide enrichment is dependent on peptide amounts. As revealed in this study, Suf proteins are present at reduced levels in normal growing

cells. $SufC_{His}$ peptide levels may not have been optimal for enrichment of detectable levels of phosphotyrosine containing peptides. A more concentrated sample may allow us to identify phosphorylated tyrosine residues. Further studies are needed to better understand the contribution of phosphorylation to Suf regulation.

4.5 References

1. Outten, F. W., Djaman, O., and Storz, G. (2004) A *suf* operon requirement for Fe-S cluster assembly during iron starvation in *Escherichia coli*. *Mol Microbiol* 52, 861-872.

2. Aslund, F., Zheng, M., Beckwith, J., and Storz, G. (1999) Regulation of the OxyR transcription factor by hydrogen peroxide and the cellular thiol-disulfide status. *Proc Natl Acad Sci U S A* 96, 6161-6165.

3. Lee, K. C., Yeo, W. S., and Roe, J. H. (2008) Oxidant-responsive induction of the *suf* operon, encoding a Fe-S assembly system, through Fur and IscR in *Escherichia coli*. *J Bacteriol* 190, 8244-8247.

4. Varghese, S., Wu, A., Park, S., Imlay, K. R., and Imlay, J. A. (2007) Submicromolar hydrogen peroxide disrupts the ability of Fur protein to control free-iron levels in *Escherichia coli*. *Mol Microbiol* 64, 822-830.

5. Yeo, W. S., Lee, J. H., Lee, K. C., and Roe, J. H. (2006) IscR acts as an activator in response to oxidative stress for the *suf* operon encoding Fe-S assembly proteins. *Mol Microbiol* 61, 206-218.

6. Zheng, M., Aslund, F., and Storz, G. (1998) Activation of the OxyR transcription factor by reversible disulfide bond formation. *Science* 279, 1718-1721.

7. Zheng, M., Wang, X., Templeton, L. J., Smulski, D. R., LaRossa, R. A., and Storz, G. (2001) DNA microarray-mediated transcriptional profiling of the *Escherichia coli* response to hydrogen peroxide. *J Bacteriol* 183, 4562-4570.

8. Schalinske, K. L., Anderson, S. A., Tuazon, P. T., Chen, O. S., Kennedy, M. C., and Eisenstein, R. S. (1997) The iron-sulfur cluster of iron regulatory protein 1 modulates the accessibility of RNA binding and phosphorylation sites. *Biochemistry* 36, 3950-3958.

9. Schalinske, K. L., and Eisenstein, R. S. (1996) Phosphorylation and activation of both iron regulatory proteins 1 and 2 in HL-60 cells. *J Biol Chem* 271, 7168-7176.

10. Brown, N. M., Anderson, S. A., Steffen, D. W., Carpenter, T. B., Kennedy, M. C., Walden, W. E., and Eisenstein, R. S. (1998) Novel role of phosphorylation in Fe-S cluster stability revealed by phosphomimetic mutations at Ser-138 of iron regulatory protein 1. *Proc Natl Acad Sci U S A* 95, 15235-15240.

11. Deck, K. M., Vasanthakumar, A., Anderson, S. A., Goforth, J. B., Kennedy, M. C., Antholine, W. E., and Eisenstein, R. S. (2009) Evidence that phosphorylation of iron regulatory protein 1 at Serine 138 destabilizes the [4Fe-4S] cluster in cytosolic aconitase by enhancing 4Fe-3Fe cycling. *J Biol Chem* 284, 12701-12709.

12. Fillebeen, C., Caltagirone, A., Martelli, A., Moulis, J. M., and Pantopoulos, K. (2005) IRP1 Ser-711 is a phosphorylation site, critical for regulation of RNA-binding and aconitase activities. *Biochem J* 388, 143-150.

13. Ayala-Castro, C., Saini, A., and Outten, F. W. (2008) Fe-S cluster assembly pathways in bacteria. *Microbiol Mol Biol Rev* 72, 110-125.

14. Chahal, H. K., Dai, Y., Saini, A., Ayala-Castro, C., and Outten, F. W. (2009) The SufBCD Fe-S scaffold complex interacts with SufA for Fe-S cluster transfer. *Biochemistry* 48, 10644-10653.

15. Layer, G., Gaddam, S. A., Ayala-Castro, C. N., Ollagnier-de Choudens, S., Lascoux, D., Fontecave, M., and Outten, F. W. (2007) SufE transfers sulfur from SufS to SufB for iron-sulfur cluster assembly. *J Biol Chem* 282, 13342-13350.

16. Outten, F. W., Wood, M. J., Munoz, F. M., and Storz, G. (2003) The SufE protein and the SufBCD complex enhance SufS cysteine desulfurase activity as part of a sulfur transfer pathway for Fe-S cluster assembly in *Escherichia coli*. *J Biol Chem* 278, 45713-45719.

17. Wollers, S., Layer, G., Garcia-Serres, R., Signor, L., Clemancey, M., Latour, J. M., Fontecave, M., and Ollagnier de Choudens, S. (2010) Iron-sulfur (Fe-S) cluster assembly: the SufBCD complex is a new type of Fe-S scaffold with a flavin redox cofactor. *J Biol Chem* 285, 23331-23341.

18. Riemer, J., Hoepken, H. H., Czerwinska, H., Robinson, S. R., and Dringen, R. (2004) Colorimetric ferrozine-based assay for the quantitation of iron in cultured cells. *Anal Biochem* 331, 370-375.

19. Beinert, H. (1983) Semi-micro methods for analysis of labile sulfide and of labile sulfide plus sulfane sulfur in unusually stable iron-sulfur proteins. *Anal Biochem* 131, 373-378.

20. Blom, N., Gammeltoft, S., and Brunak, S. (1999) Sequence and structure-based prediction of eukaryotic protein phosphorylation sites. *J Mol Biol* 294, 1351-1362.

21. Blom, N., Sicheritz-Ponten, T., Gupta, R., Gammeltoft, S., and Brunak, S. (2004) Prediction of post-translational glycosylation and phosphorylation of proteins from the amino acid sequence. *Proteomics* 4, 1633-1649.

22. Miller, M. L., and Blom, N. (2009) Kinase-specific prediction of protein phosphorylation sites. *Methods Mol Biol* 527, 299-310.

23. Saini, A., Mapolelo, D. T., Chahal, H. K., Johnson, M. K., and Outten, F. W. (2010) SufD and SufC ATPase activity are required for iron acquisition during *in vivo* Fe-S cluster formation on SufB. *Biochemistry* 49, 9402-9412.

24. Wada, K., Sumi, N., Nagai, R., Iwasaki, K., Sato, T., Suzuki, K., Hasegawa, Y., Kitaoka, S., Minami, Y., Outten, F. W., Takahashi, Y., and Fukuyama, K. (2009) Molecular dynamism of Fe-S cluster biosynthesis implicated by the structure of the $SufC_2$-$SufD_2$ complex. *J Mol Biol* 387, 245-258.

25. Annan, R. S., and Carr, S. A. (1997) The essential role of mass spectrometry in characterizing protein structure: mapping posttranslational modifications. *J Protein Chem* 16, 391-402.

REFERENCES

Adinolfi, S., Iannuzzi, C., Prischi, F., Pastore, C., Iametti, S., Martin, S. R., Bonomi, F., and Pastore, A. (2009) Bacterial frataxin CyaY is the gatekeeper of iron-sulfur cluster formation catalyzed by IscS. *Nat Struct Mol Biol* 16, 390-396.

Andrews, S. C., Robinson, A. K., and Rodriguez-Quinones, F. (2003) Bacterial iron homeostasis. *FEMS Microbiol Rev* 27, 215-237.

Annan, R. S., and Carr, S. A. (1997) The essential role of mass spectrometry in characterizing protein structure: mapping posttranslational modifications. *J Protein Chem* 16, 391-402.

Aslund, F., Zheng, M., Beckwith, J., and Storz, G. (1999) Regulation of the OxyR transcription factor by hydrogen peroxide and the cellular thiol-disulfide status. *Proc Natl Acad Sci U S A* 96, 6161-6165.

Ayala-Castro, C., Saini, A., and Outten, F. W. (2008) Fe-S cluster assembly pathways in bacteria. *Microbiol Mol Biol Rev* 72, 110-125.

Badger, J., Sauder, J. M., Adams, J. M., Antonysamy, S., Bain, K., Bergseid, M. G., Buchanan, S. G., Buchanan, M. D., Batiyenko, Y., Christopher, J. A., Emtage, S., Eroshkina, A., Feil, I., Furlong, E. B., Gajiwala, K. S., Gao, X., He, D., Hendle, J., Huber, A., Hoda, K., Kearins, P., Kissinger, C., Laubert, B., Lewis, H. A., Lin, J., Loomis, K., Lorimer, D., Louie, G., Maletic, M., Marsh, C. D., Miller, I., Molinari, J.; Muller-Dieckmann, H. J., Newman, J. M., Noland, B. W., Pagarigan, B., Park, F., Peat, T. S., Post, K. W., Radojicic, S., Ramos, A., Romero, R., Rutter, M. E., Sanderson, W. E., Schwinn, K. D., Tresser, J., Winhoven, J., Wright, T. A., Wu, L., Xu, J., and Harris, T. J. (2005) Structural analysis of a set of proteins resulting from a bacterial genomics project. *Proteins* 60, 787-796.

Bagshaw, C. (2001) ATP analogues at a glance. *J Cell Sci* 114, 459-460.

Beinert, H. (1983) Semi-micro methods for analysis of labile sulfide and of labile sulfide plus sulfane sulfur in unusually stable iron-sulfur proteins. *Anal Biochem* 131, 373-378.

Beinert, H., Holm, R. H., and Munck, E. (1997) Iron-sulfur clusters: nature's modular, multipurpose structures. *Science* 277, 653-659.

Blanc, B., Clemancey, M., Latour, J. M., Fontecave, M., and Ollagnier de Choudens, S. (2014) Molecular investigation of iron-sulfur cluster assembly scaffolds under stress. *Biochemistry* 53, 7867-7869.

Blom, N., Gammeltoft, S., and Brunak, S. (1999) Sequence and structure-based prediction of eukaryotic protein phosphorylation sites. *J Mol Biol* 294, 1351-1362.

Blom, N., Sicheritz-Ponten, T., Gupta, R., Gammeltoft, S., and Brunak, S. (2004) Prediction of post-translational glycosylation and phosphorylation of proteins from the amino acid sequence. *Proteomics* 4, 1633-1649.

Bolanos-Garcia, V. M., and Davies, O. R. (2006) Structural analysis and classification of native proteins from *E. coli* commonly co-purified by immobilised metal affinity chromatography. *Biochim Biophys Acta* 1760, 1304-1313.

Bou-Abdallah, F., Adinolfi, S., Pastore, A., Laue, T. M., and Dennis Chasteen, N. (2004) Iron binding and oxidation kinetics in frataxin CyaY of *Escherichia coli*. *J Mol Biol* 341, 605-615.

Boyd, E. S., Thomas, K. M., Dai, Y., Boyd, J. M., and Outten, F. W. (2014) Interplay between oxygen and Fe-S cluster biogenesis: insights from the Suf pathway. *Biochemistry* 53, 5834-5847.

Brand, L., and Gohlke, J. R. (1972) Fluorescence probes for structure. *Annu Rev Biochem* 41, 843-868.

Brown, N. M., Anderson, S. A., Steffen, D. W., Carpenter, T. B., Kennedy, M. C., Walden, W. E., and Eisenstein, R. S. (1998) Novel role of phosphorylation in Fe-S cluster stability revealed by phosphomimetic mutations at Ser-138 of iron regulatory protein 1. *Proc Natl Acad Sci U S A* 95, 15235-15240.

Cardamone, M., and Puri, N. K. (1992) Spectrofluorimetric assessment of the surface hydrophobicity of proteins. *Biochem J* 282 589-593.

Chahal, H. K., Dai, Y., Saini, A., Ayala-Castro, C., and Outten, F. W. (2009) The SufBCD Fe-S scaffold complex interacts with SufA for Fe-S cluster transfer. *Biochemistry* 48, 10644-10653.

Chahal, H. K., and Outten, F. W. (2012) Separate Fe-S scaffold and carrier functions for $SufB_2C_2$ and SufA during *in vitro* maturation of [2Fe-2S] Fdx. *J Inorg Biochem* 116, 126-134.

Chandramouli, K., and Johnson, M. K. (2006) HscA and HscB stimulate [2Fe-2S] cluster transfer from IscU to apoferredoxin in an ATP-dependent reaction. *Biochemistry* 45, 11087-11095.

Dai, Y., and Outten, F. W. (2012) The *E. coli* SufS-SufE sulfur transfer system is more resistant to oxidative stress than IscS-IscU. *FEBS Lett* 586, 4016-4022.

Datsenko, K. A., and Wanner, B. L. (2000) One-step inactivation of chromosomal genes in *Escherichia coli* K-12 using PCR products. *Proc Natl Acad Sci U S A* 97, 6640-6645.

Deck, K. M., Vasanthakumar, A., Anderson, S. A., Goforth, J. B., Kennedy, M. C., Antholine, W. E., and Eisenstein, R. S. (2009) Evidence that phosphorylation of iron regulatory protein 1 at Serine 138 destabilizes the [4Fe-4S] cluster in cytosolic aconitase by enhancing 4Fe-3Fe cycling. *J Biol Chem* 284, 12701-12709.

Ding, H., Yang, J., Coleman, L. C., and Yeung, S. (2007) Distinct iron binding property of two putative iron donors for the iron-sulfur cluster assembly: IscA and the bacterial frataxin ortholog CyaY under physiological and oxidative stress conditions. *J Biol Chem* 282, 7997-8004.

Eccleston, J. F., Petrovic, A., Davis, C. T., Rangachari, K., and Wilson, R. J. (2006) The kinetic mechanism of the SufC ATPase: the cleavage step is accelerated by SufB. *J Biol Chem* 281, 8371-8378.

Expert, D., Boughammoura, A., and Franza, T. (2008) Siderophore-controlled iron assimilation in the enterobacterium *Erwinia chrysanthemi*: evidence for the involvement of bacterioferritin and the Suf iron-sulfur cluster assembly machinery. *J Biol Chem* 283, 36564-36572.

Fillebeen, C., Caltagirone, A., Martelli, A., Moulis, J. M., and Pantopoulos, K. (2005) IRP1 Ser-711 is a phosphorylation site, critical for regulation of RNA-binding and aconitase activities. *Biochem J* 388, 143-150.

Fontecave, M., and Ollagnier-de-Choudens, S. (2008) Iron-sulfur cluster biosynthesis in bacteria: Mechanisms of cluster assembly and transfer. *Arch Biochem Biophys* 474, 226-237.

Giel, J. L., Rodionov, D., Liu, M., Blattner, F. R., and Kiley, P. J. (2006) IscR-dependent gene expression links iron-sulphur cluster assembly to the control of O_2-regulated genes in *Escherichia coli*. *Mol Microbiol* 60, 1058-1075.

Gupta, V., Sendra, M., Naik, S. G., Chahal, H. K., Huynh, B. H., Outten, F. W., Fontecave, M., and Ollagnier de Choudens, S. (2009) Native *Escherichia coli* SufA, co-expressed with SufBCDSE, purifies as a [2Fe-2S] protein and acts as an Fe-S transporter to Fe-S target enzymes. *J Am Chem Soc* 131, 6149-6153.

Huet, G., Castaing, J. P., Fournier, D., Daffe, M., and Saves, I. (2006) Protein splicing of SufB is crucial for the functionality of the *Mycobacterium tuberculosis* SUF machinery. *J Bacteriol* 188, 3412-3414.

Iannuzzi, C., Adinolfi, S., Howes, B. D., Garcia-Serres, R., Clemancey, M., Latour, J. M., Smulevich, G., and Pastore, A. (2011) The role of CyaY in iron sulfur cluster assembly on the *E. coli* IscU scaffold protein. *PLoS One* 6, e21992.

Jacobson, M. R., Brigle, K. E., Bennett, L. T., Setterquist, R. A., Wilson, M. S., Cash, V. L., Beynon, J., Newton, W. E., and Dean, D. R. (1989) Physical and genetic map of the major *nif* gene cluster from *Azotobacter vinelandii*. *J Bacteriol* 171, 1017-1027.

Jacobson, M. R., Cash, V. L., Weiss, M. C., Laird, N. F., Newton, W. E., and Dean, D. R. (1989) Biochemical and genetic analysis of the *nifUSVWZM* cluster from *Azotobacter vinelandii*. *Mol Gen Genet* 219, 49-57.

Jakob, U., Gaestel, M., Engel, K., and Buchner, J. (1993) Small heat shock proteins are molecular chaperones. *J Biol Chem* 268, 1517-1520.

Jameson, D. M., and Eccleston, J. F. (1997) Fluorescent nucleotide analogs: synthesis and applications. *Methods Enzymol* 278, 363-390.

Johnson, D. C., Dean, D. R., Smith, A. D., and Johnson, M. K. (2005) Structure, function, and formation of biological iron-sulfur clusters. *Annu Rev Biochem* 74, 247-281.

Jones, P. M., and George, A. M. (2012) Role of the D-loops in allosteric control of ATP hydrolysis in an ABC transporter. *J Phys Chem A* 116, 3004-3013.

Kennedy, M. C., Emptage, M. H., Dreyer, J. L., and Beinert, H. (1983) The role of iron in the activation-inactivation of aconitase. *J Biol Chem* 258, 11098-11105.

Kennedy, M. C., and Beinert, H.(1988) The state of cluster SH and S^{2-} of aconitase during cluster interconversions and removal. A convenient preparation of apoenzyme. *J Biol Chem* 263, 8194-8198.

Kim, J. H., Tonelli, M., Frederick, R. O., Chow, D. C., and Markley, J. L. (2012) Specialized Hsp70 chaperone (HscA) binds preferentially to the disordered form, whereas J-protein (HscB) binds preferentially to the structured form of the iron-sulfur cluster scaffold protein (IscU). *J Biol Chem* 287, 31406-31413.

Kim, J. H., Alderson, T. R., Frederick, R. O., and Markley, J. L. (2014) Nucleotide-dependent interactions within a specialized Hsp70/Hsp40 complex involved in Fe-S cluster biogenesis. *J Am Chem Soc* 136, 11586-11589.

Kitaoka, S., Wada, K., Hasegawa, Y., Minami, Y., Fukuyama, K., and Takahashi, Y. (2006) Crystal structure of *Escherichia coli* SufC, an ABC-type ATPase component of the SUF iron-sulfur cluster assembly machinery. *FEBS Lett* 580, 137-143.

Korkhov, V. M., Mireku, S. A., and Locher, K. P. (2012) Structure of AMP-PNP-bound vitamin B12 transporter BtuCD-F. *Nature* 490, 367-372.

Kumar, B., Chaubey, S., Shah, P., Tanveer, A., Charan, M., Siddiqi, M. I., and Habib, S. (2012) Interaction between sulphur mobilisation proteins SufB and SufC: evidence for an iron-sulphur cluster biogenesis pathway in the apicoplast of *Plasmodium falciparum*. *Int J Parasitol* 41, 991-999.

Layer, G., Gaddam, S. A., Ayala-Castro, C. N., Ollagnier-de Choudens, S., Lascoux, D., Fontecave, M., and Outten, F. W. (2007) SufE transfers sulfur from SufS to SufB for iron-sulfur cluster assembly. *J Biol Chem* 282, 13342-13350.

Lee, K. C., Yeo, W. S., and Roe, J. H. (2008) Oxidant-responsive induction of the *suf* operon, encoding a Fe-S assembly system, through Fur and IscR in *Escherichia coli*. *J Bacteriol* 190, 8244-8247.

Lima, C. D. (2002) Analysis of the *E. coli* NifS CsdB protein at 2.0 A reveals the structural basis for perselenide and persulfide intermediate formation. *J Mol Biol* 315, 1199-1208.

Loiseau, L., Ollagnier-de-Choudens, S., Nachin, L., Fontecave, M., and Barras, F. (2003) Biogenesis of Fe-S cluster by the bacterial Suf system: SufS and SufE form a new type of cysteine desulfurase. *J Biol Chem* 278, 38352-38359.

Malkin, R., and Rabinowitz, J. C. (1966) The reconstitution of *clostridial* ferredoxin. *Biochem Biophys Res Commun* 23, 822-827.

Mihara, H., Kurihara, T., Yoshimura, T., and Esaki, N. (2000) Kinetic and mutational studies of three NifS homologs from *Escherichia coli*: mechanistic difference between L-cysteine desulfurase and L-selenocysteine lyase reactions. *J Biochem* 127, 559-567.

Mihara, H., and Esaki, N. (2002) Bacterial cysteine desulfurases: their function and mechanisms. *Appl Microbiol Biotechnol* 60, 12-23.

Miller, M. L., and Blom, N. (2009) Kinase-specific prediction of protein phosphorylation sites. *Methods Mol Biol* 527, 299-310.

Monk, B. C., and Kellerman, G. M. (1976) A rapid method for the assay of mitochondrial ATPase activity. *Anal Biochem* 73, 187-191.

Moody, J. E., Millen, L., Binns, D., Hunt, J. F., and Thomas, P. J. (2002) Cooperative, ATP-dependent association of the nucleotide binding cassettes during

the catalytic cycle of ATP-binding cassette transporters. *J Biol Chem* 277, 21111-21114.

Nachin, L., El Hassouni, M., Loiseau, L., Expert, D., and Barras, F. (2001) SoxR-dependent response to oxidative stress and virulence of *Erwinia chrysanthemi*: the key role of SufC, an orphan ABC ATPase. *Mol Microbiol* 39, 960-972.

Nachin, L., Loiseau, L., Expert, D., and Barras, F. (2003) SufC: an unorthodox cytoplasmic ABC/ATPase required for [Fe-S] biogenesis under oxidative stress. *Embo J* 22, 427-437.

Okamoto, S., Van Petegem, F., Patrauchan, M. A., and Eltis, L. D. (2010) AnhE, a metallochaperone involved in the maturation of a cobalt-dependent nitrile hydratase. *J Biol Chem* 285, 25126-25133.

Ollagnier-de-Choudens, S., Lascoux, D., Loiseau, L., Barras, F., Forest, E., and Fontecave, M. (2003) Mechanistic studies of the SufS-SufE cysteine desulfurase: evidence for sulfur transfer from SufS to SufE. *FEBS Lett* 555, 263-267.

Ollagnier-de Choudens, S., Nachin, L., Sanakis, Y., Loiseau, L., Barras, F., and Fontecave, M. (2003) SufA from *Erwinia chrysanthemi*. Characterization of a scaffold protein required for iron-sulfur cluster assembly. *J Biol Chem* 278, 17993-18001.

Ollagnier-de-Choudens, S., Sanakis, Y., and Fontecave, M. (2004) SufA/IscA: reactivity studies of a class of scaffold proteins involved in [Fe-S] cluster assembly. *J Biol Inorg Chem* 9, 828-838.

Outten, F. W., Wood, M. J., Munoz, F. M., and Storz, G. (2003) The SufE protein and the SufBCD complex enhance SufS cysteine desulfurase activity as part of a sulfur transfer pathway for Fe-S cluster assembly in *Escherichia coli*. *J Biol Chem* 278, 45713-45719.

Outten, F. W., Djaman, O., and Storz, G. (2004) A *suf* operon requirement for Fe-S cluster assembly during iron starvation in *Escherichia coli*. *Mol Microbiol* 52, 861-872.

Outten, F. W. (2014) Recent advances in the Suf Fe-S cluster biogenesis pathway: Beyond the Proteobacteria. *Biochim Biophys Acta* 1853, 1464-1469.

Outten, F. W. (2014) A stress-responsive Fe-S cluster biogenesis system in bacteria-the *suf* operon of Gammaproteobacteria. In *Iron-Sulfur Clusters in Chemistry and Biology*, Rouault, T. A., Ed. de Gruyter:; 297-323.

Petrovic, A., Davis, C. T., Rangachari, K., Clough, B., Wilson, R. J., and Eccleston, J. F. (2008) Hydrodynamic characterization of the SufBC and SufCD complexes and their interaction with fluorescent adenosine nucleotides. *Protein Sci* 17, 1264-1274.

Prischi, F., Konarev, P. V., Iannuzzi, C., Pastore, C., Adinolfi, S., Martin, S. R., Svergun, D. I., and Pastore, A. (2010) Structural bases for the interaction of frataxin with the central components of iron-sulphur cluster assembly. *Nat Commun* 1, 95.

Rangachari, K., Davis, C. T., Eccleston, J. F., Hirst, E. M., Saldanha, J. W., Strath, M., and Wilson, R. J. (2002) SufC hydrolyzes ATP and interacts with SufB from *Thermotoga maritima*. *FEBS Lett* 514, 225-228.

Rees, D. C., Johnson, E., and Lewinson, O. (2009) ABC transporters: the power to change. *Nat Rev Mol Cell Biol* 10, 218-227.

Riemer, J., Hoepken, H. H., Czerwinska, H., Robinson, S. R., and Dringen, R., (2004) Colorimetric ferrozine-based assay for the quantitation of iron in cultured cells. *Anal Biochem* 331, 370-375.

Roche, B., Aussel, L., Ezraty, B., Mandin, P., Py, B., and Barras, F. (2013) Iron/sulfur proteins biogenesis in prokaryotes: formation, regulation and diversity. *Biochim Biophys Acta* 1827, 455-469.

Saini, A., Mapolelo, D. T., Chahal, H. K., Johnson, M. K., and Outten, F. W. (2010) SufD and SufC ATPase activity are required for iron acquisition during *in vivo* Fe-S cluster formation on SufB. *Biochemistry* 49, 9402-9412.

Schalinske, K. L., and Eisenstein, R. S. (1996) Phosphorylation and activation of both iron regulatory proteins 1 and 2 in HL-60 cells. *J Biol Chem* 271, 7168-7176.

Schalinske, K. L., Anderson, S. A., Tuazon, P. T., Chen, O. S., Kennedy, M. C., and Eisenstein, R. S. (1997) The iron-sulfur cluster of iron regulatory protein 1 modulates the accessibility of RNA binding and phosphorylation sites. *Biochemistry* 36, 3950-3958.

Schwartz, C. J., Giel, J. L., Patschkowski, T., Luther, C., Ruzicka, F. J., Beinert, H., and Kiley, P. J. (2001) IscR, an Fe-S cluster-containing transcription factor, represses expression of *Escherichia coli* genes encoding Fe-S cluster assembly proteins. *Proc Natl Acad Sci U S A* 98, 14895-14900.

Selbach, B. P., Pradhan, P. K., and Dos Santos, P. C. (2013) Protected sulfur transfer reactions by the *Escherichia coli* Suf system. *Biochemistry* 52, 4089-4096.

Sendra, M., Ollagnier de Choudens, S., Lascoux, D., Sanakis, Y., and Fontecave, M. (2007) The SUF iron-sulfur cluster biosynthetic machinery: sulfur transfer from the SUFS-SUFE complex to SUFA. *FEBS Lett* 581, 1362-1368.

Silberg, J. J., and Vickery, L. E. (2000) Kinetic characterization of the ATPase cycle of the molecular chaperone Hsc66 from *Escherichia coli*. *J Biol Chem* 275, 7779-7786.

Silberg, J. J., Tapley, T. L., Hoff, K. G., and Vickery, L. E. (2004) Regulation of the HscA ATPase reaction cycle by the co-chaperone HscB and the iron-sulfur cluster assembly protein IscU. *J Biol Chem* 279, 53924-53931.

Smith, P. C., Karpowich, N., Millen, L., Moody, J. E., Rosen, J., Thomas, P. J., and Hunt, J. F. (2002) ATP binding to the motor domain from an ABC transporter drives formation of a nucleotide sandwich dimer. *Mol Cell* 10, 139-149Takahashi, Y., Mitsui, A., Fujita, Y., and Matsubara, H. (1991) Roles of ATP and NADPH in formation of the Fe-S cluster of spinach ferredoxin. *Plant Physiol* 95, 104-110.

Takahashi, Y., and Tokumoto, U. (2002) A third bacterial system for the assembly of iron-sulfur clusters with homologs in archaea and plastids. *J Biol Chem* 277, 28380-28383.

Tian, T., He, H., and Liu, X. Q. (2013) The SufBCD protein complex is the scaffold for iron-sulfur cluster assembly in *Thermus thermophilus* HB8. *Biochem Biophys Res Commun* 443, 376-381.

Touati, D. (2000) Iron and oxidative stress in bacteria. *Arch Biochem Biophys* 373, 1-6.

Varghese, S., Wu, A., Park, S., Imlay, K. R., and Imlay, J. A. (2007) Submicromolar hydrogen peroxide disrupts the ability of Fur protein to control free-iron levels in *Escherichia coli*. *Mol Microbiol* 64, 822-830.

Verdon, G., Albers, S. V., van Oosterwijk, N., Dijkstra, B. W., Driessen, A. J., and Thunnissen, A. M. (2003) Formation of the productive ATP-Mg^{2+}-bound dimer of GlcV, an ABC-ATPase from *Sulfolobus solfataricus*. *J Mol Biol* 334, 255-267.

Vinella, D., Brochier-Armanet, C., Loiseau, L., Talla, E., and Barras, F. (2009) Iron-sulfur (Fe/S) protein biogenesis: phylogenomic and genetic studies of A-type carriers. *PLoS Genet* 5, e1000497.

Vinella, D., Loiseau, L., Ollagnier de Choudens, S., Fontecave, M., and Barras, F. (2013) *In vivo* [Fe-S] cluster acquisition by IscR and NsrR, two stress regulators in *Escherichia coli*. *Mol Microbiol* 87, (3), 493-508.

Wada, K., Sumi, N., Nagai, R., Iwasaki, K., Sato, T., Suzuki, K., Hasegawa, Y., Kitaoka, S., Minami, Y., Outten, F. W., Takahashi, Y., and Fukuyama, K. (2009) Molecular dynamism of Fe-S cluster biosynthesis implicated by the structure of the $SufC_2$-$SufD_2$ complex. *J Mol Biol* 387, 245-258.

Watanabe, S., Kita, A., and Miki, K. (2005) Crystal structure of atypical cytoplasmic ABC-ATPase SufC from *Thermus thermophilus* HB8. *J Mol Biol* 353, 1043-1054.

Winterbourn, C. C. (1995) Toxicity of iron and hydrogen peroxide: the Fenton reaction. *Toxicol Lett* 82-83, 969-974.

Wirtz, M., and Droux, M. (2005) Synthesis of the sulfur amino acids: cysteine and methionine. *Photosynth Res* 86, 345-362.

Wollers, S., Layer, G., Garcia-Serres, R., Signor, L., Clemancey, M., Latour, J. M., Fontecave, M., and Ollagnier de Choudens, S. (2010) Iron-sulfur (Fe-S) cluster assembly: the SufBCD complex is a new type of Fe-S scaffold with a flavin redox cofactor. *J Biol Chem* 285, 23331-23341.

Yeo, W. S., Lee, J. H., Lee, K. C., and Roe, J. H. (2006) IscR acts as an activator in response to oxidative stress for the *suf* operon encoding Fe-S assembly proteins. *Mol Microbiol* 61, 206-218.

Yu, D., Ellis, H. M., Lee, E. C., Jenkins, N. A., Copeland, N. G., and Court, D. L. (2000) An efficient recombination system for chromosome engineering in *Escherichia coli*. *Proc Natl Acad Sci U S A* 97, 5978-5983.

Zheng, L., and Dean, D. R. (1994) Catalytic formation of a nitrogenase iron-sulfur cluster. *J Biol Chem* 269, 18723-18726.

Zheng, L., Cash, V. L., Flint, D. H., and Dean, D. R. (1998) Assembly of iron-sulfur clusters. Identification of an *iscSUA-hscBA-fdx* gene cluster from *Azotobacter vinelandii*. *J Biol Chem* 273, 13264-13272.

Zheng, M., Aslund, F., and Storz, G. (1998) Activation of the OxyR transcription factor by reversible disulfide bond formation. *Science* 279, 1718-1721.

Zheng, M., Wang, X., Templeton, L. J., Smulski, D. R., LaRossa, R. A., and Storz, G. (2001) DNA microarray-mediated transcriptional profiling of the *Escherichia coli* response to hydrogen peroxide. *J Bacteriol* 183, 4562-4570.

APPENDIX A

Polyhistidine tag at C-terminus of *sufC* in the *E. coli* chromosome

A.1 Materials and Methods

Construction of sufC$_{His}$sufD strain. A DNA fragment containing a kanamycin cassette with flanking *suf* regions was amplified from pKD4 vector[1] using upstream primer (5'-AACAACTGGAGGAGCAGGGTTACGGTTGGCTGACTGAACAACAAG GCAGCAGCCATCACCATCATCACCACAGCCAGTAAGTGTAGGCTGGAGCTGC TTC-3') and downstream primer (5'-CAAGTGATGCCACTGTTGCAGCGCGTTACT GCTGTTCGGTAAGCCAGCCATATGAATATCCTCCTTA-3'). *E. coli* strain DY330[2] was transformed by electroporation with the amplified fragment and *Kan*^{R} colonies were selected at 30°C. Insertion of the kanamycin cassette was confirmed by colony PCR. Phage P1 was used to transduce the mutation into MG1655 strain, yielding MG1655*sufC$_{His}$_kan_sufD* strain. Transformation with pCP20[1] flipped-out the kanamycin cassette to yield strain MG1655*sufC$_{His}$sufD*. Loss of kanamycin was confirmed by colony PCR and decreased resistance to kanamycin. Both colony PCR tests were performed with the same upstream (5'-AACAACTGGAGGAGCAGGGTT ACGGTTGGCTGACTGAACAACAAGGCAGCAGCCATCACCATCATCACCACAG CCAGTAAGTGTAGGCTGGAGCTGCTTC-3') and downstream (5'-CAAGTGATG CCACTGTTGCAGCGCGTTACTGCTGTTCGGTAAGCCAGCCATATGAATATCCT

CCTTA-3') primers. Successful insertion of the polyhistidine tag on the chromosome was confirmed by DNA sequencing.

In vivo growth assay. MG1655 WT, *ΔsufABCDSE*, and MG1655*sufC*$_{his}$*sufD* strains were each grown in LB at 37°C overnight. OD_{600} was measured then adjusted to 2.0 in 1mL gluconate minimal media (1 X M9 minimal media, 0.2% gluconate, 0.02% $MgSO_4$, 0.1 mM $CaCl_2$, 0.0005% thiamine). 20 µL of cells was added to 2 mL (1:100 dilution) of gluconate minimal media with increasing concentrations of 2, 2'-dipyridyl (0, 150, 200 µM). Final absorbance at 600 nm was measured after an 18 hour growth at 37°C. Assays were performed in triplicate.

A.2 Results and Discussion

Incorporation of a polyhistidine-tag on SufC in the chromosome does not alter suf expression. We have successfully engineered a polyhistidine tag at the C-terminus of *sufC* in the *suf* operon on the *E. coli* chromosome. This MG1655*sufC*$_{His}$*sufD* strain retains the native promoter region at the *suf* operon and is thus regulated by the same transcription factors (i.e. Fur, OxyR, IscR) (Figure A.1). We performed control experiments to ensure the addition of the polyhistidine tag to SufC does not disrupt Suf function *in vivo*. This was necessary because we used a kanamycin resistance gene fused to the polyhistidine sequence insert for selection. The "flipping out" of the kanamycin resistance gene left a sizable scar-region between *sufC* and *sufD*. Also, in the native *suf* sequence, the start codon for the *sufD* gene overlaps the stop codon of *sufC*. To insert the polyhistidine-tag sequence at the end of the *sufC* gene, *sufD* had to be uncoupled from *sufC* and given a new start codon and ribosomal binding site.

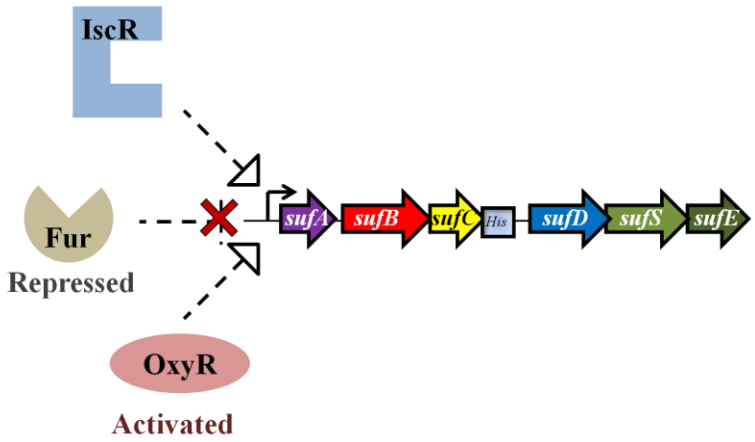

Figure A.1 Transcriptional regulation of the *suf* genes chromosomally expressed in *sufC*$_{His}$*sufD* exposed to H_2O_2 stress.

The *sufC*$_{His}$*sufD* strain grows similarly to WT in increasing concentrations of dipyridyl (Figure A.2) and SufC and SufD protein levels are similar to WT in cells induced with 200 µM dipyridyl. SufC runs at a higher molecular weight due to the additional 4 kDa from the polyhistidine tag (Figure A.3). The polyhistidine-tag is not near any critical ATP binding motifs in SufC and is far from the Q-loop, the proposed site of binding for partner proteins SufB and SufD. The results confirm the addition of the polyhistidine tag on *sufC* does not affect *suf* expression and does not disrupt Suf function *in vivo*. The *sufC*$_{His}$*sufD* strain was used to study *in vivo* Suf protein-protein interactions.

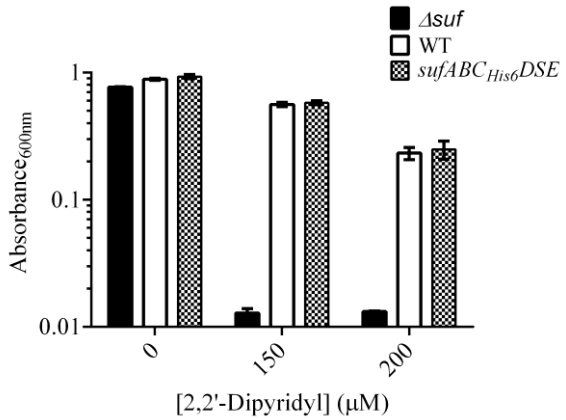

Figure A.2 *In vivo* growth assay of *ΔsufABCDSE* (black), WT (white), and *sufC$_{His}$sufD* (dotted) strains in iron starvation conditions. Strains were grown in gluconate minimal media containing increasing amounts of 2, 2'-dipyridyl.

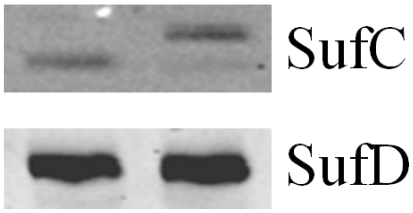

Figure A.3 Immunoblots of SufC (top) or SufD (bottom) protein levels in WT (lane 1) or *sufC*$_{His}$*sufD* (lane 2) cells induced with 200 µM dipyridyl.

A.3 References

1. Datsenko, K. A., and Wanner, B. L. (2000) One-step inactivation of chromosomal genes in *Escherichia coli* K-12 using PCR products. *Proc Natl Acad Sci U S A* 97, 6640-6645.

2. Yu, D., Ellis, H. M., Lee, E. C., Jenkins, N. A., Copeland, N. G., and Court, D. L. (2000) An efficient recombination system for chromosome engineering in *Escherichia coli*. *Proc Natl Acad Sci U S A* 97, 5978-5983.

APPENDIX B

Isolation of SufD from cells over-expressing the *sufABCDSE* genes

B.1 Materials and Methods

Isolation of SufD from cells over-expressing sufABCDSE genes. The pBAD/*Myc*-His C vector (Invitrogen) containing the entire *suf* operon under control of an arabinose-inducible promoter was used to over-express *sufABCDSE* in *E. coli* TOP10 strain.[1] 4 L cultures were grown in LB at 37°C to an OD_{600} of 0.5 and induced with 0.2% (w/v) L-arabinose. After 3 hour induction at 37°C, cells were harvested by centrifugation cell pellets frozen at -80°C. Cleared lysate was loaded onto a Phenyl FF column (GE Healthcare) in line with a Biologic DuoFlow FPLC system (Biorad). The column was washed with 3 column volumes of phenyl binding buffer (25 mM Tris-HCl, pH 7.5, 100 mM NaCl, 1 M ammonium sulfate, and 10 mM βME), then Suf proteins were eluted with ten column volumes of a linear gradient of 1-0 M ammonium sulfate. SufD protein eluted at 100% phenyl buffer B (25 mM Tris-HCl, pH 7.5, 10 mM βME). Pooled fractions were diluted with Q buffer A (phenyl buffer B) (1:3) and loaded onto a Q Sepharose column. Fractions containing SufD (30-32% buffer B) were concentrated and loaded onto an equilibrated HiLoad 16/60 Superdex 200 column. SufD fractions were collected from the center of the peak, concentrated, and stored at -80°C. Purity was determined by SDS PAGE and protein concentrations were measured by Bradford assay. SufD was identified by MALDI-TOF mass spectrometry analysis.

B.2 Results and Discussion

SufD isolated from cells over-expressing the entire suf operon. $SufBC_2D$ is isolated from cells over-expressing the entire *suf* operon.[1, 2] We recently noticed a protein that migrates similarly to SufD on SDS PAGE eluting with $SufBC_2D$ on the HIC column but eluting separately from $SufBC_2D$ on the anion exchange column (Figure B.1A). Fractions from the anion exchange column containing this protein (300-320 mM NaCl) were collected separately from $SufBC_2D$. The concentrated fractions were a faint red color. Further purification on a size exclusion column revealed the protein eluted in a symmetrical peak. Fractions were concentrated and analyzed for purity by SDS PAGE (> 90% purity, Figure B.1B). The protein band was excised from the gel, digested with trypsin, and analyzed by mass spectrometry. The protein band was identified as SufD. Concentrated final SufD was colorless and did not have any significant UV-Vis spectral features (Figure B.1B). Purified SufD was analyzed on an analytical size exclusion column and compared to protein standards to determine the apparent molecular weight. The experimental molecular weight was 78.8 kDa (Figure B.2), comparable to the experimental molecular weight of SufD isolated from cells only over-expressing *sufD* (74.9 kDa). The observed molecular weight is consistent with previously reported values for SufD (79.2 ± 1.3 kDa).[3] The theoretical molecular weight of a SufD homo-dimer is 93.6 kDa. The theoretical molecular weight of a SufD monomer is 46.8 kDa. The observed molecular weight value of as-purified SufD is not comparable to a SufD monomer or dimer. The crystal structure of SufD from *E. coli* has been resolved,[4] and the structure reveals SufD is a homo-dimer in solution (Figure B.3).

A

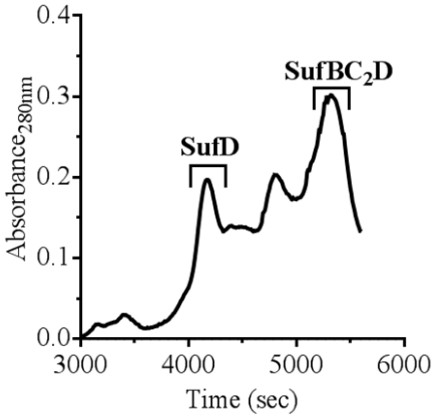

B

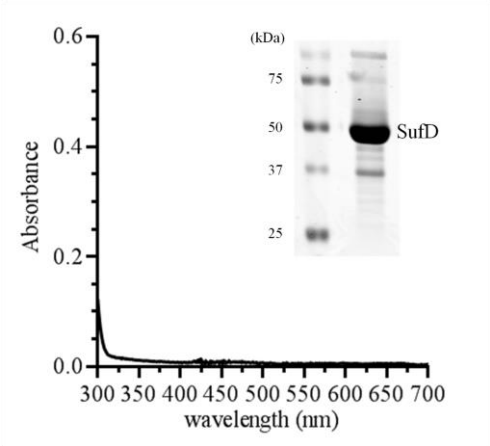

Figure B.1 Characterization of SufD. (A) SufD elutes separately from $SufBC_2D$ on anion exchange column (Q Sepharose). (B) UV-visible absorption spectrum of as-purified SufD. *Inset,* SDS PAGE analysis of purified SufD.

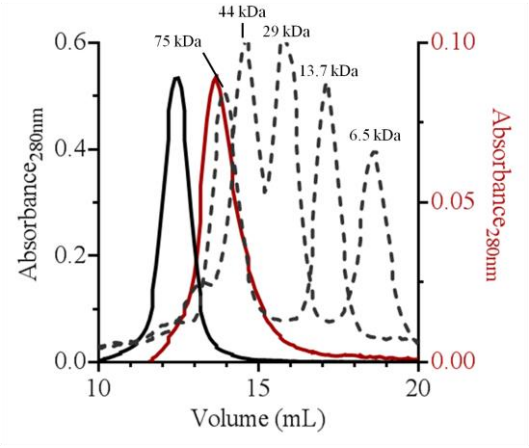

Figure B.2 Comparison of molecular size between $SufBC_2D$ (black) and SufD (red). Elution profiles from analytical size exclusion column (Superdex 200 10/300) are shown with size marker proteins: aprotinin, ribonuclease a, carbonic anhydrase, ovalbumin, conalbumin (dashed line) monitored by absorbance at 280 nm.

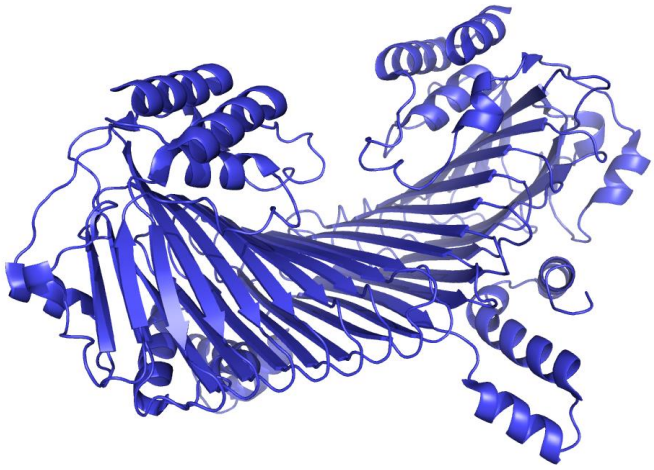

Figure B.3 *E. coli* SufD homo-dimer structure (PDB entry IVH4).[4]

We have established that $SufBC_2D$ is a stable complex that does not disassemble into sub-complexes or individual Suf proteins *in vitro* or *in vivo* (Chapter 2, this study). We discovered that SufD is distinctly separate from SufD associated with $SufBC_2D$ (Figure B.1A). The crystal structure of SufD was resolved in 2005 as a part of a bacterial structural genomics project to identify structures of novel bacterial proteins lacking sequence homology with structures available in the Protein Data Bank (Figure B.3). SufD has a beta-solenoid structure and contains 23 highly conserved His residues.[4] The presence of multiple conserved His residues makes SufD a potential candidate for involvement in metal binding, specifically iron binding. We previously reported mutation of SufD His128 to Ala increases the amount of [2Fe-2S] cluster associated with SufA purified from cells over-expressing the *suf* operon.[5] The mechanism was not determined, but the result suggests SufD is somehow involved in iron acquisition or Fe-S cluster transfer by the Suf pathway. Saini et al. reported the requirement of SufD and SufC ATPase activity for iron acquisition during Fe-S cluster formation on SufB.[6] SufD may not need to be in the $SufBC_2D$ complex to participate in the iron acquisition step. In future experiments, we will investigate if SufD binds iron and characterize the biochemical relevance of SufD in the Suf pathway.

B.3 References

1. Outten, F. W., Wood, M. J., Munoz, F. M., and Storz, G. (2003) The SufE protein and the SufBCD complex enhance SufS cysteine desulfurase activity as part of a sulfur transfer pathway for Fe-S cluster assembly in *Escherichia coli*. *J Biol Chem* 278, 45713-45719.

2. Layer, G., Gaddam, S. A., Ayala-Castro, C. N., Ollagnier-de Choudens, S., Lascoux, D., Fontecave, M., and Outten, F. W. (2007) SufE transfers sulfur from SufS to SufB for iron-sulfur cluster assembly. *J Biol Chem* 282, 13342-13350.

3. Wada, K., Sumi, N., Nagai, R., Iwasaki, K., Sato, T., Suzuki, K., Hasegawa, Y., Kitaoka, S., Minami, Y., Outten, F. W., Takahashi, Y., and Fukuyama, K. (2009) Molecular dynamism of Fe-S cluster biosynthesis implicated by the structure of the $SufC_2$-$SufD_2$ complex. *J Mol Biol* 387, 245-258.

4. Badger, J., Sauder, J. M., Adams, J. M., Antonysamy, S., Bain, K., Bergseid, M. G., Buchanan, S. G., Buchanan, M. D., Batiyenko, Y., Christopher, J. A., Emtage, S., Eroshkina, A., Feil, I., Furlong, E. B., Gajiwala, K. S., Gao, X., He, D., Hendle, J., Huber, A., Hoda, K.; Kearins, P.; Kissinger, C.; Laubert, B.; Lewis, H. A.; Lin, J., Loomis, K., Lorimer, D.; Louie, G.; Maletic, M.; Marsh, C. D.; Miller, I.; Molinari, J., Muller-Dieckmann, H. J., Newman, J. M.; Noland, B. W.; Pagarigan, B.; Park, F., Peat, T. S., Post, K. W.; Radojicic, S.; Ramos, A.; Romero, R.; Rutter, M. E., Sanderson, W. E.; Schwinn, K. D.; Tresser, J.; Winhoven, J.; Wright, T. A.; Wu, L., Xu, J.; Harris, T. J. (2005) Structural analysis of a set of proteins resulting from a bacterial genomics project. *Proteins* 60, 787-796.

5. Gupta, V., Sendra, M., Naik, S. G., Chahal, H. K., Huynh, B. H., Outten, F. W., Fontecave, M., and Ollagnier de Choudens, S. (2009) Native *Escherichia coli* SufA, coexpressed with sufBCDSE, purifies as a [2Fe-2S] protein and acts as an Fe-S transporter to Fe-S target enzymes. *J Am Chem Soc* 131, 6149-6153.

6. Saini, A., Mapolelo, D. T., Chahal, H. K., Johnson, M. K., and Outten, F. W. (2010) SufD and SufC ATPase activity are required for iron acquisition during *in vivo* Fe-S cluster formation on SufB. *Biochemistry* 49, 9402-9412.